5-2008

Body Mass Estimation from the Human Skeleton

Megan K. Moore
University of Tennessee - Knoxville

To the Graduate Council:

I am submitting herewith a dissertation written by Megan K. Moore entitled "Body Mass Estimation from the Human Skeleton." I have examined the final electronic copy of this dissertation for form and content and recommend that it be accepted in partial fulfillment of the requirements for the degree of Doctor of Philosophy, with a major in Anthropology.

Lyle Konigsberg, Major Professor

We have read this dissertation and recommend its acceptance:

Richard Jantz, Walter Klippel, Mohamed Mahfouz, R. Kent Hutson

Accepted for the Council:
Dixie L. Thompson

Vice Provost and Dean of the Graduate School

(Original signatures are on file with official student records.)

To the Graduate Council:

I am submitting herewith a dissertation written by Megan K. Moore entitled "Body Mass Estimation from the Human Skeleton." I have examined the final electronic copy of this dissertation for form and content and recommend that it be accepted in partial fulfillment of the requirements for the degree of Doctor of Philosophy, with a major in Anthropology.

Lyle Konigsberg, Major Professor

We have read this dissertation
and recommend its acceptance:

Richard Jantz

Walter Klippel

Mohamed Mahfouz

R. Kent Hutson

Accepted for the Council:

Carolyn R. Hodges, Vice Provost and Dean
of the Graduate School

(Original signatures are on file with official student records.)

Body Mass Estimation from the Human Skeleton

A Dissertation Presented for
the Doctor of Philosophy
Degree
The University of Tennessee, Knoxville

Megan K. Moore
May 2008

Dedication

To my dear Papa, for all you have been and all you have done for me. I miss you.

Acknowledgements

This research could not have been completed without the financial support and expertise of the Biomedical Engineers of the University of Tennessee. I am especially indebted to Dr. Mohamed Mahfouz for taking me under his wing and exposing me to new and innovative methods in order to achieve my anthropological goals. The extensive knowledge and constructive criticism from my advisor Dr. Lyle Konigsberg greatly improved the quality of my scholarship. The open door policy and many hours of brainstorming with Dr. Richard Jantz are responsible for the topic of this dissertation. I am indebted to Dr. Kent Hutson of the UT Medical Center for facilitating the CT scans and advising me on technical procedures. Dr. Dixie Thompson of the Department of Exercise, Sport and Leisure Studies at UT gave up a lot of free time to collaborate on bone density scans. I would like to thank Dr. Lee Meadows Jantz for her help and support and for giving me permission to use the William M. Bass Donated Collection. The Biomedical Engineering students provided their technical expertise, without which, this work could not have been completed. Thank you Emam ElHak Ali Abd ElFatah, Brandon Merkl, Mike Kuhn and Katherine Kesler. A special thanks to all of the Anthropology and Engineering volunteers who gave up their Saturdays or Sundays to help up with the scanning. The scanning was extremely physically and mentally demanding, and they worked for hours on end, without a single complaint. I thank Jenn Lilly, Donna McCarthy, Amanda Allbright, Emily Loucks, Rebecca Wilson, Elizabeth DiGangi, Anne Kroman, Lorena Villao, Katie King, Brian Pope, Genevieve Ritchie, Kate Driscoll, Courtney Eleazer, Kanchana Jagannathan and of course my ever obliging CT Tech, Todd Malone. Thanks to my wonderful friends for the patience and moral support,

especially during the final most stressful stages. Thank you: Dr. Anne Kroman, Dr. Liz DiGangi, Dr. Katy Weisensee, Dr. Graciela Cabana, Emily Hammerl, Giovanna Vidoli, Heather Worne, and Barbara Graham. This would not have been completed without my family. I love you all dearly: Monique, Mom, Dad, Michael, Dora, Nonnie, Grandma, Grandpa and my wonderfully supportive partner John Nipper. This research was supported by a grant from Zimmer Orthopaedics and NIJ Fellowship 2007- DN-BX-0013.

Dissertation Abstract

The established methods for estimating average body mass from the skeleton are of two types: biomechanical and morphometric. Neither technique currently addresses the extremes of body mass (e.g. emaciation or obesity). The goal of this research is to explore several different biomechanical methods, using data collected from high resolution computed tomographic scans and macroscopic analysis of 150 known modern individuals from the William M. Bass Donated Skeleton Collection at the University of Tennessee, Knoxville. This research will review the biomechanics of human gait and the biomechanical accommodations that occur with increased obesity and load bearing. The analysis will include cross-sectional geometry of the human femur at five locations along the diaphysis, bone mineral density scans of the proximal femur and a macroscopic evaluation of degenerative changes of the articulations of the spine, hip, knee and foot. The best single indicator of body mass for both males and females is the cross-sectional area of the proximal femur and BMD. By using pathologies combined, an accuracy rate of 87% for predicting obesity was achieved using a classification tree with sexes pooled. Furthermore, severe obesity has such a profound effect on the human skeleton as to leave a suite of traits affecting the load bearing elements of the lower limb and vertebral column.

Table of Contents

List of Figures

List of Tables

Chapter 1. INTRODUCTION

Introduction

The ability to estimate body mass from the skeleton represents an intellectual gap in forensic death investigations involving unidentified skeletal remains. Body mass estimation has received considerable attention, but previous research has failed to account for body mass extremes due to restraints of research collections. The current methods for estimating body mass from the skeleton are of two types: biomechanical and morphometric. The goal of my research is to combine biomechanical and morphometric methods, using data collected from three different methodological approaches: high resolution computed tomographic (CT) scans, dual-energy X-ray absorptiometry (DEXA) and macroscopic osteological analysis.

Morphometric analysis is limited to calculating the average body mass from the skeleton, disregarding variables of robusticity or adiposity. Biomechanical estimations confound body mass with levels of activity. To improve upon the biomechanical method, research must control for activity patterns. This can be accomplished by taking into account femoral cross-sectional shape, analogizing the long bones as engineering beams. Using several different biomechanical methods and accounting for activity can increase accuracy in body mass estimation. The ideal test case for this problem is to have a large skeletal sample of individuals of known height and weight, and the ability to determine biomechanical properties of the internal structure of the load bearing bones of the lower limb. All of these parameters are met by using CT and DEXA scans of the Bass Donated Skeletal Collection at the University of Tennessee.

Literature Review

Osteologists possess a set of skills to reveal antemortem information from human skeletal remains. The osteologist can estimate the age at death, sex, stature, and ancestry of a skeleton with a relatively high degree of accuracy. Body mass would provide a useful addition to skeletal analysis, but the accuracy of estimates is centered around average body mass, disregarding body mass extremes of emaciation and obesity. In a 2004 study, it was estimated that 32.2% of the American adult population is obese (Ogden et al., 2006). The ability to estimate body mass extremes would be a valuable asset for forensic analysis to achieve individuation of a skeleton. There are two methods currently established for body mass estimation from the skeleton. The first morphometric method calculates body mass based on allometric relationships between different measurements of the skeleton, typically stature and some measure of body breadth. The second method is based on biomechanical principles of load bearing on the diaphysis and articulations of the weight-bearing bones of the lower limb (Auerbach and Ruff, 2004).

Morphometric body mass estimation models the human body as a cylinder. The height of the cylinder is stature and the diameter of the cylinder is calculated from a measure of body breadth. Separate equations for males and females could improve this method, by controlling for sex by the width of the pelvis and the length of the clavicle (i.e. males typically have broader shoulders and narrower hips than females). Bi-iliac breadth alone works well for both highly active and sedentary normal weight individuals; in one study males are underestimated by 3% and females overestimated by 3% (Ruff, 2000). Bi-iliac breadth fails to account for any body mass extremes.

There are several biomechanical methods for estimating body mass from the skeleton. These methods are based upon the effects of load bearing and partially on aspects of aging. Load bearing typically affects the lower limb more than the upper, thus, most of the research in this area has focused on the lower limb for body mass estimation. The long bones can be modeled as engineering beams. The cross-sectional cortical area reflects the bone's strength to axial compression. The moment of inertia reflects bending strength. Polar moments of area measure the torsional strength of a bone (Frankel and Nordin, 1980). Greater bending strength in a certain direction would imply that the bone is loaded more in this direction. Many studies have investigated changing activity patterns due to the ratio of maximum to minimum bending in the femoral midshaft. It has been suggested that a high Imax/Imin ratio (or shape index) correlates strongly with greater levels of activity especially over rough terrain (Ruff *et al.,* 1983; Ruff *et al.,* 1984). A high shape index indicates more antero-posterior (a-p) elongation. If equal to one, it is more circular, if less than one, elongated in the medio-lateral (m-l) direction. Ruff (2000) looked at the relationships between cross-sectional properties and body mass and found significant relationships between all of the variables and body weight, especially with axial strength.

A second biomechanical method based on articular surface area to evaluate load bearing has received less attention. Ruff *et al.* (1991) failed to find significant relationships between body mass and the femoral head. When obese individuals were included, the prediction error lowered to 12-13% for the femoral head and 11% for shaft breadth. This is presumably because the femoral head, being part of a ball and socket joint, has constrained dimensions in adulthood, and thus fails to reflect adult weight

fluctuations. Lieberman *et al.* (2001) failed to find differences in the size of articulations of quadrupeds during extensive training, but this study may not translate well to bipeds. Eckstein et al. (2002) discovered that the articulations at the knee were significantly larger in highly active individuals with a history of increased activity. Porter (1999) also found a correlation in living individuals between body mass and the width of the ankle, combining tibial and fibular maleoli measurements *in vivo*. Bone density and degenerative properties associated with aging should be included in this section on biomechanical measures of body mass. Body mass has been shown to correlate well with bone density (Gibson et al., 2004; Looker et al., 2006; Miyabara et al., 2007, Wheatley, 2005; Wu , 2007). Osteoarthritis also has a strong positive relationship with body mass (Coggon et al., 2001; Ford et al., 2005; Moskowitz, 1993; Sharma et al., 2006; Stürmer et al, 2000).

Living bone is not homogenous in terms of its directional organization (i.e., it is anisotropic), which is a functional necessity of the non-uniform loading patterns. This can complicate mathematical modeling. Bones can be loaded by tension, compression, shear and bending forces. Bone is ultimately strongest in compression. Bending occurs mostly at the midshaft, whereas the epiphyses near the joint are mostly loaded in compression. Cortical bone is designed mostly for compression. Shear fractures occur typically in the cancellous bone. The torsional forces are distributed over the entire surface of a bone (Frankel and Nordin, 1980). Increasing surface area or cross-sectional area, increases bone strength to both compression and tension. Area moment of inertia measures the bending strength of a bone. A simple demonstration of bending strength

can be understood with a wooden ruler, if you consider the ease of bending a ruler in half along the width compared to bending it along the narrow thickness (Larsen, 1996).

The analogy of the ruler is useful for considering the diaphysis of the load bearing long bones of the lower limb (i.e. beam theory). A shape index or Imax/Imin ratio, which equals the moments of inertia in the direction of greatest bending divided by the moments of inertia in the direction of least bending strength is suggested to account for activity levels (Ruff, 1987). A higher ratio, or more antero-posterior (a-p) elongated shaft, would have greater a-p strength in bending at the midshaft. This orientation of the diaphysis has been shown to be the result of greater flexion at the knee (i.e.climbing up stairs or walking over rough terrain) (Larsen, 1997; Lovejoy, *et al.,* 1976; Ruff, 1987).

Recognizing the biomechanics of obesity provides a step closer to understanding how to recognize skeletal covariates of obesity. As the percentage of obese individuals increases rapidly in the living populations, so will the percentage representation in forensic cases. The prevalence of obesity has increased from 12.8% in 1974 to 22% in 1994 (Flegal, *et al.,* 1998) and has steadily increased to 32.2%. Approximately 50.7% of subadults are now overweight (Ogden et al., 2006). When considering that the major joints of the legs are exposed to loads that are 1.9 to 7.2 times body weight (Komistek et al., 2005), it would be reasonable to assume that obese individuals are regularly experiencing much greater axial loads than their normal weight counterparts.

As stated previously, a-p bending forces are greatest in extreme flexion of the knee, but you do not see this in obese individuals. The load-bearing elements of the lower limbs of obese individual will be affected primarily by greater axial loading. The greater axial loading in the obese individual will result in a very thick, but nonetheless

circular cross-section. Asymmetry in knee malalignment is common as a compensatory mechanism in obese individuals which leads to knee instability and osteoarthritis (Sharma *et al.,* 2000). According to several studies, there is an extremely high correlation between obesity and osteoarthritis with the data from NHANES II and the Framingham study. One study found a 'linear' relationship between knee arthritis and levels of obesity in women (Mannienen *et al*., 1996). Ford *et al.* (2005) found that obese women were 25.1 times more likely to have meniscal tears than normal weight counterparts, which is a condition that leads to osteoarthritis.

Previous studies support my hypothesis that body mass will correlate best with femoral cross-sectional area, both of which used radiographic scans of living subjects. In one study by Ruff, Scott, and Liu (1991), cross-sectional dimensions of the shaft correlated well with current weight, except for one outlier. This individual was obese, but had not been at age 18, as had been self-reported. She showed increased cortical thickness, but her midshaft diameter was normal. The cross-sectional area for her femoral diaphysis correlated extremely well with her body mass. This case indicates a potentially significant reversal in bone remodeling for an adult with endosteal deposition rather than resorption. This supports the claim that primarily axial compression is affecting the femoral shaft in obesity, because the individual's resistance to torsion was not increased by distance from the neutral axis (centroid), nor was the bending strength (area moments of inertia). Two studies found cross-sectional femoral measures correlate strongly with body mass during growth (Eckstein *et al,.*2002; Moro *et al.*, 1996). Ruff, Scott and Liu (1991) and Ruff (2000) found correlations with body mass and cross-

sectional properties in adults. In the latter study, reflecting the current body weight more than the body weight at age 18.

Previous research on cross-sectional geometry, bone density, and degenerative joint disease indicates that obesity will result in a suite of traits. The combination of decreased knee flexion and increased axial compression in ambulatory obese individuals will lead to in an increase in cross-sectional area, without an increase in area moments of inertia or torsional strength. Thus, obese individuals would have thick cortical area with a relatively round (a-p = m-l) and narrow shaft diameter for their body mass estimate, if not flattened mediolaterally (m-l > a-p). Greater bone mineral density and greater bone density should be evident. The load bearing elements of the lower limbs of obese individual will be subjected to greater compressive loads.

At the other end of the load-bearing spectrum, emaciated individuals will be more likely represented by individuals suffering from low bone density (osteopenia), increased fracture risk (osteoporosis) and reduced cortical area. Approximately 1.5 million low trauma fractures a year in the US are a result of osteoporosis. Many factors influence bone density including diet, exercise, body mass, peak bone mass, sex, age and ancestry. All of these factors also affect body mass, so maybe this relationship between BMI and BMD is the most important. Body mass index also plays a dominant role in bone density. A larger BMI tends to be associated with greater bone density than a smaller BMI (Gibson et al., 2004; Looker *et al*., 2006; Miyabara et al 2007; Wheatley, 2005; Wu, 2007).

Lifestyle factors contributing to osteopenia in young women include low body weight, poor nutrition, reduced beta cell hormones, excessive dieting and non-

participation in high school sports (Gibson et al., 2004; Reid, 2007; Turner, 2000). Female athletes in endurance or appearance based sports (gymnastics, ballet, running) with extreme diets are more likely to develop early onset osteoporosis. Ridout (1999) showed that bone density of young female athletes would sometimes be equivalent to elderly women. Again, the main factors were excessive exercise, low body weight and amenorrhea. Thirty to forty percent of young female athletes were anemic due to low fat, low iron and high fiber diets. Decreased cortical thickness is one way to evaluate osteoporosis (Bloom *et al*., 1970) and decreased cortical thickness has been seen in nutritionally stressed populations in Africa and the United states (Hummert, 1983; Martin *et al.*, 1987).

In summary, this research intends to explore this suite of traits in the same sample of skeletons. Previous research has focused independently on bone mineral density, cross-sectional geometry or pathological response to obesity or emaciation. Bone mineral density research suggests that larger individuals should have more bone density and emaciated individuals have osteoporosis, whether due to starvation or illness. Studies of the cross-sectional geometry of the femur suggest greater cortical area with increased body mass. Obesity is recognized as a risk factor for osteoarthritis, which is rarely seen associated with osteoporosis. Diabetes mellitus and high protein diets are highly correlated with the condition DISH of the spine. The current research will tie all of these skeletal responses together in the same sample of known origin in order to develop a comprehensive model of the effects of body mass on the skeleton.

Research Design and Methods

The research sample consists of 150 modern individuals of known age, weight, height and occupation from the William M. Bass Donated Skeletal Collection at the University of Tennessee, Knoxville. During the summer of 2005, CT scans were conducted at the University of Tennessee Medical Center with the financial and technical support of the Center for Musculoskeletal Research and the Department of Biomedical Engineering. The Bass Donated Skeletal Collection offers a unique opportunity to study individuals of known age, height and weight. High-resolution CT scans were collected using a GE Lightspeed 16 Slice computed tomography scanner. The DICOM images were converted to JPEG files and manually segmented into three-dimensional bone surface models. A subset of femora was density (DEXA) scanned at the Department of Exercise, Sport and Leisure Studies. The robust research methodology cross-validates modern techniques of computed tomography and densitometry with traditional osteological methods of biological anthropology, thus serving to increase reliability and applicability.

This research reviews the biomechanics of human gait and the biomechanical accommodations that occur with greater obesity and load bearing. The project will includes three major modes of analysis: cross-sectional geometry and shape analysis, bone density, and osteological analysis of degenerative conditions. Chapter 2 provides a summary of previous research in body mass estimation. The William M. Bass Donated Skeletal Collection is described in Chapter 3, with a summary of trends in body mass for the collection over the past few decades. Chapter 4 focuses on the cross-sectional geometry of the human femur, because of the load bearing and survivability of this

element. Cross-sectional CT data at five locations along the shaft are evaluated for geometric properties of area (both medullary and cortical), moments of inertia, torsional rigidity and radius of gyration. Bone mineral density calculations of the proximal femur are investigated using dual-energy X-ray absorptiometry (DEXA) in Chapter 5. This chapter also combines the methods of cross-sectional geometry to develop a comprehensive model for body mass estimation. Finally, an osteological analysis explores osteoarthritis and other degenerative changes of the articulations of the spine, hip, knee and foot in Chapter 6. My preliminary findings indicate that a significant covariate of body mass, at least for females and the elderly, is the cross-sectional area of the femoral waist (least circumference) ($r=.82$, $n=24$) (Moore et al., 2007). A large cross-sectional area and increased bone density of the femoral midshaft should correspond to a high body mass index (BMI) and a reduced cortical area and reduced density as seen in osteoporosis will correspond to a decrease in BMI. By controlling for cross-sectional shape and thus activity levels, the correlation coefficient will increase for both males and females. The greatest obstacle will be to control for the covariates of activity and aging from the forces imposed by body mass alone, thus accounting for lifetime fluctuations in body mass. Severe obesity should have such a profound effect on the human skeleton as to leave a suite of traits affecting the load bearing elements of the lower limb and vertebral column at one end of the spectrum and an absence of these traits at the other end of the spectrum associated with emaciation.

Computed tomography (CT) is superior to magnetic resonance (MRI) and ultrasound for imaging the skeleton. CT performs multiple two-dimensional slices of three-dimensional objects and mathematically reconstructs the cross-sectional image

from the X-ray measurement of thin slices (Brant, 1994). In essence, the CT creates 3-dimensional radiographs. The advantages of CT data are numerous: rapid data acquisition, relatively non-destructive (some DNA degradation), provides high-resolution three-dimensional data of both internal and external bone surfaces and information on bone density.

In conjunction with a team of biomedical engineers and anthropologists, CT scans were conducted of the individuals from the William M. Bass Skeletal Collection in the Department of Anthropology at the University of Tennessee. To facilitate data acquisition we developed a system that permitted rapid data collection, consisting of six identical sets of two boxes lined with foam. We standardized the positioning of the boxes in the CT scanner by strapping a board to the scanner table.

For the statistical analysis, the covariates of body mass (bone density, cross-sectional area, osteoarthritis, DISH, heel spurs) will be evaluated by multiple regression equations. A classification tree and logistic regression will serve to demonstrate the relationships between the categorical variables in order to develop a predictive model for estimating body mass.

Implications for policy and practice

The findings of the internal structural changes from three-dimensional CT models can validate evidence from osteological analysis, enabling wide-scale application of osteological methods that are fast, inexpensive and less labor intensive. In a forensic investigation with unidentified human skeletal remains, X-rays of a single femur in two different planes could be used to approximate cortical area at the midshaft and establish a

ratio of Imax/Imin to estimate activity levels. Using only radiographs in conjunction with an osteological analysis of the vertebral pathologies, osteoarthritis and heel spurs, practitioners could potentially estimate body mass of the individual.

Chapter 2. BODY MASS ESTIMATION

Osteologists possess a set of skills to reveal information from human skeletal remains. The osteologist creates a biological profile to estimate the age, sex, stature, and ancestry of a skeleton with a relatively high degree of accuracy. Body mass would be a useful addition to skeletal analysis, but the accuracy of estimates is centered around average body mass, disregarding body mass extremes of emaciation and obesity. These body mass extremes would be extremely useful for forensic analysis and individuation of a skeleton, not to mention the information it could provide about historic or prehistoric populations. There are two methods currently used to estimate body mass from the skeleton. The first morphometric method calculates body mass based on allometric relationships between different measurements of the skeleton, typically stature and some measure of body breadth. The second method is based on biomechanical principles of load bearing on the diaphysis and articulations of the weight-bearing bones of the lower limb (Auerbach and Ruff, 2004). Morphometric analysis is limited to calculating the average body mass from the skeleton, disregarding variables of robusticity or adiposity. Biomechanical estimations confound body mass with levels of activity. To improve upon the biomechanical method, research must control for activity patterns, which can be accomplished by taking into account femoral cross-sectional shape. Using multiple biomechanical methods together can serve to increase confidence in body mass estimation. The ideal test case for this problem is to have a large skeletal sample of individuals of known height and weight, and the ability to determine the biomechanical properties of the internal structure of the load bearing bones of the lower limb.

Morphometric Methods

Morphometric body mass estimation models the human body as a cylinder. The height of the cylinder is stature and the diameter of the cylinder is calculated from some measure of body breadth. Bi-iliac breadth measures the width of the pelvis as a measure of body breadth. This measurement is done by articulating the pelvis and subsequently accounting for tissue thickness. This model seems to work well when comparing size and proportions for adaptation to tropical vs. cold climates, in accordance with Bergmann's and Allen's rules of surface area to volume ratios in the trunk and extremities (Ruff, 1991; Ruff and Walker, 1993). To improve upon this method, I suggest either calculating separate equations for males and females or to additionally utilize the clavicle as a natural control for sex differences in body breadth at different regions (i.e. males typically have broader shoulders and narrower hips than females). Bi-iliac breadth alone works well for both highly active and sedentary normal weight individuals; in one study males are underestimated by 3% and females overestimated by 3% (Ruff, 2000). This method relies heavily on the stature measurement; therefore the use of accurate stature formulae from appropriate reference populations is very important. For my research, I will focus on a modern sample of known origin, thus the selection of a reference population and relevant regression equations are not necessary.

Biomechanical Methods

There are several biomechanical methods for estimating body mass from the skeleton. These methods are based upon the effects of load bearing and partially on aspects of aging. Load bearing affects the lower limb more than the upper, thus, most of

the research in this area has focused on the latter for body mass estimation. The long bones can be modeled as engineering beams. The cross-sectional cortical area reflects the bone's strength to axial compression. The moment of inertia reflects bending strength. Polar moments of area measure the torsional strength of a bone (Frankel and Nordin, 1980). Greater bending strength in a certain direction would imply that the bone is loaded more in this direction. Many studies have investigated changing activity patterns due to the ratio of maximum to minimum bending in the femur and tibia. It has been suggested that a high Imax/Imin ratio correlates strongly with greater levels of activity, especially over rough terrain (Lieberman et al., 2004; Ruff et al., 1983; Ruff et al., 1984). Ruff (2000) looked at cross-sectional properties to estimate body mass. Ruff et al. (1991) did not find significant relationships between body mass and the femoral head. This is might reflect constrained dimensions in adulthood, and thus the inability to correspond to adult weight fluctuations. This same joint may behave differently during growth and development, but there has been little research in this area. Lieberman et al. (2001) did not find changes in articulations of quadrupeds during extensive training. This study may not translate well to bipeds. On the contrary, Eckstein et al. (2002) discovered that the articulations at the knee were significantly larger in highly active individuals with a history of increased activity. Porter (1999) also found a correlation in living individuals between body mass and the width of the ankle. Bone density and degenerative properties associated with aging should be included in this section on biomechanical measures of body mass.

The skeleton serves many purposes. It acts as a support system for other organs, it provides levers for action, and it must support the weight of the organism while

withstanding forces during locomotion and impact (Schmidt-Nielsen, 1984). Due to the fact that bone is plastic, bone will adapt and model or remodel itself as necessary according to the strain applied. Roux first made the observation in 1881 that bone trabeculae appear to follow engineering principles, a finding later supported by Wolff in 1892. They recognized a principle of "functional adaptation" in bones, where bone will reinforce itself along the direction of principal strain (Cowin, 2001). Bones are anisotropic and extremely complex mechanical systems able to respond simultaneously to multiple forces (axial, bending and torsion). Bones can change in material properties during growth, development and aging. As a result, the shape of a bone will reflect weight-bearing throughout life due to levels of activity and to body mass. Intrinsic factors (hormone levels, nutrition, etc.) can also play a role in bone metabolism. The skeleton will at least be strong enough for locomotion, able to withstand impact according to the individual's activity level. The problem to focus on is how to separate activity patterns and aging from the forces imposed by body weight alone, accounting for lifetime fluctuations in body weight.

During growth and development, bones are extremely plastic to forces of load bearing, due to their more elastic material properties. The ultimate shape of the diaphysis and articulations are altered by these forces. Increased surface area at the joints provides greater resistance to axial compression, which is the predominant force affecting the epiphyses (Frost, 1993; Eckstein, et al. 2002). For example, if bones undergo extreme axial loading, the bones will accommodate by increasing in cross-sectional area. Greater or lesser activity can confound some of these findings, but it is important to keep in mind that the shape of bone can reflect specific activities. If you have two individuals

experiencing heavy loads, one from greater activity, the other from obesity, both will have increased bone deposition on the bone shaft, but the more active individual will likely have a greater Imax/Imin ratio, because anterior-posterior (a-p) elongation is associated with extreme flexion at the knee (Lieberman et al., 2004; Ruff, et al. 1983; Ruff et al., 1984; Ruff et al, 1991). The obese individual will only be experiencing greater axial loading. Asymmetry in knee malalignment is common as a compensatory mechanism in obese individuals as I will explain later in this chapter (Maffeis-Claudio, et al., 2001; Sharma et al., 2000). The greater axial loading in the obese individual will result in a very thick, but nonetheless circular cross-section.

Adult bone responds slightly differently to forces of loading over time. The fusion of the epiphyses and increased mineralization compared to juvenile bone gives greater strength and stiffness to adult bone, thus becoming more brittle. The articulations are unable to expand in the same way as for juveniles. Frost (1993, 1997b) and Eckstein et al. (2002) posit that degenerative processes are an attempt to compensate for this by increasing surface area with osteoarthritis, and ultimately increasing compressive strength at the epiphyses. In addition to the expansion of the joint surfaces, gradual bone loss will simultaneously reduce long bone cortices. Bone has been shown to increase in diameter with age, while losing bone mineral density. Essentially this maintains and increases bending strength into adulthood, but with reduced strength in compression, and likely in individuals of decreased body mass, with less compressive forces acting on their bones. Women experience an accelerated bone loss following menopause, which has been established in prehistoric populations as well (Bloom, 1970; Ericksen, 1976; Nelson, et al., 2000; Ruff et., 1982; Ruff et., 1984). Clinical studies show that smaller women are

more prone to osteoporosis than are larger women (Gibson et al. 2004; Miyabara et al., 2007; Wu, 2007). This could either be due to increased estrogen stores in adipose tissue of heavier women or beta cell hormones, recognized for maintenance of bone metabolism, or due to decreased bone strength from decreased compression, or a combination of the two (Reid, 2007).

The paradox of skeletal function is that it must be "strong enough for support, but light enough for locomotion" (Rubin, 1990). The ability to maintain this balance is contained within the bone itself. This balance is maintained through a collaborated effort between an extensive network of osteocytes and basic multicellular units (BMUs) made up of osteoblasts and osteoclasts. BMUs respond to signals from the osteocytes via bone resorption followed by apposition (Frost, 1993; Rubin, 1990). This process is often referred to as Wolff's Law, but I prefer the term functional adaptation (Bertram, et al., 1991; Carter, et al., 1991; Cowin, 2001).

One particular problem in attempting to estimate body mass from the skeleton is that body mass may fluctuate throughout life. There is a certain duration of lag time in bone turnover. We need to establish how long it takes bone to remodel in response to body mass (Frost, 1993). It is clear that the patterns of bone loss and deposition occur differently between childhood and adulthood. Activity patterns should change the overall shape of the shaft. As an adult, the cross-sectional shape may remain somewhat constant, but bone loss will occur endosteally, which is the pattern for this type of bone loss with aging. The most confounding issue will be in determining whether someone has become bedridden, because his or her bones are no longer active levers, and thus will experience extreme bone loss regardless of size (Frost, 1997b).

Engineering Beam Theory

Bones can be loaded by tension, compression, shear and bending forces. Bone is strongest in compression. Bending occurs mostly on the midshaft, whereas the epiphyses are mostly loaded in compression. Shear fractures occur typically in the cancellous bone, while cortical bone is designed mostly for compression. Torsion is distributed over the entire surface of a bone (Frankel and Nordin, 1980). Living bone is seldom loaded by a single force, which makes it very complicated to model mathematically. The larger the cortical area, the stronger and more stiff the bones are to compression and tension. Polar moment of inertia is a measure of the torsional strength of the bone, which is directly related to the distance from the neutral axis, which typically goes through the center of the medullary canal (although this can fluctuate depending on the direction of force(s) being applied). The further from the neutral axis, the stronger the bone is to torsion. Area moment of inertia measures the bending strength of a bone. Larsen (1997) used the analogy of the bending strength in terms of a wooden ruler. If you try to bend the ruler along the width of the ruler, it yields quickly and fails. If you try to bend it along the narrow thickness of the ruler, it is more difficult to bend and break.

The analogy of the ruler is useful for considering the diaphysis of the load bearing long bones of the lower limb. One main focus in the research by Ruff is on the Imax/Imin ratio. Imax and Imin are both in fourth powers, like variances weighted by units of square area. Dividing one by the other gives a unit-less "shape" variable. This ratio is also known as the shape index. Manouvrier first recognized a difference in this ratio in 1888 from non-human primates to modern humans, the latter having a more round diaphysis. He attributed this rounder quality to being more civilized (Kennedy,

1989). The purpose of a higher ratio or more anterior-posterior elongated shaft, going back to the ruler analogy, is that the shaft would have greater a-p strength in bending, usually at the midshaft. This orientation of the diaphysis has been shown to be the result of greater flexion at the knee, related to climbing up stairs or over rough terrain (Larsen, 1997; Lovejoy, et al., 1976; Ruff, 1987). This ratio is useful because it automatically controls for size differences (Ruff, Hayes, 1983). This research has been corroborated by studies on modern elite athletes (Ruff, 2000), and in studies of *in vitro* loading in bones (Rubin, et al., 1990).

Biomechanics of Obesity

The population of obese individuals is rapidly increasing in the United States. The prevalence of obesity has increased from 12.8% in 1974 to 22% in 1994 and is steadily increasing (Flegal, et al., 1998). Recent estimates have 32.2% of adults as obese and claim that 50.7% of subadults are overweight in America (Odgen et al., 2006). This generation of obese juveniles is only now reaching adulthood, so we are not yet aware of the long-term effects of childhood obesity. The most difficult task is to recognize the biomechanical affects of obesity in childhood versus adulthood. In this chapter, I will consider bone acquisition during growth and development compared to adulthood, with respect to obesity. The greatest obstacle in the literature review is a lack of data in the clinical research. Extreme outliers are typically removed from any analyses. However, a few anecdotal descriptions exist in the literature to provide pertinent information to formulate my hypothesis.

During growth and development, material properties of the bone change from elastic to stiff. Endochondral ossification of the long bones occurs primarily through modeling or apposition of lamellar bone. Because of the higher percentage of collagen, young bone can adapt efficiently to its environment. This is especially true near the joint epiphyses (Frost, 1993; Rubin, 1990). There appears to be contradictory evidence for the ability of epiphyses to change according to levels of weight bearing in humans. Ruff and colleagues (1991) found a poor correlation between body mass and the femoral head, but this joint has constrained dimensions. Eckstein et al., (2002) discovered that the knee joint showed significant increases in articular area for tri-athletes versus matched size control subjects. The tri-athletes had been extremely active throughout their lives, thus, these articular area increases could have developed during childhood. Of note, there was no difference in the cartilage thickness between the two groups, as the researchers had originally predicted. Frost (1997) suggests that sudden heavy loading in children causes increases in spongiosa and compact bone (Frost, 1997b).

Adult bone formation occurs via a completely different process of Haversian remodeling. When the bone is stressed, micro-fractures can form in the cement junction, between osteocytes to help dissipate the force. If beyond a certain threshold, the basic multicellular units or BMUs will begin to increase bone apposition, and decrease resorption to accommodate the increased load. When the threshold has been brought to the lower end of the spectrum, the remodeling is turned off (Frost, 1997b). In remodeling, secondary osteons will overlay the primary lamellar bone (Robling, 1998). Bone remodeling in adults is mostly subperiosteal expansion with endosteal resorption, although, there is some scant evidence of endosteal apposition in obese individuals (Ruff,

et al., 1994). Whether this endosteal bone deposition in obese individuals is modeling or remodeling is beyond the scope of the present research.

Recognizing the biomechanics of obesity will take us a step closer to understanding how to recognize markers of obesity in the skeleton. This is becoming increasingly important due to the inevitable increased representation of obesity in forensic cases. Rates of obesity are increasing dramatically in the US and in other affluent parts of the world. In the US, the cause is most likely multi-factorial: a combination of decreased activity and increased calorie consumption. There does appear to be a threshold in obesity, for permanent immobilization, which could create confounding expressions in the skeleton. In the following paragraphs, I will review the biomechanics of obesity and try to predict some potential problems for the interpretation from skeletal remains.

Locomotion in obese individuals is markedly different from normal weight individuals. This knowledge will allow us to recognize patterns on the skeleton reflecting this difference. The gait of pre-pubescent obese children varies markedly from their non-obese counterparts. Obese children have a longer cycle duration, longer stance phase, and slower pace. Obese children showed more gait asymmetry, consistently favoring the right side. Nearly seventy percent of the obese children in one study required help from the researcher to stand from a sitting position without the use of their upper body (Hills et al., 2002). In morbidly obese individuals, their arms provide much of the support to stand erect in order to avoid injury to middle and lower back (Galli et al., 2000). This functional impairment due to childhood obesity perpetuates the cycle of obesity with individuals maintaining a positive energy balance. When considering that the knee joints

are exposed to loads that are anywhere from 1.9 to 7.2 times body weight (Komistek et al., 2005), it would be reasonable to assume that obese individuals are experiencing much greater axial loads than their normal weight counterparts. This should be evident in the axial strength of the bone expressed by increased mid-shaft cross-sectional area.

The knee is typically very stable in vertical alignment in the extended position. This normal vertical alignment is relatively rare for obese individuals. In a study by Herrington et al. (2004), less than ten percent of obese individuals exhibited normal knee alignment. To measure the alignment or malalignment of the knee for the purpose of biomechanics, the Q-angle, or quadriceps angle is a standard measure. One common method for measuring the Q-angle is to measure the angle formed by a line drawn through the anterior superior iliac spine (ASIS point) to the center of the patella. A second line from the center of the patella to the tibial tuberosity creates the Q-angle. Having an angle greater than 15-20 degrees is related to patellar pain and lateral dislocation. Men typically have a Q-angle between 10 and 14 degrees. Due to the broadness of the female pelvis and relatively shorter stature, women have a slightly greater Q-angle, between 15-17 degrees. This implies that biomechanically, women are already at a disadvantage. The most efficient Q-angle is at ten degrees. The knock-kneed condition, also known as *genu valgum* occurs if the Q-angle exceeds 17 degrees. The bowlegged or *genu varum* malalignment occurs when the Q-angle is extremely small or slightly negative. In a study on the effects of obesity on foot biomechanics, researchers found that the obese women showed a significantly higher Q-angle. Q-angles measured between 10 and 25 degrees in women with average body mass, but the severely obese women had Q-angles with a mean of 34 degrees.

In a study by Sharma et al. (2000), more than half of the nearly 300 individuals studied exhibited the varus malalignment. Another 40% had valgus malalignment, with only 10% having normal alignment. Most of the individuals showed direction symmetry, but the actual Q-angle was rarely symmetric. They found a correlation between the varus malalignment, joint space and BMI, but not for the valgus condition. Joint space was significantly smaller on the medial side of the knee joint compared to the lateral side in the varus condition. In this study of obese individuals with the valgus condition, there was less knee flexion and more plantar flexion. This along with severe out-toeing (eversion) may explain the high correlation of *pes planus*, or flat-footed condition with obesity. In the varus condition, the medial tibial plateau was supporting one hundred percent of the body weight. In the valgus, the weight was more distributed across the tibial plateau, with the medial side supporting a majority of the total body weight. The researchers' suggested that the osteoarthritis of the knee was due to malalignment caused by the varus condition. This may be expressed as differences in bone density and severity of osteoarthritis from the medial to the lateral sides of the tibial plateau.

Using the data from NHANES II and the Framingham study, there is an extremely high correlation between obesity and osteoarthiritis. One study found a 'linear' relationship between knee osteoarthritis and levels of obesity in women (Mannienen et al., 1996). Syed and colleagues (2000) proposed that quadriceps fatigue is responsible for osteoarthritis of the knee. This fatigue causes changes in gait pattern, which reduces shock absorption. They proposed women were more prone to osteoarthritis because women tend to have lower lean mass, and thus will experience muscle fatigue more rapidly. Hills et al. (2002) came to a similar conclusion, claiming that the increase in

lean muscle mass in males may add to the increase in musculoskeletal support and increased shock absorption during walking.

With obesity, I predict that most of the force on a bone will be axial. As stated previously, a-p bending forces are greatest in extreme flexion of the knee, but you do not see this in obese individuals. One particularly relevant study was conducted by Ruff, Scott, and Liu (1991). This study compared body mass estimates with skeletal measures of femoral cross-sectional geometry from radiographs of living subjects. Researchers asked subjects to report their current weight and their weight at age 18. There was one outlier, and when removed, cross-sectional dimensions of the shaft correlated well with current weight. The outlier was an obese individuals but she had not been so at age 18. Her cortical thickness was 1.5 SD above the mean, but her midshaft diameter was normal. The cross-sectional area for her femoral diaphysis correlated extremely well with her body mass, within 1% when using the sex specific formula. This case indicates a potentially significant reversal in bone remodeling/modeling for an adult showing endosteal deposition rather than resorption. This supports the claim that primarily axial compression is affecting the femoral shaft in obesity. Her resistance to torsion was not increased by distance from the neutral axis, nor was the area moments of inertia. Larsen and Ruff (1994) may also have discovered an archaeological example of obesity in an Amerindian population from Spanish Florida post-contact. They found evidence for decreased sedentism, but did not mention endosteal apposition. These authors did note that historical documentation suggested this population was corpulent, perhaps after adjusting to the high calorie maize diet associated with increased sedentism. They did show decreased bending strength post-contact. In a study by Moro et al. (1996), the

authors found that cross-sectional femoral measures correlated strongly with body mass during growth. This is consistent with research by Eckstein et al. (2002). Ruff, Scott and Liu (1991) and Ruff (2000) found correlations with body mass and cross-sectional properties in adults, with the latter study reflecting current body weight more than body weight at age 18.

Bone mass measurements can be accomplished in a variety of ways, but most often with dual energy X-ray absorptiometry (DEXA) in living patients. This technique has been criticized for not reflecting the actual strength of the bone, and bone density measures alone can be misleading. First of all, compensatory subperiosteal apposition associated with aging will increase the overall strength of the bone, but will appear as a decrease in density via DEXA. This technology does not predict density well in non-circular cross-sections. Furthermore, bone mass as measured through ash density, does not appear to correlate with cross-sectional properties. This is perhaps due to the varying isometric material properties within the cortical bone. The study by Moro et al. (1996) is the first that I have found in which body mass correlated better with cross-sectional properties than height, sex or activity level. In the study by Ruff, Scott and Liu (1991), they found an increase in cross-sectional area, without an increase in bone breadth.

From this literature review, obesity appears to form a suite of traits, which could be evaluated much the same way as sex or age assessment. The combination of decreased knee flexion and increased axial compression in ambulatory obese individuals will lead to an increase in cross-sectional area, without an increase in area moments of inertia or torsional strength. Thus, obese individuals will have thick cortical areas with a relatively round (Imax = Imin) and narrow shaft diameters for their body mass estimate.

Females should be more likely to exhibit *genua valgus*, and males to have *genua varus*, with corresponding OA expressions. As juveniles will likely show greater plasticity during growth, I predict that adults, who were obese as children, will have larger articulations at the knee, and potentially at the ankle as well. As a result, their joints will be better adapted to prevent knee osteoarthritis, but the hip may not be as well adapted, and would lead to osteoarthritis. Adult onset obesity will lead to greater knee osteoarthritis. The greatest predicament will be in recognizing the threshold at which an individual becomes bed-ridden. Frost (1997b) recognized that even obese individuals begin to show the effects of osteoporosis due to immobilization. Adult bone does have a fairly strong conservation mode (Frost, 1993), but the effects of OA should remain, as should the ultimate diameter, because adult bone resorption typically occurs endosteally.

Metabolic Processes of Bone Synthesis and Resorption

The skeleton appears to be a stable structure, yet the skeleton is a dynamic system, constantly remodeling in response to mechanical forces and metabolic processes. Bone acts as a reservoir of calcium to maintain normal function of the body and heart. Osteoclasts operate to resorb existing bone to release minerals and remove organic waste, while osteoblasts synthesize new bone matrix or osteoid. Osteoblasts mature into osteocytes, which become intricately woven into the network of calcified bone matrix. Osteocytes maintain the ability to communicate complex information of mechanical forces to make necessary modifications.

Bone remodeling is influenced by both mechanical factors and chemical factors. The mechanisms for bone metabolism from diet and genetic influences are not

completely understood, but recent research has explored this relationship. Chemical mechanisms for bone metabolism include hormones from nutrition, beta cell hormones, adipocyte hormones, calcium intake and calcitropic hormones (Reid, 2007). In terms of hormones from nutrition, consuming glucose causes an increase in calcitonin and a decrease in parathyroid hormone (PTH). This causes bone turnover to decrease. Amylin is a co-secretion of insulin and further prevents resorption. Other chemicals dependent on diet that potentially influence metabolism include glucose dependent insulinotropic polypeptide (GIP), glucagons-like peptide (GLPI & II), insulin-like growth factor (IGF I) and Ghrelin. Beta cell hormones produced in the pancreas may affect bone turnover due to insulin sensitivity and resistence. Obesity often leads to hyperinsulinemia, symptomatic of insulin resistence. This reduces the body's ability to respond to use the insulin it produces to lower glucose levels. This affects bone turnover because osteoblasts have both insulin and IGF I receptors. Furthermore, in cases of hyperinsulinemia, there is androgen and estrogen overproduction in the female ovaries. This leads to more free hormones and subsequently reduced osteoclast action (Francis, 2003; Reid, 2007). The adipocyte hormone estrogen has long been known to play a vital role in bone metabolism in females. Leptin has recently received attention for its role. Leptin influences bone turnover at the hypothalamus in both osteoblasts and chondrocytes, reinforcing the effect of insulin. The hypothalamus is the part of the central nervous system that controls energy balance and homeostasis. In rats, a low dose of leptin appears to be good for bone mineral content, but high doses can actually cause obesity. Adipinectin and resistan are two other adipocyte hormones that may play a role in both obesity and bone metabolism. Calcium intake is touted as the remedy for low

bone density, but the clinical research shows contradictory evidence. Dietary intake can confound the results of longitudinal studies in humans. Finally, the calcitropic hormone vitamin D can be sequestered in adipose tissue of obese individuals. On the other hand, Vitamin D intake can possibly prevent the development of adipocytes (Reid, 2007). This recent research into serum levels emphasizes the relationship that greater adiposity plays in higher bone density. Regardless of the mechanism, obesity is related to increased bone mineral content.

Pathologies

Having an appreciation for the biomechanics of obesity and the relationship between body composition and bone, it is important now to revisit some degenerative bone diseases with a fresh perspective. Most degenerative diseases of bone are attributable to age, but many are not an inevitable consequence of aging. Four degenerative pathologies will be considered and include osteoarthritis (OA), diffuse idiopathic skeletal hyperostosis (DISH), heel spurs and osteoporosis.

Osteoarthritis

Osteoarthritis (OA) is the most common form of arthritis. OA results from mechanical and biological events that involve diarthrodial or synovial joints. Stürmer et al. (2000) claims that OA is mechanical rather than systemic in terms of the risk due to obesity. OA is a slow, progressive articular disease with gradual development of joint pain (Moskowitz, 1993). The results of OA can be ulceration, loss of articular cartilage, sclerosis, eburnation of subchondral bone, osteophytes and subchondral cysts. Joint pain, stiffness, reduced movement and variable degrees of non-systemic inflammation are

symptoms of OA (Sharma et al., 2006). Hough (1993) suggests that OA is inherently a non-inflammatory disorder, describing the condition as a deterioration of cartilage and formation of new bone at the joint margins (see figure 2.1). Also known as degenerative joint disease (DJD), OA can be due to either 'wear and tear' or trauma. If OA is the result of trauma, it is classified as secondary OA. Primary osteoarthritis is a response to intensive or infrequent activities, but there is no difference in the manifestation due to these different etiologies (Bridges, 1991). Moderate mechanical loading is necessary for cartilage health. Dynamic compression can lead to increased chondrocyte anabolism and increased cartilage thickness, as seen in animal studies. High intensity exercise or sudden increase at an older age, as well as severe inactivity, can conversely lead to catabolic changes (Griffin et al., 2005). Interestingly, osteoporosis and OA are rarely found together (Hough, Jr. 1993; Moskowitz, 1993). Dequeker et al. (1983) suggested that perhaps osteoporosis protectts against OA.

Figure 2.1. Osteoarthritis of the knee, showing lipping, eburnation and porosity.

Risk Factors for Osteoarthritis

There has been a recent increase in osteoarthritis, affecting 15% of the population (Sharma et al., 2006). Messier et al. (1996) reported that knee OA is found in 33% of adults over 63 years. This is likely an underestimate, as early stages of OA can be asymptomatic and underreported. Autopsies show much earlier signs of OA than do radiographs and have shown evidence of OA as early as the twenties. By the age of 40, 90% of all autopsies show some OA in the weight bearing joints (Moskowitz, 1993). Under 45 years, OA may be more common in men but after 55, it is higher in frequency and more severe in women (Moskowitz, 1993). Postmenopausal women are more likely to have knee, hip and hand arthritis than men, but estrogen was not found to predispose women to OA (Holmberg et al., 2005; Sharma et al., 2006). Hip OA is more common in

males according to Moskowitz (1993). This author went on to say that, age is the strongest identified risk, but OA is not inevitable. In the Framingham longitudinal study, age did not affect the risk of knee OA. A strong relationship exists between OA and occupation. Runners, however, show no difference in DJD or joint space of the knee compared to non-runners (Bridges, 1991). Sports with heavy loading and twisting at the knee are risk factors for OA, but habitual physical activity is not (Griffin et al., 2005).

There exists a strong relationship between body mass and the development of osteoarthritis. This relationship seems to be causal, as weight gain in obesity precedes the development of OA (Griffin et al., 2005). As BMI increases, strain and torque increase, leading to higher risk of injury (Ford et al., 2005). Hough (1993) claimed obesity is accepted as a definitive risk for osteoarthritis. Felson (1988) reported that increased body mass was found to be associated with OA throughout the body including the hands, feet, knee, hip and spine.

Previously in this chapter, I demonstrated that obese individuals are more likely to have knee malalignment than normal alignment. Sharma and colleagues (2006) observed knee alignment and found that the individuals with varus malalignment were four times more likely to have medial OA at the knee. Valgus malalignment was more likely to cause lateral OA at the knee. In this study, for every one degree of valgus angle, the average loss of lateral tibial cartilage volume is 8.0 μl. The authors stated that meniscal tears are related to loss of cartilage volume. After reviewing patient records for OA, a survey study by Holmberg et al. (2005) found that individuals who were overweight at any time were more likely to have OA. The odds ratios for obesity and OA were several times greater for OA than occupation. The highest risk, based on this survey, was for

those individuals who had been obese since the age 30. The risk was significantly lower for those with a BMI less then twenty. In a case-control study looking at meniscal tears, the researchers found a dose-response relationship with body mass index in both sexes. Odd ratios were 15.0 for males and 25.1 for women with a BMI over 40 (Ford et al., 2005). Another study found odds ratios of 13.6 for individuals with a BMI>36 and only 0.1 for BMI<20 (Coggon et al., 2001). In a study by Stürmer et al. (2000), the odds ratio for obese individuals to have bilateral knee OA was 8.1 and only 5.9 for overweight individuals. Sharma et al. (2006) found that if an individual has unilateral knee OA, 46% of the top tertile for BMI developed OA in the opposite knee as well. Another study found that obese individuals had more severe cartilage defects, with larger medial tibial area overall. These results revealed a dose response relationship (Ding et al., 2005). With increased bone density, there is a positive correlation with OA (Moskowitz, 1993).

Heel Spurs

Heel spurs on the inferior surface of the calcaneous are the result of an inflammatory condition called plantar fasciitis. Chronic inflammation due to increased tensile loads can cause degeneration of the plantar fascia (plantar aponeurosis). As the fascia is pulled from the calcaneous, a bony spur develops (see figure 2.2). This condition is assumed to be the result of repetitive microtrauma, similar to osteoarthritis. Plantar fasciitis can result in *pes planus* or flat-footedness, which is a collapse of the foot's arch. This condition is common in runners and military personnel. Plantar fasciitis peaks between 40-60 years, but occurs at younger ages in runners. With the arch collapsed, stress fractures can occur in the metatarsals (Buchbinder, 2004). Two million

Americans a year suffer from heel spurs and as much as 10% of the population will have them at some point in their life. In a matched case-control study for age and gender, researchers considered the risk factors of obesity, standing posture and amount of dorsiflexion. The odds ratio for obesity (BMI>30) was 5.6 compared to normal weight individuals (BMI<25). For those individuals who spent the majority of the day on their feet, the odds ratio was 3.6. The most important variable was reduced dorsiflexion, which is caused by a shortened Achilles tendon. All of these factors would have increased the tensile loads on the plantar fascia (Riddle et al., 2003).

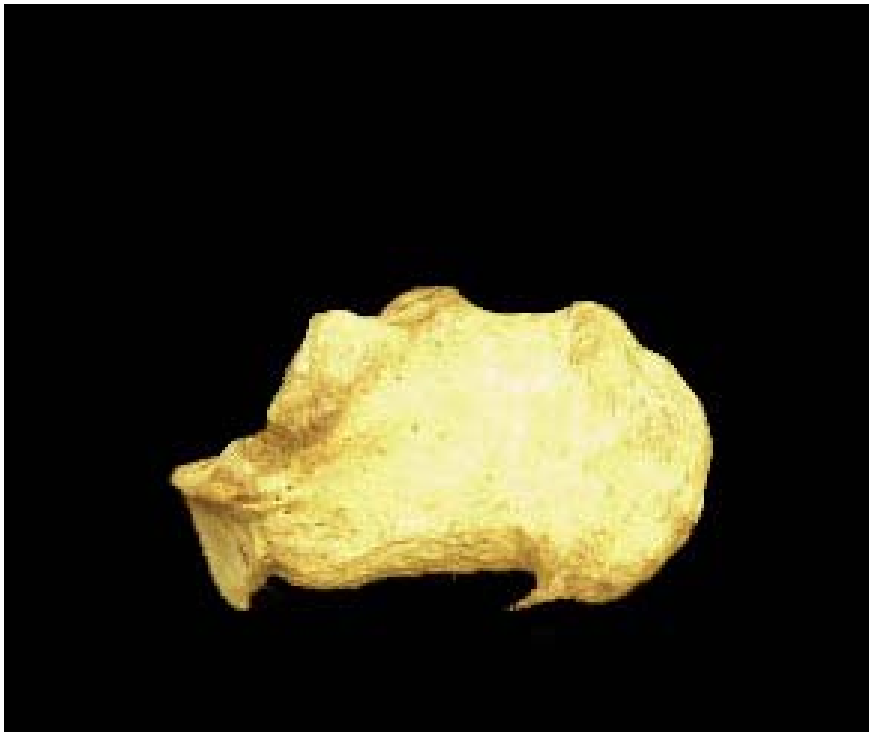

Figure 2.2. Heel spur on the inferior and posterior right calcaneous.

DISH

Diffuse idiopathic skeletal hyperostosis (DISH), also known as Forestier's disease, is a combination of ankylosis of the spine and ossification of muscle attachments (entheses) throughout the body. The unique manifestation on the spine resembles candle wax melting and flows along the right anterior of the spinal column (see figure 2.3). DISH does not form on the left side of the spine because of the pulsation from the descending aorta. If the condition is on the left, it is indicative of a right sided aorta. It appears to be a calcification of the anterior longitudinal ligament, mostly in the thoracic spine. The condition is diagnosed if three or more vertebrae are fused together and disc space is preserved. Other manifestations of the disease are ossifications of the muscle attachments of the rotator cuff and deltoid tuberosity of the humerus, ulnar olecranon, bicipital tuberosity of the radius, iliac crest and iscial tuberosity of the pelvis, trochanters and linea aspera of the femur, entheses of patella, tuberosity and *linea m. solei* of the tibia and heel spurs of the calcaneous. Due to this diffuse nature, individuals with DISH are classified "bone formers" (Moskowitz, 1993).

Figure 2.3. DISH from the anterior (left) and right lateral aspects (right).

There tend to be correlations of DISH with obesity and diabetes mellitus. Both DISH and OA increase with age, are hypertrophic diseases and often co-occur. DISH is unusual in individuals less than forty years of age, with an average age of 65 years. It is 6.9 times more common in males. In an archaeological samples, DISH was significantly correlated with high status and a high protein diet (Jankauskas, 2003) and with monasteries (Patrick, 2005). DISH often associated with gout and ossification of the posterior longitudinal ligament, but not with rheumatoid arthritis. In one study, 40% of DISH patients had Type II diabetes, but this was not confirmed in subsequent studies (Rogers et al., 2001). DISH often goes undiagnosed because it does not cause back pain, only stiffness and reduced movement. DISH is common in patients with hyperglycemia and high levels of insulin. Moskowitz, (1993) reports that DISH is found in 50% of the Pima Indians who also had elevated levels of Vitamin A. By giving high doses of

vitamin A derivatives (retinoids) in another study, a similar ossification developed in the spine.

Osteoporosis

The World Health Organization defines osteoporosis as exceeding 2.5 standard deviations below the mean value for bone mass in young adults. Osteoporosis is defined as severe if there has been one or more fragility fractures (Francis, 2003). Horner *et al*. (2002), define osteopenia as having a BMD t-score between –1 and –2.5 standard deviations below peak bone mass, and osteoporosis exceeding –2.5 standard deviations below the mean. A new suggestion for differentiating different forms of bone loss was offered by Frost (1997a). He suggests broadening the definition of physiologic osteopenia to include everyone with a below normal BMD for their age, height, weight, etc., who only fracture when they fall. Osteoporosis would then be the "naturally irreversible osteopenia," with spontaneous fractures without obvious injuries. This definition may prove useful in the future, but I will use the definition offered by the WHO and Horner et al. (2002). Primary osteoporosis is that due to menopause and aging. Gennari *et al.* (1998) describe secondary osteoporosis as having identifiable causal agents other than menopause and aging, whereas Francis (2003) defines secondary osteoporosis as an accelerated form of the disease.

Osteoporosis is an extremely costly disease, on the individual and on the economy. Approximately 1.5 million low trauma fractures a year in the US are a result of osteoporosis. The mortality rate in the elderly in the six months following a hip fracture is 10-20%, 25% of those survivors will require assisted or nursing homecare

(Messinger-Rapport et al., 2002). Many factors influence bone density including diet, exercise, weight, peak bone mass, sex, age and ancestry. Bone density in older life is directly dependent on bone density earlier in life and peak bone mass. The higher an individual's peak bone mass, the less likely they will suffer from osteoporosis later in life.

There are three main stages in the life cycle of bone: growth, consolidation and involution, according to Francis (2003). During growth, osteoblast function exceeds osteoclast resorption, in which 90 percent of the bone mass is deposited. When the epiphyses fuse, growth ends and consolidation is the phase in which the bone is fortified until peak bone mass is reached in the early or mid-thirties. Involution is then the stage when bone loss exceeds bone formation. Sex and age are the number one factors affecting bone density. Bone density decreases by about 0.3-0.5% per year for men and women after age 40. For women, the rate of loss increases to 2-3% per year following menopause and then levels out. Osteoporosis affects the trabecular and cortical bone differently. The rate is not the same for trabecular and cortical bone. Following menopause, women will lose approximately 15% of their cortical bone, whereas the trabecular bone loss is relatively constant throughout adult life. Trabecular bone can be built up again, but cortical bone loss is relatively irreversible. Overall, women will lose about 35% of their cortical bone and 50% of their trabecular bone after the age of 30. In general, the rate of loss in bone mineral density (BMD) is approximately 1% per year until the age of 65. The process is accelerated to 2% per year BMD lost for the five years following menopause in women (Zhang-Wong et al, 2002). "Overall, women lose 35-50

percent of trabecular and 25-30 percent of cortical bone mass with advancing age, whilst men lose 15-45 percent of trabecular and 5-15 percent of cortical bone" (Francis, 2003).

Exercise does increase bone mass, but more slowly than muscle mass is increased. Increased calcium intake, along with Vitamin D can maintain a healthy calcium balance in the elderly. However, calcium supplementation does not appear to have much effect on perimenopausal women's bone density. Ancestry plays a large role in bone density. Black women are less prone to osteoporosis than white women and tend to have much greater bone density throughout life. Body mass index also plays a role in bone density. Larger BMIs tend to be associated with greater bone density than smaller BMI (Gibson et al., 2004; Looker et al., 2006; Miyabara et al., 2007; Wheatley, 2005; Wu, 2007). Saitoglu et al (2007) found a more significant correlation with body typing. They discovered that endomorphic body types, defined as having a round body with fat and soft body structure, had greater bone mineral density of the spine, femoral neck and total femur. This trend is not observed in obese children, girls especially, and in institutionalized elderly males with little exercise (Goulding et al. 2002; Paniagua, 2006; Pollock et al., 2007).

Risk Factors for Osteoporosis

Osteoporosis is due to an imbalance of bone metabolism, with resorption exceeding new bone synthesis (Molina-Perez, *et al.*, 2000). As mentioned previously, there are many causes of this imbalance. If we eliminate age as a factor, we can explore the causes of secondary or accelerated osteoporosis more closely. Sex of the individual, genetic make-up, diet, body mass and activity patterns all play a significant role in bone

metabolism. Estrogen has been shown to decrease osteoclast bone resorption and increase osteoblast collagen synthesis. Women are four times more likely to develop osteoporosis than are men (Deltoff, et al., 1998), mostly due to the sharp decline in estrogen after menopause. Lifestyle factors contributing to osteopenia in young women include low body weight, low dairy consumption during childhood, use of the birth control shot Depo-Provera, excessive dieting and non-participation in high school sports (Turner, *et al.*, 2000). Extreme physical activity while young can help to increase peak bone mass and reduce a woman's chance of osteoporosis, unless she develops amenorrhea as a result (Gibson et al., 2004; Kelsey, 1989; Miyabara et al 2007). Female athletes in endurance or appearance based sports are more likely to develop early onset osteoporosis. One study showed that the bones of young female athletes would sometimes be equivalent to sixty, seventy, or eighty year old women. Again the main factors were excessive exercise, low body weight and amenorrhea. Thirty to forty percent of young female athletes were anemic due to low fat, low iron and high fiber diets (Ridout, 1999). Greater adolescent activity levels and the number of menstrual cycles following menarche was strongly correlated with bone mineral density (Gibson et al., 2004; Miyabara et al., 2007). Legroux-Gerot *et al.,* (1999) reported the probable causes of osteoporosis in a population of males. Old age was the definite cause in only 8.8% of the individuals. Renal tubule dysfunction was the likely cause in 12.5% of the individuals, 19.4% was glucocorticoid-induced, and 28.1% were due to multiple factors. In 22.5% of the cases, alcohol was the likely factor.

Because osteoporosis is a metabolic disease, diet plays a major role. Vitamin D affects calcium absorption, thus both are necessary for bone building and strength.

Fluoride in water has been shown to reduce rates of vertebral fracture, but only at the level of >2 ppm. Calcium intake by itself produces somewhat contradictory results. It retards the loss of cortical bone mass, but not trabecular. The influence of calcium intake is much less significant on bone mass than estrogen supplements. Inactivity greatly decreases bone density, especially from prolonged immobilization (Kelsey, 1989). The role of genetics in osteoporosis cannot be overlooked. White and Asian women are more prone to osteoporosis with differing fracture patterns. White females tend to have hip fractures, whereas Asian females tend to have spinal fractures. Blacks tend to have greater bone density at all ages, whether this is due to a genetic component, lifestyle or difference in Vitamin D metabolism remains to be seen (Kelsey, 1989).

Chapter 3. MATERIALS

This research would not be possible without access to the William M. Bass Donated Skeletal Collection from the Department of Anthropology at the University of Tennessee. This sample consists of modern human skeletons of more than five hundred known individuals. The collection was started in 1981 and consists of predominantly white American males with twentieth century birth years. The rate of donation has increased over recent years to approximately one hundred individuals per year. Demographic information is available for most individuals and includes stature, weight, age, sex and cause of death. Occasionally, donations will include data on occupation, chronic disease history and a photograph of the individual. Recent donations have more complete personal information than earlier years of the body donation program. Information on stature and weight was converted to metric data and calculated for body mass index (BMI = kg/m^2). Height and weight can either be self-reported, taken at the time of autopsy or an estimate. All estimates are removed from this analysis. Only individuals with height and weight information and only white males and females are included in this analysis to maintain adequate statistical sample size. There has been a demographic shift in BMI for donated individuals from the early years of the donation program to the present. The average BMI for all individuals donated (n=326) to the collection gradually increases from 23 in the 1980s, to 25 in the 1990s to BMI=29 (28 with the outlier removed) since the year two thousand (see Figure 3.1).

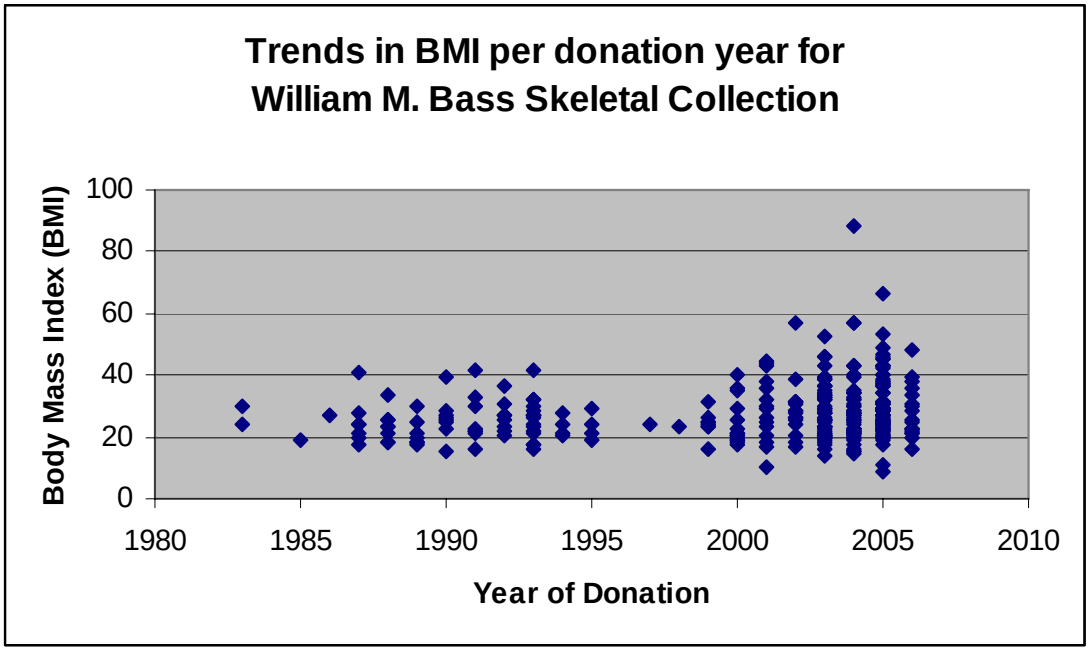

Figure 3.1. Temporal trends in BMI per donation year for the Bass Collection

The donated individuals decomposed naturally in the outdoor Anthropological Research Facility at the University of Tennessee. The remains were further cleaned in water (heated to less than 100 °C) to remove debris and any adhering soft tissue and then air-dried. This method may reduce as much as 10% of the bone density (Galloway et al., 1997), but all of the bones were processed in this same manner to maintain consistency. Some of the skeletal remains from the eighties were subsequently preserved with shellac, which may also have an effect on bone mineral density. This preservation method did not impede the creation of bone models from the CT scans.

Chapter 4. CROSS-SECTIONAL GEOMETRY

Introduction

Bone strength depends on three characteristics of bone: material properties, microstructure, total bone mass/volume and macrostructure (Ruff, 1981). The material properties include chemical composition and bone density. Microstructure of the bone is defined by the modeling and remodeling of Haversian systems. Macrostructure is a combination of geometric properties and trabecular orientation. This chapter will explore the macrostructure of bone, examining geometric properties of the human femur as it responds to load-bearing and body mass. Ledley et al. (1974) noted three decades ago that the only non-invasive method for reconstructing cross-sections sufficiently for biomechanical analysis was computerized tomographic (CT) scanning. The same is still true today with even better quality of images, faster scanning time and reduced cost. The resultant 3-D radiographs can be segmented into 3-D computer surface models that permit automated measurement. This enables automation of the analysis.

Computer Imaging and Analysis

Computerized tomography (CT), Magnetic Resonance and ultrasound are all types of cross-sectional tomography. They perform multiple two-dimensional slices of three-dimensional objects. For a CT scan, the computer mathematically reconstructs the cross-sectional image from the X-ray measurement of thin slices. Changes due to absorption and scatter as the narrow X-ray beam passes through the subject are interpreted by detectors on the opposite side of the subject. As the tube rotates around

the subject, this process is repeated many times automatically. The voxel dimensions, or pixels to form a volume measurement, are determined by an algorithm chosen, between one and ten millimeters in resolution. This type of scan is extremely rapid and produces superior detail compared to magnetic resonance (Brant, 1994). Pietrusewsky (2000) claimed that for anthropology, "the discipline's most notable contributions to science" are anthropometry (measurement of the living) and osteometry (measurement of the skeleton). This research strives to advance anthropometric morphometric techniques in the postcranial skeleton.

Quantifying bone size and shape remains a fundamental task for many anthropological research endeavors, including questions of human variation, allometry, recognizing secular trends, reconstructing past activity patterns as well as numerous other bioarchaeological and forensic applications. (Jantz et al.1984, King et al., 1998; Krogman and Iscan, 1986; Meadows et al., 1995; Ruff, et al., 1991; Trotter and Gleser, 1952). Geometric morphometric techniques are replacing traditional linear measurement in much of anthropology as the preferred method of capturing bone shape and size. The requirement of corresponding landmarks, however, has made the application of these techniques to the post-crania difficult since most bones lack sufficient well-defined landmarks.

Computed tomography (CT) scanning provides data potentially suitable for the application of geometric morphometric techniques to post-cranial elements. In addition, the advantages of CT data are numerous and include: rapid data acquisition, non-destructive, provides high resolution three-dimensional data of both internal and external bone surfaces and information on bone density. The potential for CT data has been

recognized for several decades in anthropology (Lovejoy et al., 1976; Ruff and Leo,1986), although its use has mainly been limited to cross-sectional geometry and costs are often prohibitive for large scale application.

Materials and Methods

In conjunction with a team of biomedical engineers and anthropologists, CT scans were conducted of more than five hundred individuals from the William M. Bass Skeletal Collection in the Department of Anthropology at the University of Tennessee. We developed a methodology for rapidly collecting CT data of skeletal elements, which reduced later image processing time. In addition, our team established a method to make these suitable for geometric morphometric techniques and created a statistical atlas of the skeleton. For this part of the study, a subset of those skeletons, a total of 110 white males and 59 white females, were included. Only those individuals in the sample with associated body mass information were selected in this part of the analysis. Skeletons too fragile for transportation, were excluded and not CT scanned.

CT Data Collection

To facilitate data acquisition we developed a system that permitted rapid data collection. Six identical sets of two boxes (one 125cm x 32cm x 3cm the other 150cm x 22cm x 5cm) were built from foam core board. Each box was lined with low density polyurethane foam with an outline drawn for each bone. I made a slice down the center of strip of foam in which to place the vertebral spinous processes in order. All foam elements were glued into position in the boxes. Each set of two boxes was large enough to hold the skeletal elements of one large individual. All bones were positioned so that

they neither touched another bone nor the foam core board. We scanned the following elements for each individual: cranium, mandible, all vertebrae, sacrum, os coxae, scapulae, clavicles, humeri, radii, ulnae, femora, tibiae, fibulae, tali, calcanea, and metatarsals (Figure 4.1). We standardized the positioning of the boxes in the CT scanner by strapping a piece of plywood to the scanner table. The plywood had eight dowels that were used as reference markers to maintain the same position of the boxes in each scan. All individuals were scanned at The University of Tennessee Medical Center Outpatient Diagnostic Center. Scanning was conducted using a GE Lightspeed 16 slice computed tomography scanner (Figure 4.2).

CT Specifications

- GE Lightspeed 16 Slice computed tomography scanner: Parameters

    Table – 1.5 m length

    2. Mass – 150 at .8 seconds
    3. FOV – 32 cm
    4. Resolution - .625 mm slices
    5. 100 KV
    6. Use Bone Algorithm 512/512 mm

Figure 4.1. Orientation of skeletons in the scanning boxes

Figure 4.2. Aligning boxes for scanning

Image Segmentation and Model Creation

Segmentation is the process of selecting regions from three-dimensional images and separate objects based on threshold values. We used the commercially available program Amira to segment the high resolution DICOM images. There are two types of image segmentation: manual and automatic.

For manual segmentation, the researcher opens a series of DICOM images in the program Amira . Starting at one end of the bone, the researcher opens a single DICOM slice. The grayscale value of the region of interest is selected, using maximum and minimum thresholds values as a criterion. This shades in the area of interest. The voxel values correspond to the different densities of the object scanned. Cortical bone is dense and appears very light gray to white. Trabecular bone appears as a range of darker gray voxel values. In the program Amira, the entire shaded area can be selected and enclosed in a colored outline. This area of interest is termed a "label." The researcher then continues manual segmentation down several slices of the bone from one epiphysis. The researcher then moves to the opposite end of the bone and manually segments the image. Once both proximal and distal slices are given the same label, a simple click on the same gray value anywhere in between will automatically detect the entire bone. It is necessary to check through each slice to verify that the entire bone was accurately selected. Figure 4.3 depicts manual segmentation of a femur and a vertebra in relation to an original DICOM slice.

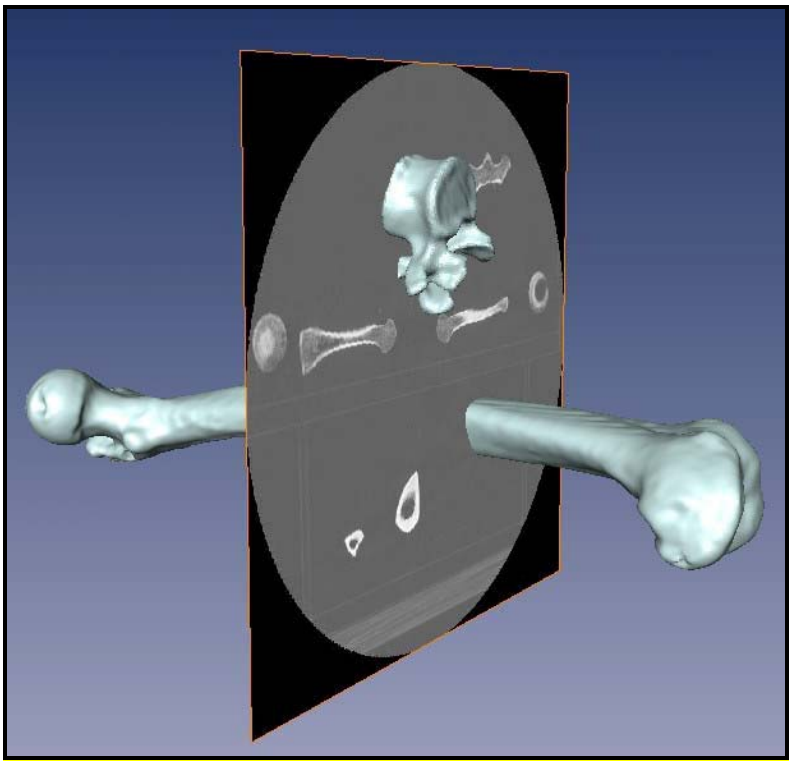

Figure 4.3. Example of manual segmentation in relation to a DICOM slice

The medullary canal is segmented separately from the subperiosteal surface. This is necessary because the endosteal surface of the bone has some trabecular bone and thus has lower voxel values. After selecting the entire bone as the region of interest, the software then interpolates the information between each slice and a surface model is generated. The surface model for the femur is made up of a 3-dimensional triangular mesh consisting of 800,000 to 1,000,000 data points, after smoothing algorithms are applied (see Figure 4.4). The smoothing reduces the amount of information to facilitate the atlas creation.

Automatic segmentation (see Figure 4.5) follows a similar format. The main distinction is that the maximum and minimum thresholds for every slice are set simultaneously. This saves a great deal of time, but renders poorer models. If two bones

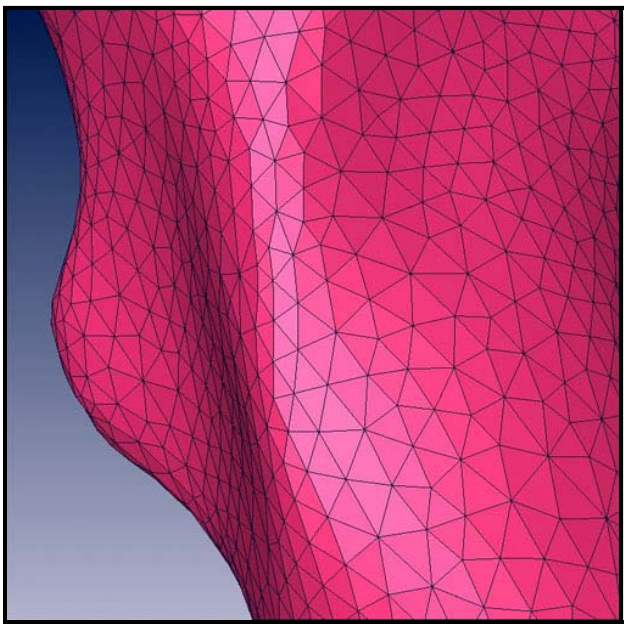

Figure 4.4. Close-up image of 3D triangular mesh

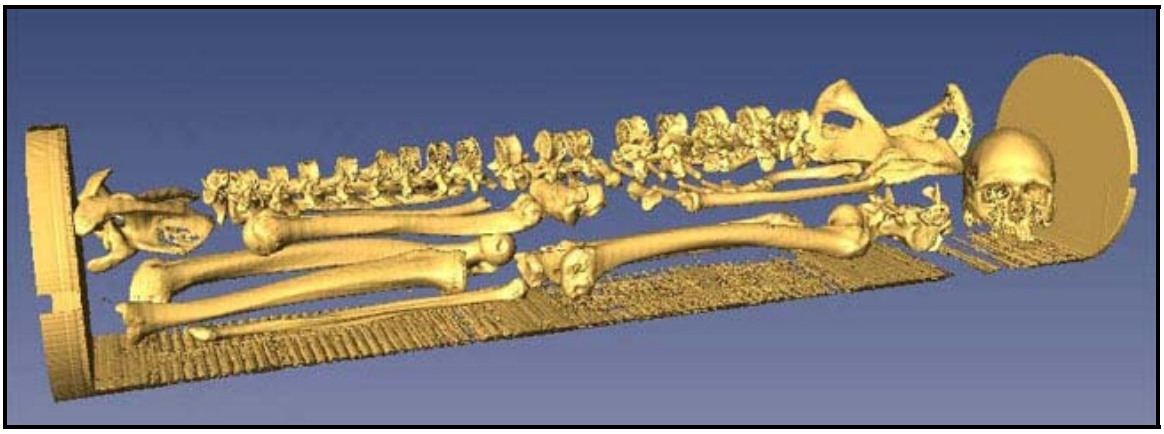

Figure 4.5. An example of automatic segmentation

inadvertently touch during the scan, the bones will be recognized as a single label. This method does not recognize the subtle differences in gray scale values for the cortical and trabecular bone, which also results in poorer models.

Bone Atlas

The next phase of the research was the creation of a statistical shape atlas of each bone. Multiple femur models are required to create a shape atlas. One original model serves as a template. The number of points for each model is reduced to 7,500 evenly distributed points. An atlas is a database of bone models concisely representing a single bone element. An atlas can be used to examine variation among human populations. The atlas can be useful for teaching purposes or for anatomical simulation. It could even be used to facilitate better automatic segmentation. Anthropology could benefit greatly from the statistical bone atlas to recognize subtle variations between different populations. This method could be useful to forensic anthropology, paleoanthropology, and bioarchaeology. Fragmentary bones could be reconstructed to estimate full length and width measures. The team with which I have worked has been able to discriminate sex with the femur using canonical variates analysis at 95.4% accuracy and the patella with 93.5% accuracy (Mahfouz et al., 2007a and 2007b). For my project, the atlas has been used to automatically recreate cross-sections for biomechanical analysis.

To create the atlas, linear transformations are applied to align the template femur to a second femur model (Mahfouz et al., 2006a and 2006b). These transformations include translation, rotation, scale, and shear. Once all possible transformations are complete, a nonlinear deformation algorithm adjusts the template until the differences

between the two models fall below a certain value. The 7,500 points of the template are projected onto the new model, discarding the original second femur model. Now both bones have the same number of points and triangular faces. The template is updated by averaging the differences between the original template and the new bone. This is repeated for every femoral model created for each sex. The result is a number of femoral models with the same number of points and faces in approximately the same position. This allows for point-to-point comparisons between femur models and the creation of an average femur for geometric morphometric comparisons. Principal components analysis (PCA) is used to describe the shape differences of the atlas models. The first principal component is able to capture 96% of the variation, for which scale has already been removed.

Cross-sectional Geometry

Complete femur models included both external surfaces and a separate model of the internal medullary canal surface. Each femur atlas model was placed in separate folders with corresponding folders containing the aligned canal models. The canals and atlas femora were run simultaneously through a program designed by my colleague in biomedical engineering. The MATLAB program was specifically designed for this project and is based on the program SLICE created by Nagurka and Hayes (1980). The femora were aligned according to several reference axes for measurement. These reference axes correspond to those used in previous research (Ruff, 1981). Landmarks were established for various homologous points (i.e. points of articulation, maximum distance points, etc). The landmarks were chosen based on geometric shape parameters

that would not vary from one individual to the next. All of the left bones were automatically mirrored when added to the bone atlas to simplify analysis. The reference axes were based on the centers of articulations at the epiphyses. The reference axes allow the x, y and z coordinates to be easily determined. As mentioned in Chapter 2, the femur was modeled as an engineering beam. It is difficult to assess the reference axis for the femur in comparison to the tibia due to the complex curvature of the femoral shaft in the sagittal plane and lack of identifiable centers of articulation. The femur was divided into two segments when establishing the reference axes, the femoral neck and the diaphysis. The neck reference axis was a longitudinal axis through the center of the neck to the center of the head. There are two potential reference axes for the long axis of the shaft. One axis follows the center of the curved shaft. The second and more 'ideal' axis corresponds to the straight axis from the midpoint of the distal articulation to the cervical axis at the proximal end of the shaft. When laying the femur on the table, dorsal side down, the diaphysis is not parallel to the table. An ideal axis is established by raising the proximal end approximately 1-2 cm. This method has become standard in this research (Ruff, 1981; Gilbert, 1976). This serves as the z axis of the femur, with the more positive z being proximal. The medio-lateral direction served as the x axis with the more positive x being lateral. The y axis corresponds to the antero-posterior (a-p) direction being more positive anteriorly. The xz plane refers to the frontal plane, the yz to the sagittal plane and the xy to the transverse plane. The middle sixty percent is typically used in this type of analysis because the distal ends of the femoral shaft consist of a significant amount of trabecular bone changing the macro-structural properties of the bone. Transverse cross-sections were analyzed at five locations perpendicular to the femoral shaft: 80%, 65%,

50%, 35% and 20%. The 80% position is the most proximal cross-section and the 20% the most distal (see figure 4.6).

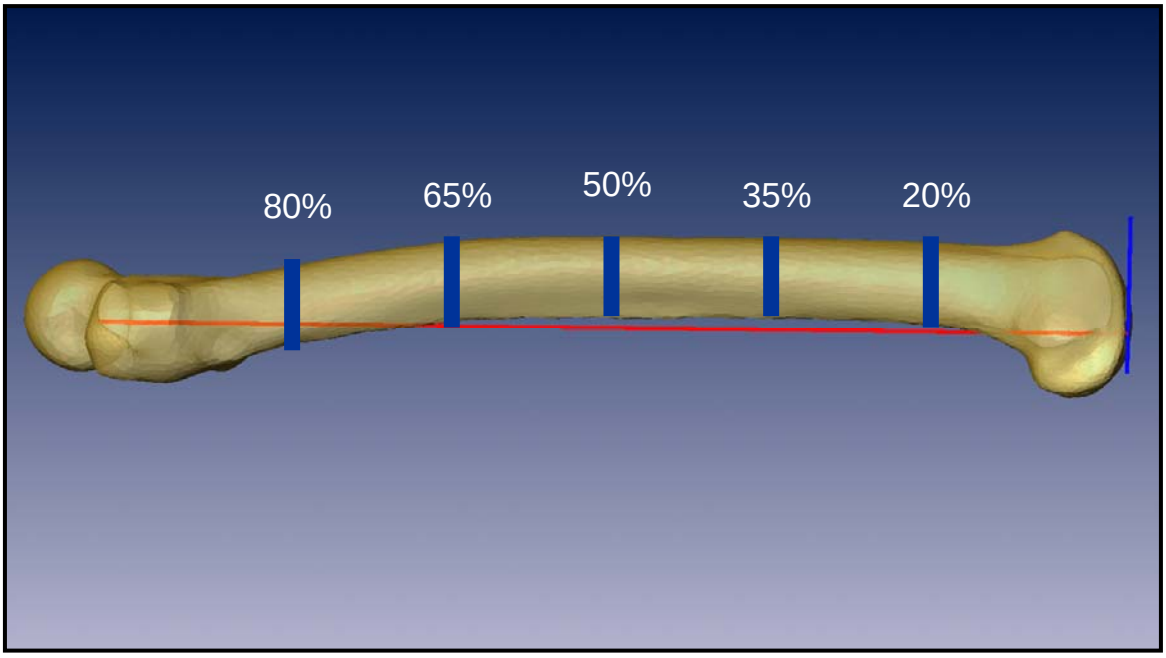

Figure 4.6. Biomechanical Atlas with five cross-sections

In addition to these cross sections, the angles between the axes were calculated. I was particularly interested to discover if any relationship exists between the collo-diaphyseal (neck) angle and body mass and whether extreme obesity might decrease that angle. Comparable to SLICE (Nagurka and Hayes, 1980), this program explored the geometric parameters of the femoral shaft. In chapter two, I explained engineering beam theory applied to the femoral shaft. The moments of inertia are length measures from the area of the centroid to the outer perimeter of the bone. The second moment of inertia (Ix) in the medilateral direction is perpendicular to the Iy direction, which runs antero-posteriorly. The second moments of area about the principal axes are the directions of maximum and minimum bending strength, with the greatest distance from the centroid

(Imax), which is perpendicular to the minimum second moment of inertia (Imin). By taking these principal 2nd moments and dividing the Imax by the Imin, we arrive at a shape index, in which size has been removed. This same equation can be applied to the 2nd moments of inertia in the AP and ML directions. Several researchers suggest that this shape parameter reflects activity patterns (Larsen, 1997; Lovejoy et al., 1976; Ruff 1987). If the shaft is elongated in the AP direction, this then reflects activities of more deep bending at the knee and hip. If the index is close to one, this would indicate a more circular cross section and less deep bending. If this is true, it can be useful for applying to body mass estimation. Previous research shows that obese individuals have a very different pattern of locomotion. From the clinical and biomechanical analysis of gait patterns in obesity, a more medio-lateral saunter is common, less bending of the knee and greater compressive loads. These might suggest that we would find cross-sections that are more circular in obese individuals with greater surface area, but not necessarily greater bending strength. In addition, we might find more medio-lateral flattening in the proximal shaft due to this sauntering gait in obesity. A list of the cross-sectional measurements is given below. Images of the computer models and axes is exhibited below in Figures 4.7, 4.8 and 4.9. The total list of measurements taken and definitions of the statistical codes can be found in the appendix (Tables A.1 and A2).

Cross-sectional Measurements

a. Total cross-sectional area

b. Cross-sectional area of cortical bone

c. Cross-sectional area of medullary canal

d. 2^{nd} moments of inertia (area) Ix and Iy perpendicular through centroid – Ix for mediolateral direction, Iy for anteroposterior direction

e. product of inertia about x and y axes translated to centroid

f. second moments of area about principal axes

g. angle between translated x and y axes and principal axes

h. maximum distance along major axis from area of centroid to outer perimeter

i. maximum distance along minor axis from area of centroid to outer perimeter

j. polar moment of area = J or Ip – approximating torsional rigidity

k. centroid – center of cortical area

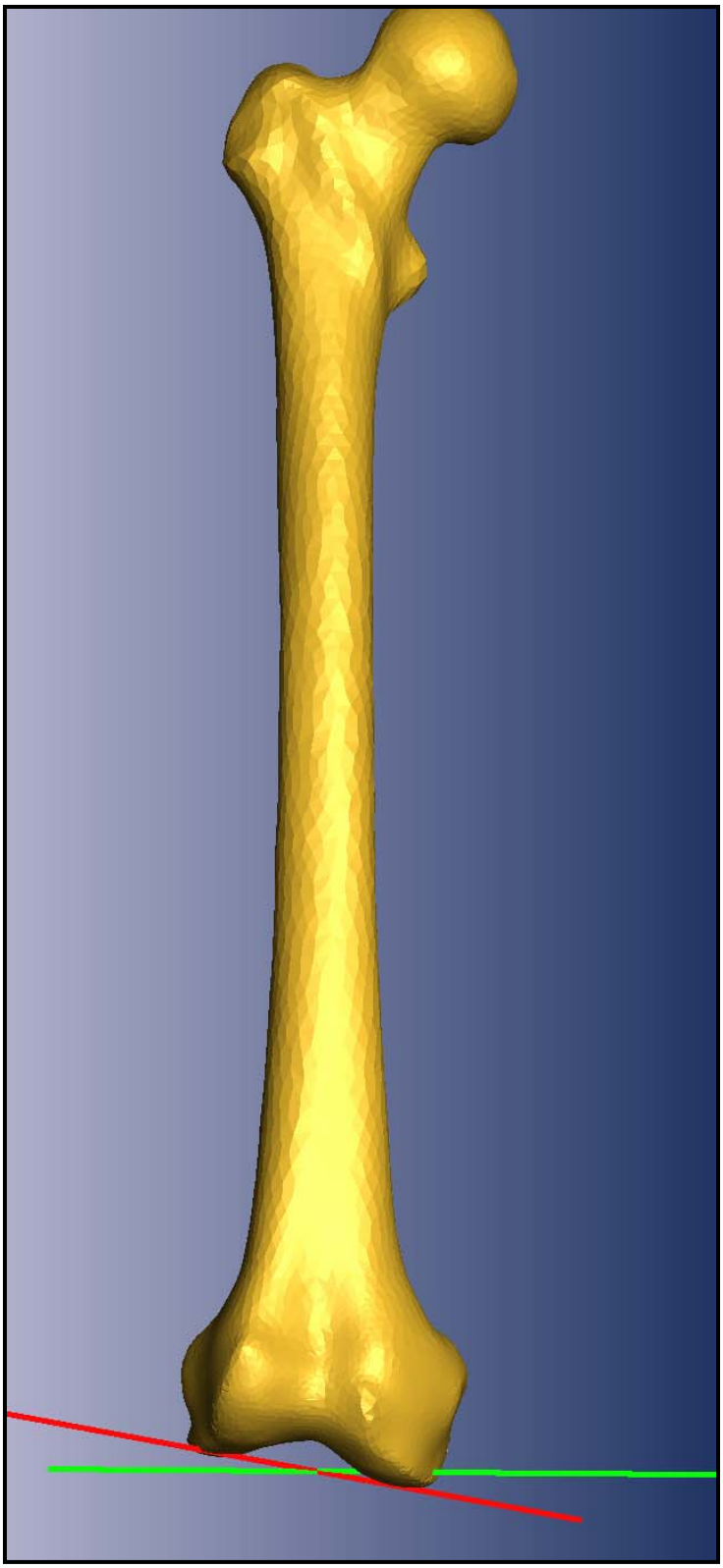

Figure 4.7. Average Point Between Distal Condyles

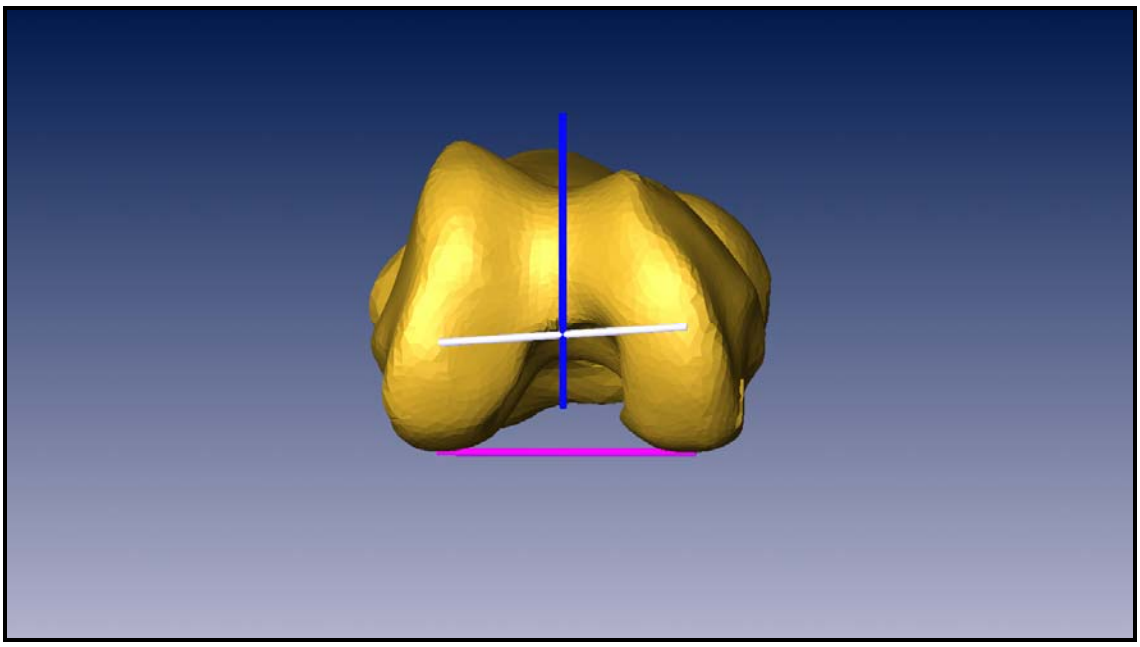

Figure 4.8. Proximal end with Y axis in blue and X axis in white

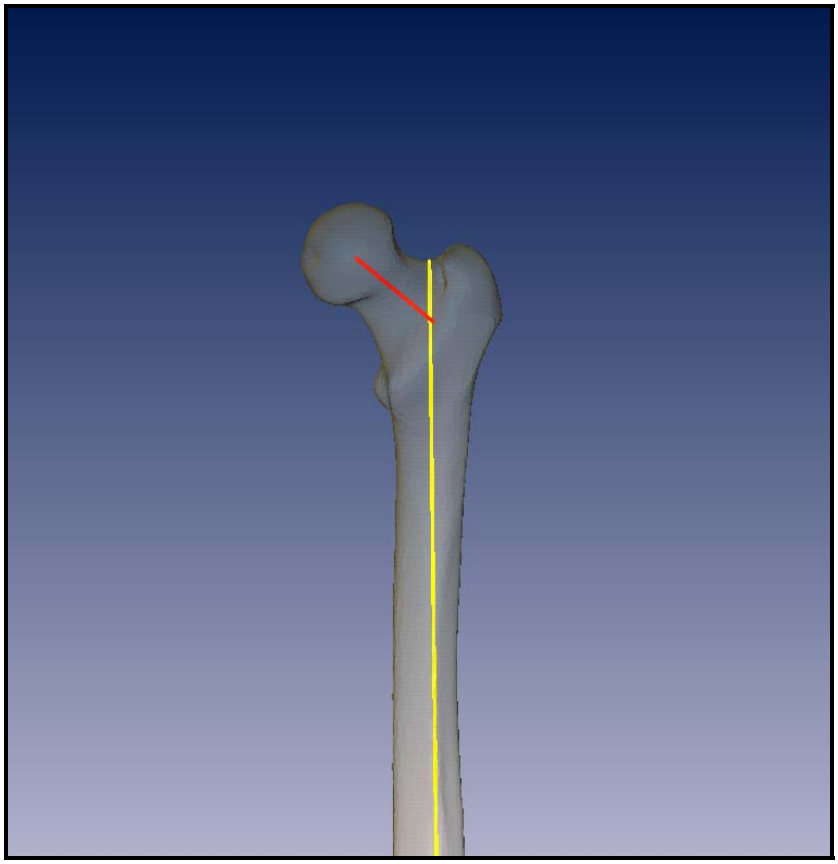

Figure 4.9. Collo-Diaphyseal (Neck) Angle

The data were analyzed using the statistical package NCSS 1997 (Number Cruncher Statistical Systems, Kaysville, UT). Correlation matrices were run comparing all variables to age, height, weight and BMI. The shape indices created for Iy/Ix and Imax/Imin were included in these correlations. To develop the best multiple regression model, I ran a variable selection using Principal Variables Analysis (PVA). PCA is not useful for data reduction, but by combining multivariate methods of PCA and McHenry's variable selection for PVA (McHenry, 1978), this can sometimes improve the variable selection. To begin PVA, PCA is run to find the highest eigenvalues and store the first few factor scores. The factor scores are then multiplied by the square root of the eigenvalues. The final step is to run a multivariate regression using McHenry's algorithm for variable selection with the transformed factors as the dependent. This technique can help select the best variables for the multiple regression. Unfortunately, this method was not any better than running McHenry's algorithm alone with weight or BMI as the dependent. Robust multiple regression was run with weight (kg) as the dependent variable. Missing values were ignored.

Results

Positive correlations with height and maximum femur length and biomechanical femur length are relatively strong for females (r = 0.61) and males (r = .59) as expected. None of the cross-sectional geometric length and shape variables correlated with age above r =.5. All correlations were typically higher for weight than for BMI for both males and females. Variables showing strong relationships in both males and in females were cortical area at 80%, torsional strength at different locations and length measurements of maximum and minimum moments of inertia along the shaft. For females the greatest correlations are at proximal cortical area (r = .62) and the minimum moment of inertia at the proximal shaft (r = .59) (see Table 4.1 below). For males, the cortical area at 80% was also a strong correlation (r = .57), but the highest was from the principal moment of inertia at the midshaft, which is a shape parameter (see Table 4.2 below).

Table 4.1. Correlations for Female Cross-sectional Variables and Weight or BMI

Cross-sectional Variable	Weight	BMI (kg/m^2)
Centroid to external bone perimeter along major axis 35%	0.497	0.408
Centroid to external bone perimeter along major axis 65%	0.500	0.413
Centroid to external bone perimeter along major axis 80%	0.502	0.438
Cortical Area 35%	0.575	0.508
Imin 35%	0.561	0.461
J 35%	0.537	0.431
Imax 50%	0.538	0.444
Imin 50%	0.571	0.481
J 50%	0.584	0.488
Total Area 65%	0.500	0.401
Imin 65%	0.575	0.477
J 65%	0.557	0.459
Cortical Area 80%	0.618	0.554
Imin 80%	0.588	0.504
J 80%	0.537	0.432

Table 4.2. Correlations for Male Cross-sectional Variables and Weight or BMI

Cross-sectional Variable	Weight	BMI (kg/m^2)
Centroid to external bone perimeter along minor axis 50%	0.495	0.430
Iy – 2nd Moment of Inertia 20%	0.499	0.441
Imin 20%	0.562	0.495
J 20%	0.537	0.464
Imax 35%	0.503	0.422
J 35%	0.501	0.420
Imax 50%	0.582	0.509
Imin 50%	0.512	0.435
J 50%	0.561	0.483
Cortical Area 80%	0.568	0.522
Imin 80%	0.502	0.443

The multiple regression equations combining only the selected cross-sectional variables are not extremely strong for males or females. For females, the best equation included the percentage of medullary canal area to bone area in the most proximal slice, the location of the centroid at the midshaft and the radius of gyration Kmin, which is a transformation of the Imin at the most distal shaft (Kmin = √(Imin/Area)). The R-squared (0.62) dropped to 0.25 with the predicted R-squared or Press statistic. The predicted R-squared or Press statistic is calculated by systematically removing each variable and recalculating the regression for the removed variable. Thus, the equation only works well for the current sample. The square root of mean squared error is high at 14.56 kg (see output 4.1 below). When I removed Kmin, the equation was significant for each independent variable, but the R-squared fell to .54, the Predicted R-squared fell to .32 and the square root of mean squared error fell to 17.0 kg (see output 4.2 and 4.3 below). The model for males was even less predictive. The variables selected for males were minimum moment of inertia at proximal shaft, the area of the centroid xy at the 20% slice, the torsional rigidity J at midshaft and 80% and the maximum radius of gyration at the 65% slice. The R-squared value (.47) was not very high with a high square root of means squared error of 17.5 kg. The R-squared Press was insignificant at 0.1. There were too many variables involved in this equation and the potential for collinearity between variables was consequently high.

Output 4.1. Multiple Regression Equations for Females

Run Summary Section

Parameter	Value	Parameter	Value
Dependent Variable	Weight_kg	Rows Processed	149
Number Ind. Variables	3	Rows Filtered Out	90
Weight Variable	None	Rows with X's Missing	1
R2	0.6178	Rows with Weight Missing	0
Adj R2	0.5953	Rows with Y Missing	3
Coefficient of Variation	0.2002	Rows Used in Estimation	55
Mean Square Error	211.9795	Sum of Weights	48.301
Square Root of MSE	14.55952	Completion Status	Normal
Ave Abs Pct Error	21.800		

Regression Equation Section

Independent Variable	Regression Coefficient b(i)	Standard Error Sb(i)	T-Value to test H0:B(i)=0	Prob Level	Reject H0 at 5%?	Power of Test at 5%
Intercept	6.4725	27.8782	0.232	0.8173	No	0.0560
IM_Percentage_80	-126.9853	32.5179	-3.905	0.0003	Yes	0.9693
Ivv_50per	25.4906	4.6281	5.508	0.0000	Yes	0.9997
Kmin_20	52.3891	23.1527	2.263	0.0279	Yes	0.6026

Estimated Model

6.473-126.985*IM_Percentage_80+ 25.491*Ivv_50per+ 52.389*Kmin_20

PRESS Section

Parameter	From PRESS Residuals	From Regular Residuals
Sum of Squared Residuals	21304.95	10810.95
Sum of |Residuals|	840.4354	788.8312
R2	0.2468	0.6178

Output 4.2. Multiple Regression Equations for Females

Run Summary Section

Parameter	Value	Parameter	Value
Dependent Variable	Weight_kg	Rows Processed	149
Number Ind. Variables	2	Rows Filtered Out	90
Weight Variable	None	Rows with X's Missing	1
R2	0.5414	Rows with Weight Missing	0
Adj R2	0.5237	Rows with Y Missing	3
Coefficient of Variation	0.2332	Rows Used in Estimation	55
Mean Square Error	288.6567	Sum of Weights	52.049
Square Root of MSE	16.9899	Completion Status	Normal
Ave Abs Pct Error	21.711		

Regression Equation Section

Independent Variable	Regression Coefficient b(i)	Standard Error Sb(i)	T-Value to test H0:B(i)=0	Prob Level	Reject H0 at 5%?	Power of Test at 5%
Intercept	57.8450	17.0180	3.399	0.0013	Yes	0.9155
IM_Percentage_80	-132.9370	36.7655	-3.616	0.0007	Yes	0.9439
Ivv_50per	31.0269	4.6086	6.732	0.0000	Yes	1.0000

Estimated Model

57.845-132.937*IM_Percentage_80+ 31.027*Ivv_50per

PRESS Section

Parameter	From PRESS Residuals	From Regular Residuals
Sum of Squared Residuals	22333.7	15010.15
Sum of |Residuals|	857.7637	811.0504
R2	0.3176	0.5414

Output 4.3. Multiple Regression Equations for Males

Run Summary Section

Parameter	Value	Parameter	Value
Dependent Variable	Weight_kg	Rows Processed	149
Number Ind. Variables	5	Rows Filtered Out	59
Weight Variable	None	Rows with X's Missing	0
R2	0.4676	Rows with Weight Missing	0
Adj R2	0.4330	Rows with Y Missing	7
Coefficient of Variation	0.2173	Rows Used in Estimation	83
Mean Square Error	306.5384	Sum of Weights	75.556
Square Root of MSE	17.50824	Completion Status	Normal
Ave Abs Pct Error	19.095		

Regression Equation Section

Independent Variable	Regression Coefficient b(i)	Standard Error Sb(i)	T-Value to test H0:B(i)=0	Prob Level	Reject H0 at 5%?	Power of Test at 5%
Intercept	71.8589	18.3894	3.908	0.0002	Yes	0.9712
I2_80per	30.9978	5.6294	5.506	0.0000	Yes	0.9997
Iuv_20per	21.8227	5.5275	3.948	0.0002	Yes	0.9737
J_50per	8.0884	2.3816	3.396	0.0011	Yes	0.9183
J_80per_	-16.3706	4.1166	-3.977	0.0002	Yes	0.9754
Kmax_65	-88.6091	30.8246	-2.875	0.0052	Yes	0.8102

Estimated Model

71.86+ 30.998*I2_80per+ 21.823*Iuv_20per+ 8.088*J_50per-16.372*J_80per_-88.609*Kmax_65

PRESS Section

Parameter	From PRESS Residuals	From Regular Residuals
Sum of Squared Residuals	43771.78	23603.46
Sum of |Residuals|	1481.628	1352.001
R2	0.0126	0.4676

Discussion

Though there are some strong individual correlations with body mass in both males and females, the multiple regression equations using cross-sectional geometry alone are not useful as predictive models. Three variables repeat in both males and females: cross-sectional area at 80%, torsional rigidity at several locations and the moments of inertia in various directions. The shape indices (Imax/Imin, Iy/Ix, and Kmax/Kmin) do not show any clear relationship with body mass, but may still in fact reflect activity. The variable that shows the strongest unilinear relationship is cross-sectional area at the proximal section. This differs from Ruff, Scott, and Liu (1991) who found a strong correlation with the midshaft area and body mass. Finding a strong correlation at the proximal midshaft may reflect the change in locomotion patterns. There does not appear to be a clear correlation between the canal area and body mass, as was predicted with endosteal apposition in obese individuals. Though these equations do not show any promise in this chapter, in the next chapter, I combine the results in multiple regression equations with bone mineral density and dramatically improve the predictability of the models.

Chapter 5. BONE DENSITY

Introduction

Forensic Anthropologists have the skills to create a biological profile from just a few scattered human remains. This toolkit includes the ability to estimate age, sex, ancestry, stature, and recognize different patterns of trauma. The ability to estimate body mass from the human skeleton has received considerable attention, but previous research has failed to take into account extremes of body mass. To consider body mass, we must first explore load bearing and bone strength. Bone strength is defined by two main features: bone quality and biomechanical properties. Long bone cross-sectional geometry is used to study biomechanical properties. Bone density and quality are often used synonymously, but micro-structure also reflects bone quality. Bone density is a reflection of age, sex, genetics, lifetime activity levels, nutrition, and body mass. The previous chapter explored the relationship of cross-sectional geometry and body mass. In this chapter, I will turn my focus to bone quality to explore the relationship of body mass and bone mineral density of the proximal femur using Dual Energy X-ray Absorptiometry (DEXA).

Many recent articles have recognized the strong relationship between bone density and body mass, without recognizing the common theme. Overweight menopausal women tend to have strong bones compared to women who are thin (Heaney et al., 1997; Reid, 2002, 2007, Wheatley, 2005). HIV patients tend to have low bone density, in addition to being relatively thin. Anorexia Nervosa in females is associated with low bone density, regardless of heavy athletic training (Gibson et al., 2004). One

researcher mentions the ability to prevent osteoporosis by increasing body weight (Reid, 2007). Many mechanisms have been suggested for this relationship. Increased estrogens stores in body fat can help increase osteoblast action. Hyperinsulinemia can cause the overproduction of hormones in the ovaries, reducing osteoclast action, while simultaneously causing an increase in calcitonin (DiMonaco et al., 2007; Reid, 2007). Regardless of the mechanism, there exists a strong relationship between bone density and body mass.

Certain factors may confound this relationship. Age plays a role when considering menopause in older females. Fortunately, this factor exaggerates the relationship. Bone density increases in obese children, but not sufficiently for increased body mass (Bianchi, 2007; Goulding et al., 2002; Pollock et al., 2007). Non-ambulatory status dramatically reduces bone density regardless of body mass (Paniagua, 2006). Astronauts who spend prolonged periods in zero gravity experience decreased bone density (Traon et al., 2007).

Bones must be strong enough to support the weight of an ambulatory individual, or otherwise fail, and hence fracture. As individuals become obese or emaciated, this relationship becomes exaggerated. The goal of this experiment is to test the hypothesis that body mass will correlate well enough with bone mineral density in order to estimate the body mass of unidentified human remains. This research combines both density and biomechanical properties to create the best predictive model for estimating body mass from the human skeleton. Dual energy X-ray absorptiometry (DEXA) is a simple and inexpensive means of establishing bone mineral content (BMC) and areal bone mineral density (BMD = BMC/area) at different regions of the body. This particular analysis

examines the BMD of the proximal femur using standard DEXA measures: total BMD, BMD of the greater trochanter, BMD of Ward's triangle and BMD of the femoral shaft in comparison to reported body weight and calculated body mass index (BMI = weight divided by height squared = kg/m^2). Ward's triangle is a triangular shaped area of low density in the femoral neck, but is typically disregarded by clinicians for osteoporosis risk.

A similar research project to estimate body mass from bone density was published by Wheatley (2005). This researcher found a significantly strong correlation of body mass to bone density ($R^2 = .49$), but felt the correlations were not strong enough for forensic applications. Wheatley suggested that future attempts should account for activity patterns. For this reason, I will introduce briefly my work with cross-sectional geometry as a way to account for activity patterns or simply, bone shape. There are multiple applications for bone density scans. Clinically, bone density scans help predict osteoporotic fracture. For bioarchaeology, bone density can be used to compare the health and activity of past populations to modern living humans. Obesity has become a global problem, increasingly so in juveniles. As the percentage of obese individuals increase in the overall population, so will their representation in forensic cases. Bone density analysis could be useful for body mass estimation to help individuate human skeletal remains.

The three goals for this research project are to first corroborate previous research that bone density indeed correlates well with the body mass. The aim is to explore the relationship of bone density in different regions of the proximal femur to body weight and body mass to determine the best predictive model. The second goal is to combine the

density and cross-sectional variables to develop a comprehensive regression formula. Finally, the hope is that this will lead to body mass estimation regression formula to be used by other researchers.

There are four ways to clinically determine bone density: Dual Energy X-ray Absorptiometry (DEXA), Quantitative Computed Tomography (QCT), Peripheral Quantitative Computed Tomography (pQCT) and Ultrasound. The advantages of DEXA are that it looks at integral bone mass and areal density, is relatively low radiation, so it is not detrimental to the patient and it is not limited to the periphery of the bone. DEXA is relatively sensitive to subtle changes in bone density and body composition (the proportion of fat and lean tissue mass). The disadvantages of DEXA are that it does not determine volumetric density, it provides only a summary measure of density across a scan path. It inaccurately assumes a cylindrical cross-section and it is unable to distinguish trabeculae from cortex. DEXA, however, is commonly used for bone density calculation and has become the gold standard for living populations. Like ultrasound, DEXA provides both T and Z scores for quickly diagnosing osteoporosis. The T-score compares the subject to the optimal bone density of a young healthy individual. The Z-score compares the subject's density to sex and age-matched individuals. If the T-score falls below 2.5 standard deviations, the individual is diagnosed with osteoporosis.

Methods

This research focuses on the proximal femur of a sample of skeletal remains with twentieth century birth years from the William M. Bass Donated Skeletal Collection at

the University of Tennessee. The sample consists of 34 white females between the ages 32-91 (mean = 62) and 35 white males between the ages of 34 and 65 (mean = 52).

Height and weight data was available for all individuals to determine the body mass index (BMI)(kg/m^2) (Figure 5.1). All skeletons decomposed naturally at the Anthropology Research Facility. Soft-tissue was removed from the femora and the bones simmered in a large pot of water until clean. This process can reduce the bone density by up to 10% according to Galloway et al. (1997), but this process was consistent for all femora in this study. Body mass categories of emaciated (BMI<17.9), normal weight (18<BMI<24.9), overweight (25<BMI<29.9), obese (30<BMI<39.9) and morbidly obese (BMI>40) are designated by the World Health Organization standards. My categories are consistent, except for collapsing overweight individuals into the average weight category. The logic for this is that my sample is significantly older than the normal population. It

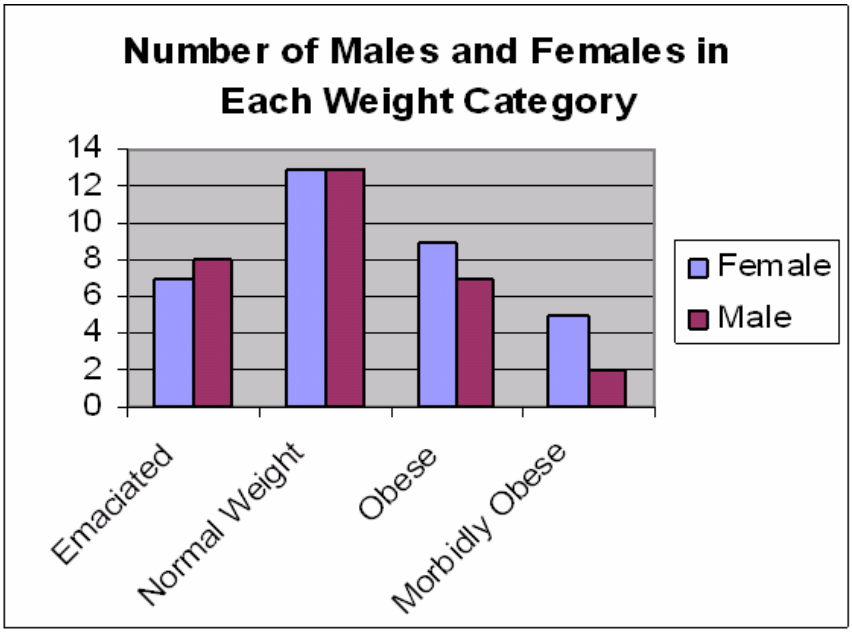

Figure 5.1. Histogram of the number of females in each BMI category

has recently been suggested that a higher BMI might be beneficial for older individuals to be considered healthy. This would raise the healthy range from 25 up to 28 for the elderly population. This may make any of the findings in this part of the study more conservative.

To conduct the density scans, each dry femur was placed in a plastic container 65 cm long, 14 cm tall and 11 cm wide. The container is designed as a planter box, but conveniently accommodates any size of femur. A two cm thick cube of low-density foam was placed under the lesser trochanter to make the shaft approximately parallel to the table surface. Both distal condyles were set directly on the bottom of the box. Leveling the femur in this way approximates anatomical position (see Figure 5.2). In this study, we did not try to rotate the proximal femur to more accurately represent anatomical position. As a result, the lesser trochanter is visible in the density scans, which would not be the case in living individuals.

Figure 5.2. DEXA scanning setup with "leveled femur"

The bone was placed with the posterior side down on the bottom of the plastic container and the anterior side facing up. The box was filled with dry white rice to a depth of approximately 12 cm over the proximal end of the bone only. The rice served as a human soft-tissue density equivalent for the DEXA scans, as per GE, the manufacturer of the DEXA Lunar scanner (see Figure 5.3). No cover was placed on the plastic container. The box was positioned on the table so that the femur was in approximate anatomical position, as if a patient were laying on the table. In this way, the machine was fooled to believe a patient was lying on the table, so as to be able to use the standard DEXA software. The arm of the machine was brought to a level just superior to midshaft. The areas of interest were manually selected on the computer by moving the rectangular field of view over the femoral neck. Two triangular fields of view were placed over the greater and lesser trochanters. Standard measurements of bone mineral density (BMD)(g/cm2) were calculated automatically for the femoral neck, Wards triangle, the greater trochanter, proximal shaft and total BMD.

Figure 5.3. DEXA scanning of femur with rice as soft-tissue equivalent

The DEXA scanner used in this study is from the Department of Exercise, Sport and Leisure Studies at the University of Tennessee. The user interface for the DEXA machine is designed to recognize living individuals, so the age is calculated by entering the individual's birthdate. To compensate for this, we subtracted the age of the decedent from the scanning date to arrive at a birthdate that was entered into the computer. To standardize the amount of radiation in each scan, the weight of the individual was set to 90 lbs, thus using the "thin mode." This is consistent with a soft-tissue thickness of 12 cm, suggested by the manufacturer. If we reported a higher body weight, the machine expected more soft-tissue equivalent material over the bone and would abort the scan. This had no bearing on the results except for z-scores but maintained a constant level of radiation through the rice and dry bone to ensure an accurate reading. This aspect of the research differs from previous research with living subjects because the DEXA scanner must accommodate different tissue thicknesses for obese and emaciated individuals.

Methods for the cross-sectional geometry are described in the previous chapter. Computed tomographic (CT) scans were conducted on the skeletons in this study. With a multi-disciplinary team of anthropologists and biomedical engineers, three-dimensional surface models of each bone were created and added to a bone atlas to allow automatic morphological comparison. These models include both medullary and subperiosteal surfaces. An algorithm similar to Slice (Nagurka and Hayes,) was used to calculate the the cross-sectional geometry at five locations along the biomechanical axis of the femoral shaft (20%, 35%, 50%, 65%, 80%). I used the ratio of principal and 2nd moments of inertia at the femoral midshaft as shape indices (Imax/Imin and Iy/Ix). Ruff and

colleagues (1984) suggest that this shape index reflects with activity patterns. The more a-p elongation indicates greater activity, especially over rough terrain or up and down stairs. If this is true, by using the shape index in the model as a partial correlation, we can account for activity.

Results

Correlation matrices using Pearson correlation coefficients for both females and males are found in the Tables 5.1 and 5.2. Additionally, for the females in table 5.1, partial correlations with age are provided. In table 5.2, partial correlations with cross-sectional shape at the mid-shaft (Imax/Imin at 50%) are included for males. Using partial correlations of midshaft shape improved the correlation for males, but lowered the correlations for females. The opposite occurred when using a partial correlation of age. The correlations increased for the females and decreased for the males. The best correlations for females without accounting for cross-sectional shape are for total BMD and Shaft BMD.

Table 5.1. Pearson and Partial Correlations (Age) for Females BMD with weight and BMI

Pearson Correlation Matrix for Females BMD with Weight and BMI (n=28)				
	Weight (kg)	**BMI**	**Weight kg/ (with Age)**	**BMI (with Age)**
Total BMD	0.660	0.654	0.747	0.710
Neck BMD	0.623	0.604	0.710	0.654
Wards BMD	0.487	0.469	0.546	0.489
Troch BMD	0.643	0.632	0.695	0.657
ShaftBMD	0.667	0.667	0.758	0.728

Table 5.2. Pearson and Partial Correlations (Shape) for Males BMD with weight and BMI

Pearson Correlation Matrix for Males BMD with Weight and BMI (n=28)				
	Weight (kg)	**BMI**	**Weight kg/ (with Shape: Imax/Imin)**	**BMI (with Shape: Imax/Imin)**
Total BMD	0.464	0.452	0.498	0.512
Neck BMD	0.500	0.450	0.593	0.588
Wards BMD	0.361	0.310	0.478	0.477
Troch BMD	0.451	0.450	0.482	0.482
ShaftBMD	0.446	0.444	0.462	0.489

When comparing the different Female BMI categories using ANOVA, the results were significant ($p<0.05$) at all locations between the emaciated and obese and between emaciated and average (Table 5.3). When comparing obese to average weight individuals, there were no significant differences. For males, the results were nearly the same (Table 5.4). There were significant differences between the average and emaciated and the obese and emaciated both at all locations except for between the obese and emaciated individuals at Ward's triangle. The relationship of bone density and BMI category is shown below for females (Figure 5.4) and for males (Figure 5.5). The trend of lesser density to greater density is clear for females and males, but more pronounced for females.

Table 5.3. Differences in BMD between different BMI categories for females (ANOVA)

FEMALES	Total BMD (g/cm^2)	Neck BMD	Wards Triangle BMD	Greater Trochanter BMD	Proximal Shaft BMD
Average BMI vs. Obese	0.107	0.082	0.020	0.103	0.123
Average BMI vs. emaciated	0.245*	0.231*	0.253*	0.176*	0.303*
Obese vs. emaciated	0.352*	0.313*	0.273*	0.279*	0.426*

*p<.05

Table 5.4. Differences in BMD between different BMI categories for females (ANOVA)

MALES	Total BMD (g/cm^2)	Neck BMD	Wards Triangle BMD	Greater Trochanter BMD	Proximal Shaft BMD
Average BMI vs. Obese	0.012	0.003	0.064	0.017	0.047
Average BMI vs. emaciated	0.236*	0.256*	0.287*	0.192*	0.248*
Obese vs. emaciated	0.248*	0.286*	0.235	0.209*	0.295*

*p<.05

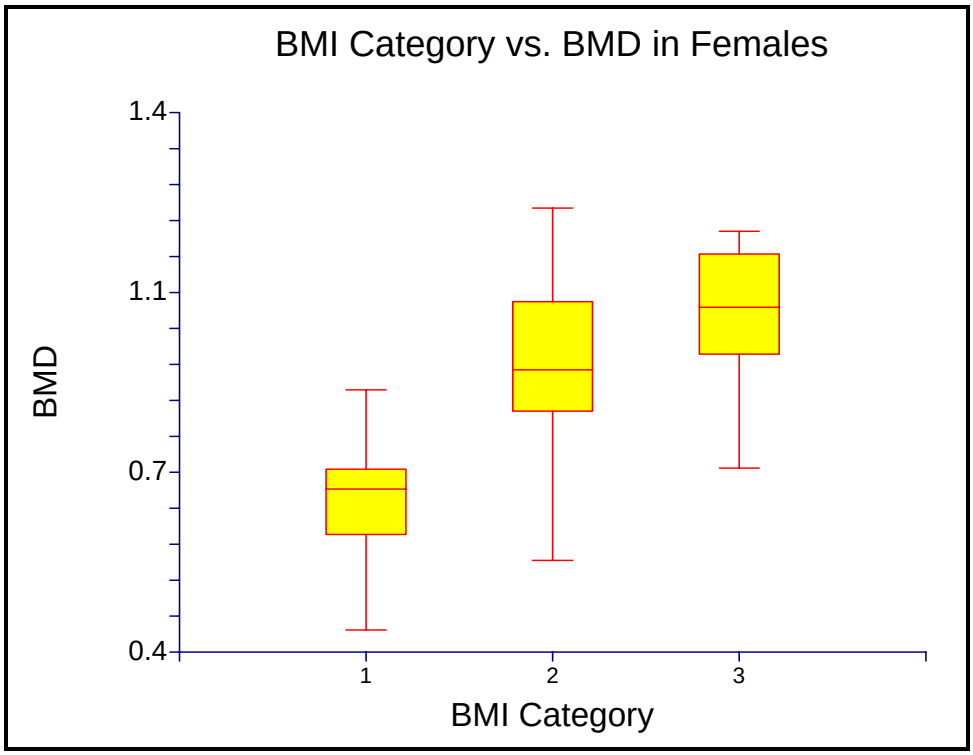

Figure 5.4. Boxplots for different BMI categories compared to total BMD in Females

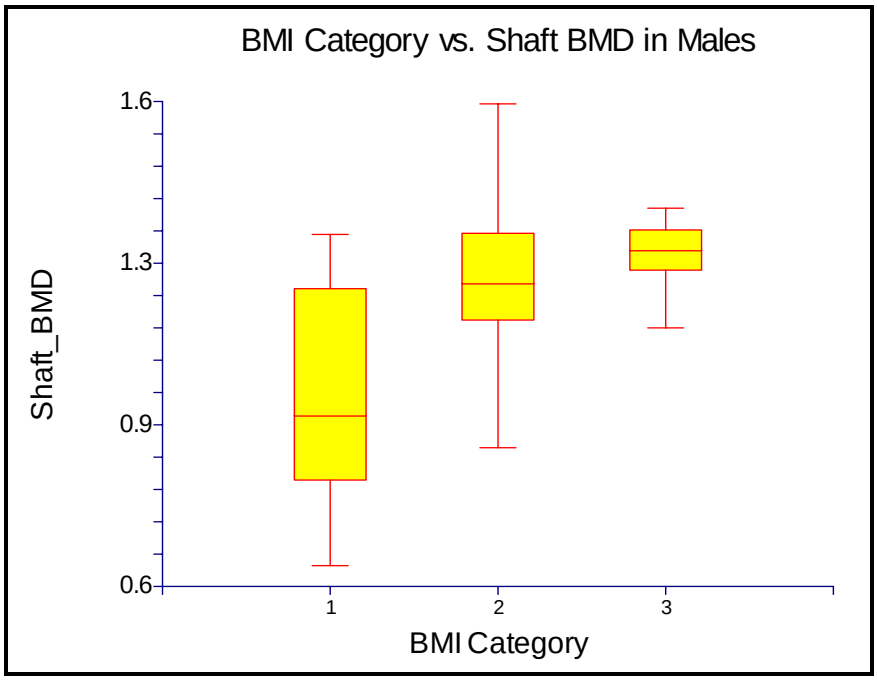

Figure 5.5. Boxplots for different BMI categories compared to Shaft BMD in Males

The data from the previous chapter on cross-sectional geometry has been combined in this chapter for multivariate regressions. Separate equations were created for males and females, as well as for the sexes pooled. Correlation matrices examine the individual relationships with each variable compared to sex. The complete matrices are available in the appendix. Principal Variable Analysis (PVA) was applied to determine the best combination of traits to use in the predictive model. PVA is a combination of Principal Components Analysis (PCA) and McHenry's algorithm for variable selection. PCA is useful for data screening to preliminary determine relationships between variables (McHenry, 1978). PCA claims to provide data reduction, but ultimately creates more data in the form of new factor scores. It allows a reduction in structure, but not in the database. Interpretation of principal components can be difficult. Rotations may or many

not help and often the researcher attempts to force interpretations. The ability to choose one variable for each principal component is not always possible. One way to get around these problems is to combine multivariate techniques together. The solution in many cases is PVA (Seaver, personal communication, 2007). Principal Variables Analysis takes the optimum number of PC scores. In this chapter, I take the top three or four eigenvalues. The PC scores are saved and multiplied by the appropriate square root of the eigenvalue. Finally, a multivariate regression analysis with variable selection is run using McHenry's algorithm. The statistical software packages NCSS97 was used to run PVA and multiple regression.

The variable selection method, McHenry's algorithm, was used separately for the cross-sectional variables and density variables. The best variables for each sex were then subjected to a second variable selection. The best two or three variables were used to create robust multiple regression equations in NCSS. For females, using McHenry's algorithm for variable selection with BMI as the dependent, Shaft BMD was selected first (R-squared = .45) and then Total BMD and Ward's triangle combined (R-squared = .60). For males, Neck BMD was selected first (R-squared = .24) and then Neck BMD and Ward's BMD combined (R-squared = .48) using McHenry's variable selection. To avoid problems with collinearity, only the strongest density variable was included to develop each multiple regression equation.

The best regression formula to predict body mass in females (see output 5.1) includes the area of the canal at 65%, the radius of gyration at 65% and shaft bone mineral density (R^2 = 0.73, SQRT MSE = 14.8 kg). Adding age to the female regression formula made no difference. The best regression formula (R^2 = 0.81, SQRT MSE = 10.3

kg) for males included, Neck BMD, the distance from the centroid in the A-P direction at the proximal cross-section and the shape variable at midshaft (Imax/Imin) (see output 5.2).

Results – Female

Output 5.1. Best Multiple Regression Equation for Females

Run Summary Section

Parameter	Value	Parameter	Value
Dependent Variable	Weight_kg	Rows Processed	149
Number Ind. Variables	5	Rows Filtered Out	90
Weight Variable	None	Rows with X's Missing	29
R2	0.7828	Rows with Weight Missing	0
Adj R2	0.7335	Rows with Y Missing	2
Coefficient of Variation	0.2064	Rows Used in Estimation	28
Mean Square Error	218.8327	Sum of Weights	26.786
Square Root of MSE	14.793	Completion Status	Normal
Ave Abs Pct Error	21.066		

Regression Equation Section

Independent Variable	Regression Coefficient b(i)	Standard Error Sb(i)	T-Value to test H0:B(i)=0	Prob Level	Reject H0 at 5%?	Power of Test at 5%
Intercept	-317.9996	74.1871	-4.286	0.0003	Yes	0.9835
Height_m	112.7201	45.2849	2.489	0.0209	Yes	0.6626
IM_TotalArea_65	-98.9688	42.4507	-2.331	0.0293	Yes	0.6060
Kmax_65	217.2282	93.9662	2.312	0.0305	Yes	0.5988
Shaft_BMD	169.4005	30.1042	5.627	0.0000	Yes	0.9997
Wards_BMD	-139.2644	34.4143	-4.047	0.0005	Yes	0.9716

Estimated Model

-318.000+ 112.720*Height_m-98.969*IM_TotalArea_65+ 217.228*Kmax_65+ 169.400*Shaft_BMD-139.264*Wards_BMD

PRESS Section

Parameter	From PRESS Residuals	From Regular Residuals
Sum of Squared Residuals	12089.52	4814.32
Sum of |Residuals|	458.0867	336.6383
R2	0.4546	0.7828

Normality Tests Section

Test Name	Test Value	Prob Level	Reject H0 At Alpha = 20%?
Shapiro Wilk	0.9340	0.077880	Yes
Anderson Darling	0.4703	0.246552	No
D'Agostino Skewness	-2.6989	0.006956	Yes
D'Agostino Kurtosis	1.5841	0.113170	Yes
D'Agostino Omnibus	9.7937	0.007470	Yes

Results – Male

Output 5.2. Best Robust Multiple Regression Formula for Body Mass Estimation in Males

Run Summary Section

Parameter	Value	Parameter	Value
Dependent Variable	Weight_kg	Rows Processed	149
Number Ind. Variables	3	Rows Filtered Out	59
Weight Variable	None	Rows with X's Missing	63
R2	0.8306	Rows with Weight Missing	0
Adj R2	0.8064	Rows with Y Missing	2
Coefficient of Variation	0.1418	Rows Used in Estimation	25
Mean Square Error	113.6638	Sum of Weights	23.729
Square Root of MSE	10.66132	Completion Status	Normal
Ave Abs Pct Error	10.342		

Regression Equation Section

Independent Variable	Regression Coefficient b(i)	Standard Error Sb(i)	T-Value to test H0:B(i)=0	Prob Level	Reject H0 at 5%?	Power of Test at 5%
Intercept	-359.0596	48.8692	-7.347	0.0000	Yes	1.0000
F_A_per80	105.7358	30.6187	3.453	0.0024	Yes	0.9085
F_B_per65	134.4009	43.7403	3.073	0.0058	Yes	0.8339
Neck_BMD	73.0208	10.8310	6.742	0.0000	Yes	1.0000

PRESS Section

Parameter	From PRESS Residuals	From Regular Residuals
Sum of Squared Residuals	4282.783	2386.939
Sum of |Residuals|	249.1966	214.6753
R2	0.6961	0.8306

Normality Tests Section

Test Name	Test Value	Prob Level	Reject H0 At Alpha = 20%?
Shapiro Wilk	0.9247	0.065498	Yes
Anderson Darling	0.7033	0.066397	Yes
D'Agostino Skewness	2.7029	0.006874	Yes
D'Agostino Kurtosis	1.7294	0.083734	Yes
D'Agostino Omnibus	10.2964	0.005810	Yes

Discussion& Conclusion

In conclusion, bone mineral density has a strong correlation with body mass in the proximal human femur for both white males and females. These results support my previous research, which showed a strong correlation (r = .82) between BMI and cross-sectional area of the femoral waist (Moore et al., 2007). It was unexpected to get such a high correlation in the current research without controlling for age in females. As I mentioned earlier, age exaggerates the differences rather than confounding. Furthermore, there are significant differences in bone mineral density between different weight classifications in both males and females. This correlation is not as strong in males between the average weight and the obese males. This could be because males tend to have vocations or avocations that require heavier lifting than female occupations. Accounting for shape at the midshaft in males dramatically decreased the prediction error. It is clear from this research that males and females must be considered separately when attempting to estimate body mass.

One advantage of this study over previous studies is that by using skeletal femora with a uniform depth of soft-tissue equivalent material, any inconsistencies that arise from different thicknesses of living tissue are removed. Another advantage is the ability to directly compare the results found here with the cross-sectional geometry of the same bones gathered from CT scanned data. In a living population, this would require exposing patients to excessive amounts of radiation. By using a skeletal sample, the resolution can be increased to provide more accurate models. This allows the addition of a shape variable to better predict body mass, which improves upon previous research and increases the power of the model for males. One drawback of this study is the small

sample size in terms of density scans. The results found in this research are consistent with many other studies, thus increasing my confidence in the results found here.

I intend to continue this research in the future to increase sample size with DEXA scans to better validate my findings. It is important to explore the biomechanics of body mass in children, comparing obese and normal weight to answer two important questions. First, will obesity change the adult bone shape? Second, will childhood obesity allow children to better adapt to adult obesity or make it worse? Finally, our current knowledge of bone turnover rates is relatively scant. There exists a need to explore bone turnover rates in response to weight gain or loss in both children and adults.

When unidentified human remains are found, it is the responsibility of the forensic anthropologist to estimate age, sex, stature, and ancestry in order to narrow down the possible matches to missing persons. With the prevalence of obesity in our society, the ability to estimate body mass from the skeleton would add one more useful tool for the forensic anthropologist to establish identification. Furthermore, this research could be applicable to the bioarchaeologist or paleoanthropologist to reconstruct past cultures.

Chapter 6. OSTEOLOGICAL ANALYSIS OF PATHOLOGIES

The previous two chapters explored the relationship of bone density and femoral shaft shape to body mass. In chapter two, I explained the etiology and risk factors of four common bone diseases: osteoarthritis (OA), diffuse idiopathic skeletal hyperostosis (DISH), heel spurs and osteoporosis. This chapter will test the correlations between these four pathologies and body mass. Though these diseases are often considered separately, there does appear to be a relationship between them. OA, DISH and heel spurs often co-occur in a single individual, yet OA and osteoporosis are rarely found in the same patient. Age is often touted as the main cause for these degenerative changes, but these diseases are not an inevitable consequence of aging. In reviewing the literature, the common theme that moves to the fore is body mass. Obese individuals tend to have more severe OA of the knees and heel spurs. DISH has a high incidence in individuals with Type II diabetes and hyperinsulinemia, which is also common in obese individuals. Osteoporosis is rarely seen with OA and has been proposed to have some sort of preventive mechanism against OA. There is, however, a strong relationship between body mass and osteoporosis in ambulatory individuals, with below average body mass predisposing patients to osteoporosis.

The research sample used is from the William M. Bass Donated Skeletal Collection. Eighty-one individuals are used in this analysis, white females and white males. The variables chosen are heel spurs, diffuse idiopathic skeletal hyperostosis (DISH), osteoarthritic (OA) lipping, porosity and eburnation of the proximal tibia for

both the medial and lateral sides, as well the femoral head. I include measurements of the width and breadth of the proximal tibia, the femoral head and bi-iliac breadth. The latter two measures have been used in previous research for both biomechanical and morphometric body mass estimation respectively (Auerbach and Ruff, 2004; Ruff, 2000).

Introduction

Body mass affects the skeleton as a continuum from obesity at one extreme to emaciation at the other. The skeleton continually strives to maintain enough bone to be strong enough for support, but light enough for locomotion. On one end of the spectrum with emaciation, the reduced load bearing causes bone to atrophy and the resorption of minerals. Osteoporosis is diagnosed clinically when bone mineral density (BMD) falls 2.5 standard deviations below the young healthy mean, whereas osteopenia is BMD between 1.0 to 2.5 S.D. below the young mean. Osteopenia has been observed in individuals who suffer from nutrient deficiencies due to diet restriction, as is the case with female elite runners (Gibson et al., 2004), anorexia nervosa (Misra et al., 2007), patients with HIV (Jones et al., 2007) and individuals suffering from extreme famine (Hummert, 1983). On the other end of the spectrum with obesity, bones become hypertrophic, with ossification of entheses and ligaments and increased bone density. The previous chapter explored the relationship of bone density; this chapter will focus on hypertrophic bone pathologies of DISH, heel spurs and osteoarthritis.

It was noted by Dequeker and colleagues (1983) that osteoporosis seems to provide some sort of preventive mechanism for osteoarthritis. These researchers recognized an important phenomenon in bone metabolism and biomechanics, but

proposed the wrong etiology. The reason you do not see osteoarthritis commonly with osteopenia traces back to the body mass continuum. With low body mass, joint articulations are not subjected to heavy loads and are hence less likely to compensate with osteoarthritis (OA). As BMI increases, strain and torque increase, leading to a higher risk of injury (Ford et al., 2005). OA occurs because of repeated injury to the joint capsule, which is common in people who either regularly or infrequently overload their joints. A certain amount of loading appears necessary for joint health. As body mass increases toward the extreme of obesity, other biomechanical compensations occur with locomotion. Knee malalignment is more common in extreme obesity than normal alignment. With knee malalignment, the joints are more prone to injury. Osteoarthritis of the knees could be a mechanism to create more surface area to increase compressive strength at the joint, which would be necessary for greater body mass loads. Other biomechanical compensations occur with extreme obesity. The gait of an obese individual often changes to a more medio-lateral movement as opposed to the antero-posterior pendulous gait of normal bipedal locomotion. The cycle of obesity is perpetuated by decreased activity and increased risk for injury. A sedentary lifestyle in obese individuals necessitates body mass to be mobilized by the upper limb. In sit-to-stand studies of obese individuals (Galli et al., 2000), the activity is very different from normal weight individuals. Normal weight subjects leaned forward to place their center of gravity slightly in front of their feet to stand. They did not require upper limb strength to push them to a standing position. The obese subjects, on the contrary, regularly require their arms to help raise them to a standing position. With excess body mass about their abdomen, leaning forward to place their center of gravity in front of their feet causes

the lower back to support excessive body mass. These obese subjects, without the aid of their arms, attempted to stand without leaning forward. This forces the quadriceps muscles to do all of the work when standing, which quickly fatigue after a few trials. This simple exercise clarifies two major pathological phenomena that occur in the skeleton of obese individuals. First, extreme adiposity around the abdomen will put excessive strain on the mid back when standing. Secondly, the arms play a major role in the locomotion of obese individuals. This explains the distribution of OA in obese individuals. The arms and wrists are typically not equipped to handle the heavy load of lifting the body mass from a seated position. Obese individuals are more likely to have wrist and hand osteoarthritis (Holmberg et al., 2005; Hough, Jr., 1993; Moskowitz, 1993; Oliveria et al., 1998). Previous researchers have failed to recognize the important role that the upper limb plays in obese locomotion. As a result, they have mistakenly interpreted OA in the arm and wrist as systemic as opposed to load bearing. Furthermore, the thoracic and lumbar spine are subjected to repeated injury during the sit-to-stand, as well as being overburdened regularly during walking and due to a sedentary lifestyle. This explains the etiology of diffuse idiopathic skeletal hyperostosis. As a result of injury and to reinforce the spine, the body sacrifices flexibility for durability. The anterior longitudinal ligament fuses to the vertebrae, preserving disk space.

Other expressions of this diffuse syndrome are also the result of excess body mass. The malalignment of the knee mentioned earlier, genua valgus (knock-kneed) malalignment and genua varus (bow-legged) malalignment are common in obese individuals. In order to compensate for increased body mass and to widen the base, eversion of the foot is extremely common. This puts an extreme amount of stress on the

arch of the foot and commonly leads to plantar fasciitis, which manifests on the skeleton as heel spurs. Heel spurs are included in the diffuse syndrome of DISH. The final trait commonly seen in DISH is osteoarthritis, which was previously explained in this and earlier chapters. The entire phenomenon of DISH can thus be explained by the abnormal locomotive accomodations that occur as a result of extreme obesity in both gait and sit-to-stand activities. If these predictions are true, the evidence should be apparent in the skeletal pathologies of a large sample of modern humans of known body mass. Osteoarthritis should better correlate with body mass than with age and the suite of traits attributed to DISH should be associated with individuals of extreme obesity (Patrick, 2005).

Some confounding issues in this chapter may be due to different activity patterns, either vocational or avocational. The pathologies described are degenerative changes due to trauma or repetitive activities. Trauma can occur in many different occupations. The important point that I would like to make is that the pattern of degenerative changes should differ if due to obesity versus some other activity. Runners commonly get heel spurs, as do those individuals who have occupations in which they stand on their feet all day (Buchbinder, 2004; Riddle et al., 2003). But one would expect neither runners nor people standing all day to have the condition DISH in the spine. If a healthy weight individual suffers from a knee injury in one leg, and they favor that leg during healing, it is unlikely that their body weight would put excessive strain on the contra-lateral leg. If this were to happen in severely obese individuals, 46% would develop OA in the other leg as a result (Sharma et al., 2006). The odds-ratio for bi-lateral knee OA in obese individuals compared to normal weight is 8.1 (Stürmer et al., 2000).

Materials and Methods

In order to test this hypothesis, I conducted an osteological analysis of 81 individuals from the William M. Bass Donated Skeletal Collection housed at the University of Tennessee Department of Anthropology. The sample was chosen based on availability of height and weight information, including only white males and females. I analyzed each skeleton in entirety for all pathologies and measurements. This was conducted blindly in terms of body mass information. Though DISH is considered to be a diffuse syndrome, I recorded only the spinal manifestation and heel spurs individually. Presence of the vertebral trait of DISH was recorded if three or more vertebrae were fused along the anterior right side of the vertebral bodies and only if disc space was preserved. A note was made on the severity of the manifestation and which vertebrae were involved. Heel spurs were scored from zero to 3 based on the severity of the heel spur (see Figure 6.1). Only those heel spurs on the inferior surface of the calcaneous were recorded.

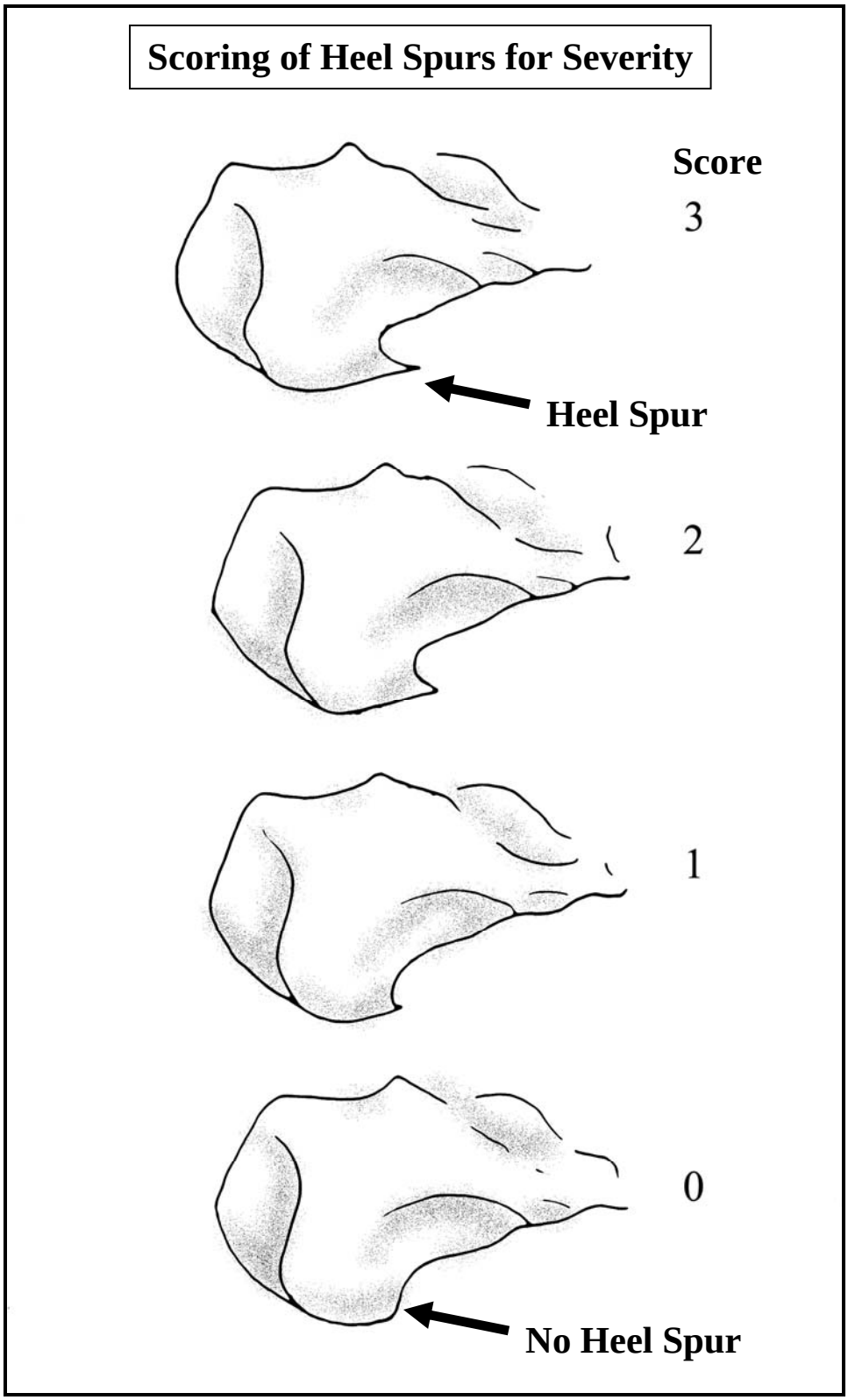

Figure 6.1. Scoring Procedure for Heel Spurs Showing Posterior Calcaneous

There can be a significant amount of inter-observer error when scoring for arthritis, but collecting enough data can give a reasonable approximation (Moskowitz, 1993). Bridges (1985) and Ortner (2003) recommend providing as much detail as possible. The scoring procedure is consistent with Bridges (1991), but I collapse the slight and mild categories, so that I have only scores of zero to three (e.g. 0 = absent, 1 = trace, 2 = moderate, 3 = severe). Osteoarthritis was scored for variations in severity and location. Three locations on the skeleton were the focus in this study. I scored both right and left sides when possible. I divided the tibial plateau into medial and lateral condyles and recorded them separately. The femoral head was also scored for OA. Osteoarthritis was broken down into lipping, extent of lipping, porosity, eburnation and extent of eburnation. The extent of lipping and eburnation were defined as the proportion of the circumference of the articulation affected, from zero to three. A score of two, for example, was recorded when two-thirds of the tibial condyle was affected with lipping.. Porosity proved to be a more arbitrary designation and did not correspond well with eburnation or lipping, as there may be signs of porosity due to bone deposition or resorption.

The statistical software package NCSS 2004 was used for most statistical analyses. Principal Component Analysis (PCA) was used initially to check for outliers Chi-square tests were run initially to clarify unilinear relationships at each location, comparing the different BMI categories: Emaciated, Normal, Obese, and Morbidly Obese. BMI categories were then collapsed into Obese (BMI>30) and Not Obese (BMI<30). Logistic Regression was run for each variable. Finally, I used a separate program to create a classification tree (decision tree) of the categorical variables. The

Computational Intelligence Program at the University of British Columbia provides applets through their website for decision trees, neural networks and fuzzy logic, among other complex algorithms. Decision trees are useful in developing predictive models from categorical data in terms of simple yes and no responses. The applet is set up to randomly separate the sample into a training and a testing set.

Results - Females

Chi-square tests were initially run for each independent variable to tease apart some of the relationships between the different BMI categories: Emaciated (BMI<17.9), Normal Weight (18<BMI<24.9), Overweight (25<BMI<29.9), Obese (30<BMI<39.9) and Morbidly Obese (BMI>40). Significant differences (p=.017) between female BMI categories existed for the condition DISH. Eighty percent of the morbidly obese exhibited moderate to severe DISH. Tables for counts and percentages of DISH by BMI categories are shown in Table 6.1 below. Significant differences between female BMI categories existed for both right (p=.012) and left (p=.021) side heel spurs. Only Obese and Morbidly Obese categories had a class 3 spur on the left calcaneous and only morbidly obese had a class three spur on the right. Tables for counts and percentages of Right and Left Heel Spurs by BMI categories can be found in tables in the appendix. When collapsing the classes of spurs into present and absent, the moderate (2) to severe spurs (3) were put into a category of present and mild (1) was included in the absent category. I condensed all of the categories for pathologies in this way. The differences were no longer significant (p=0.11), but 60% of the morbidly obese had large spurs and

55.6% of the obese had large spurs. None of the emaciated had any heel spurs (see Table 6.2).

Table 6.1. DISH presence and BMI category - Females

Females			
	DISH Present		
BMI_Code	0	1	Total
Emaciated	4 (66.7%)	2 (33.3%)	6
Normal	15 (88.2%)	2 (11.8%)	17
Overweight	3 (100%)	0 (0%)	3
Obese	4 (44.4%)	5 (55.6%)	9
Morbidly Obese	1 (20%)	4 (80%)	5
Total	27 (67.5%)	13 (32.5%)	40

Table 6.2. Large Heel Spur and BMI Category (by count and percentage) in females

Females			
2	Big_Spur		
BMI_Code	0	1	Total
Emaciated	5 (100%)	0 (0%)	5
2Normal	11 (68.8%)	5 (31.3%)	16
Overweight	3 (100%)	0 (0%)	3
Obese	4 (44.4%)	5 (55.6%)	9
Morbidly Obese	2 (40%)	3 (60%)	5
Total	25 (65.8%)	13 (34.2%)	38

Significant differences (p=.014) were evident for lipping severity on the left medial side for the female BMI categories. These tables can be found in the appendix. The collapsed tables of dummy variables for OA on the left medial side can be found below, Table 6.3. When the severity classes of lipping were collapsed into present and absent, the differences were still significant (p=.003). Emaciated females had no left medial arthritis of the knee. Of the normal weight individuals, 5.9% had OA in this location, as did, 33.3% of the obese individuals and 80% of the morbidly obese.

In terms of severity of lipping on the left lateral side, 80% of the morbidly obese were affected. Only 11.1% of the obese had severe and only 5.9% of the normal weight had severe lipping in this location. None of the emaciated nor the overweight had severe lipping on the left lateral side and these results were significant (p=.023) (See appendix). By collapsing the categories, you see a clear trend of increasing OA on the left lateral side toward morbid obesity (see table 6.4 below). In the morbidly obese category, 80% of the females were affected with OA on the left lateral side of the knee, 33.3% of the obese and only 17.6% of the normal weight showed the condition. None of the overweight and no emaciated individuals showed OA in this location. After collapsing classes of the OA on the right lateral side, there are significant differences in OA (p=.037), with a clear trend toward more osteoarthritis in morbidly obese with 80%, 33.3% in both the overweight and obese categories, 17.5% in the normal weight and none of the emaciated affected (see table 6.5 below).

Multiple regression did not yield a very predictive model in terms of the pathologies for females. Using McHenry's algorithm of variable selection, the best variables chosen were OA of the left medial side and the breadth measurement of the

proximal right tibia. The R-squared value was only 0.53 and the R-squared press value was 0.42. The square root of the mean squared error was rather large at 17.68 kg (see output 6.1 below).

Table 6.3. Percentage and Counts of Obese with and without OA in Females

Female Counts			
	OA_TLM		
BMI_Code	0	1	Total
Emaciated	5 (100%)	0 (0%)	5
Normal	16 (94.1%)	1 (5.9%)	17
Overweight	3 (100%)	0 0%)	3
Obese	6 (66.7%)	3 (33.3%)	9
Morbidly Obese	1 (20%)	4 (80%)	5
Total	31 (79.5%)	8 (20.5%)	39

Table 6.4. Percentage and Counts of Obese with and without OA on the Left Lateral Proximal Tibia in Females

Female Counts			
	OA_TLL		
BMI_Code	0	1	Total
Emaciated	5 (100%)	0 (0%)	5
Normal	14 (82.4%)	3 (17.6%)	17
Overweight	3 (100%)	0 (0%)	3
Obese	6 (66.7%)	3 (33.3%)	9
Morbidly Obese	1 (20%)	4 (80%)	5
Total	29 (74.4%)	10 (25.6%)	39

Table 6.5. Percentage and Counts of Obese with and without OA on the Right Lateral Proximal Tibia in Males

Female Counts			
	OA_TRL		
BMI_Code	0	1	Total
Emaciated	6 (100%)	0 (0%)	6
Normal	14 (82.4%)	3 (17.6%)	17
Overweight	2 (66.7%)	1 (33.3%)	3
Obese	6 (66.7%)	3 (33.3%)	9
Morbidly Obese	1 (20%)	4 (80%)	5
Total	29 (72.5%)	11 (27.5%)	40

Output 6.1 – Female Multiple Regression Using Pathology Variables

Run Summary Section

Parameter	Value	Parameter	Value
Dependent Variable	Weight_kg	Rows Processed	149
Number Ind. Variables	2	Rows Filtered Out	90
Weight Variable	None	Rows with X's Missing	21
R2	0.5363	Rows with Weight Missing	0
Adj R2	0.5082	Rows with Y Missing	2
Coefficient of Variation	0.2550	Rows Used in Estimation	36
Mean Square Error	312.6747	Sum of Weights	35.882
Square Root of MSE	17.68261	Completion Status	Normal
	Ave Abs Pct Error	22.016	

Descriptive Statistics Section

Variable	Count	Mean	Deviation	Minimum	Maximum
OA_TLM	36	0.2229511	0.4214394	0	1
Prox_RTib_m_L	36	7.005674	0.3378593	6.4	7.9
Weight_kg	36	69.33696	25.21336	31.725	137.7

Regression Equation Section

Independent Variable	Regression Coefficient b(i)	Standard Error Sb(i)	T-Value to test H0:B(i)=0	Prob Level	Reject H0 at 5%?	Power of Test at 5%
Intercept	-129.1004	71.3158	-1.810	0.0794	No	0.4199
OA_TLM	28.2643	8.2599	3.422	0.0017	Yes	0.9132
Prox_RTib_m_L	27.4257	10.3032	2.662	0.0119	Yes	0.7336

Estimated Model

-129.100+ 28.264*OA_TLM+ 27.426*Prox_RTib_m_L_breadth

PRESS Section

Parameter	From PRESS Residuals	From Regular Residuals
Sum of Squared Residuals	12827.34	10318.26
Sum of |Residuals|	558.8193	508.9221
R2	0.4235	0.5363

Normality Tests Section

Test Name	Test Value	Prob Level	Reject H0 At Alpha = 20%?
Shapiro Wilk	0.9507	0.110397	Yes
Anderson Darling	0.6391	0.095647	Yes
D'Agostino Skewness	0.7081	0.478895	No
D'Agostino Kurtosis	-1.1741	0.240371	No
D'Agostino Omnibus	1.8798	0.390668	No

Results – Males

For the males, the Chi-square results revealed significant differences between BMI categories. There was a clear trend increasing toward greater obesity for DISH. None of the emaciated had DISH, 16.7% of the normal were affected, 28.5% of the overweight, 50% of the obese and 66.7% of the obese had the condition (p=.016) (see table 6.6 below). When looking at heel spurs in males, only overweight and morbidly obese have severe spurs on the left side. There are no significant differences between the BMI categories on the right side. When collapsing the categories of severity and side, there is a trend from no spurs in the emaciated to 50% in the morbidly obese, but the Chi-square results are not significant (p=0.275) (see table 6.7 below).

For osteoarthritis of the right medial side in males, differences between BMI groups were significant before and after collapsing the categories. After collapsing the categories, there is no OA in the emaciated or the normal weight groups, but a clear trend shows increasing OA toward the morbidly obese: 14.3% in overweight, 22.2% in obese, and 44.4% in the morbidly obese (p=.024). No significant differences exist in the males between the BMI categories for rights side spurs, lateral OA on either side or left medial OA (see table 6.8).

The multiple regression equations were no better for the males than for the females. The variables selected using McHenry's algorithm for males were OA of the left lateral, OA of the right medial and an anterior-posterior breadth measurement of the proximal tibia. The R-squared value was only 0.42 and the validation R-squared Press was extremely low at 0.16. The square root of the mean squared error was high, 20.99 kg (see output 6.2).

Table 6.6. Percentage and Counts of Obese with and without DISH in Males

Counts Section			
	DISH Present males		
BMI_Code	0	1	Total
Emaciated	6 (100%)	0 (0%)	6
Normal	20 (83.3%)	4 (16.7%)	24
Overweight	5 (71.4%)	2 (28.6%)	7
Obese	5 (50%)	5 (50%)	10
Morbidly Obese	3 (33.3%)	6 (66.7%)	9
Total	39 (69.6%)	17 (30.4%)	56

Table 6.7. Percentage and Counts of Obese with and without Big Heel Spurs Males

ounts Section			
	Big Spur Males		
BMI_Code	0	1	Total
Emaciated	6 (100%)	0 (0%)	6
Normal	19 (79.2%)	5 (20.8%)	24
Overweight	5 (71.4%)	2 (28.6%)	7
Obese	6 (66.7%)	3 (33.3%)	9
Morbid Obese	4 (50%)	4 (50%)	8
Total	40 (74.1%)	14 (25.9%)	54

Table 6.8. Percentage and Counts of Obese with and without OA

Counts Section			
	OA_TRM MALES		
BMI_Code	0	1	Total
Emaciated	5 (100%)	0 (0%)	5
Normal	23 (100%)	0 (0%)	23
Overweight	6 (85.7%)	1 (14.3%)	7
Obese	7 (77.8%)	2 (22.2%)	9
Morbid Obese	5 (55.6%)	4 (44.4%)	9
Total	46 (86.8%)	7 (13.2%)	53

Output 6.2. Males Multiple Regression using Pathology Variables

Run Summary Section

Parameter	Value	Parameter	Value
Dependent Variable	Weight_kg	Rows Processed	149
Number Ind. Variables	3	Rows Filtered Out	59
Weight Variable	None	Rows with X's Missing	40
R2	0.4190	Rows with Weight Missing	0
Adj R2	0.3765	Rows with Y Missing	5
Coefficient of Variation	0.2510	Rows Used in Estimation	45
Mean Square Error	440.5534	Sum of Weights	43.617
Square Root of MSE	20.98936	Completion Status	Normal
	Ave Abs Pct Error	21.096	

Regression Equation Section

Independent Variable	Regression Coefficient b(i)	Standard Error Sb(i)	T-Value to test H0:B(i)=0	Prob Level	Reject H0 at 5%?	Power of Test at 5%
Intercept	-112.6355	62.7346	-1.795	0.0800	No	0.4183
OA_TLL	-43.7642	11.6411	-3.759	0.0005	Yes	0.9564
OA_TRM	47.2897	13.8496	3.415	0.0015	Yes	0.9152
Prox_LTib_a_p	39.0194	12.5030	3.121	0.0033	Yes	0.8615

Estimated Model

-112.636-43.764*OA_TLL+ 47.290*OA_TRM+ 39.0194*Prox_LTib_a_p_breadth

PRESS Section

Parameter	From PRESS Residuals	From Regular Residuals
Sum of Squared Residuals	26052.32	18062.69
Sum of |Residuals|	843.184	778.2393
R2	0.1621	0.4190

Normality Tests Section

Test Name	Test Value	Prob Level	Reject H0 At Alpha = 20%?
Shapiro Wilk	0.9282	0.008114	Yes
Anderson Darling	0.7869	0.041277	Yes
D'Agostino Skewness	3.2210	0.001278	Yes
D'Agostino Kurtosis	1.9354	0.052942	Yes
D'Agostino Omnibus	14.1204	0.000859	Yes

Results Pooled

The sexes were pooled in the final analysis stages for logistic regression and classification trees. Using logistic regression, the relationships between BMI and the pathologies are shown in table 6.9 below. Only the collapsed dummy variables of present and absent and obese versus not obese were used for the logistic regression (obese = BMI>30). The odds ratios for females for DISH, heel spurs and all locations of OA had significant Wald probabilities. The odds ratios ranged from 5.1 for heel spurs, 9.9 for DISH and 23.9 for left medial OA. For males the odds ratios were not significant for heel spurs, left lateral OA or right lateral OA. Males only showed significant odds ratios for DISH at 6.5, and for the right and left medial tibial plateaus, 4.4 and 15.5 respectively. This might fit the model of being more varus aligned. Males and females seem to be favoring different knees, perhaps reflecting sex differences in knee malalignment. OA is worse on the left medial side for females and on the right medial side for males. When pooling the sexes, all OA sites had significant odds ratios ranging from 3.6 to 7.9, with the most severe for the left medial OA, DISH and then right medial OA. When comparing age as the dependent variable rather than weight, only DISH and OA of the right medial tibia were significant with odds ratios less than 3.8.

Table 9. Logistic Regression Odds Ratios for Females, Males, Sexes Pooled and for Age as Dependent

Females	Pathology	N	Odds Ratio	p – Value
	DISH	40	9.900	0.003*
	Heel Spur	38	5.066	0.027*
	OA Tibia Left Lateral	38	6.999	0.017*
	OA Tibia Left Medial	39	23.999	0.006*
	OA Tibia Right Lateral	40	5.499	0.025*
	OA Tibia Right Medial	40	5.600	0.019*
Males	**Pathology**	**N**	**Odds Ratio**	**p - Value**
	DISH	53	6.417	0.004*
	Heel Spur	51	2.700	0.127
	OA Tibia Left Lateral	53	2.679	0.186
	OA Tibia Left Medial	53	4.375	0.037*
	OA Tibia Right Lateral	50	3.333	0.133
	OA Tibia Right Medial	50	15.500	0.016*
Pooled	**Pathology**	**N**	**Odds Ratio**	**p - Value**
	DISH	93	7.692	0.000*
	Heel Spur	89	3.594	0.008*
	OA Tibia Left Lateral	91	4.163	0.008*
	OA Tibia Left Medial	92	7.958	0.000*
	OA Tibia Right Lateral	90	4.082	0.009*
	OA Tibia Right Medial	90	6.741	0.001*
Pooled Age as Dependent	**Pathology**	**N**	**Odds Ratio**	**p - Value**
	DISH	90	3.041	0.027*
	Heel Spur	86	1.653	0.302
	OA Tibia Left Lateral	88	2.667	0.086
	OA Tibia Left Medial	89	2.358	0.135
	OA Tibia Right Lateral	88	2.284	0.151
	OA Tibia Right Medial	88	3.770	0.029*

The best predictive model for BMI from the pathologies was in the form of classification trees. Two separate classification trees were created from the pooled sexes data using an applet from the University of British Columbia Computational Intelligence program (Amershi et al., 1999). The classification tree uses an information gain algorithm from a set of categorical data in the form of yes and no answers. For the first tree, the starting node was OA of the left medial tibia. The training set of 23 was randomly chosen from the sample of 80 males and females. I included a variable in the trees for age. The age category was broken down into older age as above 55 years and younger age as below 55. I chose to look at age as a categorical variable due to the error involved with age estimation from human skeletal remains. This tree resulted in 15 nodes, with seven splits and a depth of three. When the tree was tested, the algorithm accurately classified individuals as obese 83% of the time (see figure 6.2). For the second tree, a completely different random testing sample of 30% was selected. This tree started with DISH as the first node and had 13 total nodes, with six splits. This tree classified subjects as obese with 87% accuracy (see figures A.1 and A.2 in the appendix).

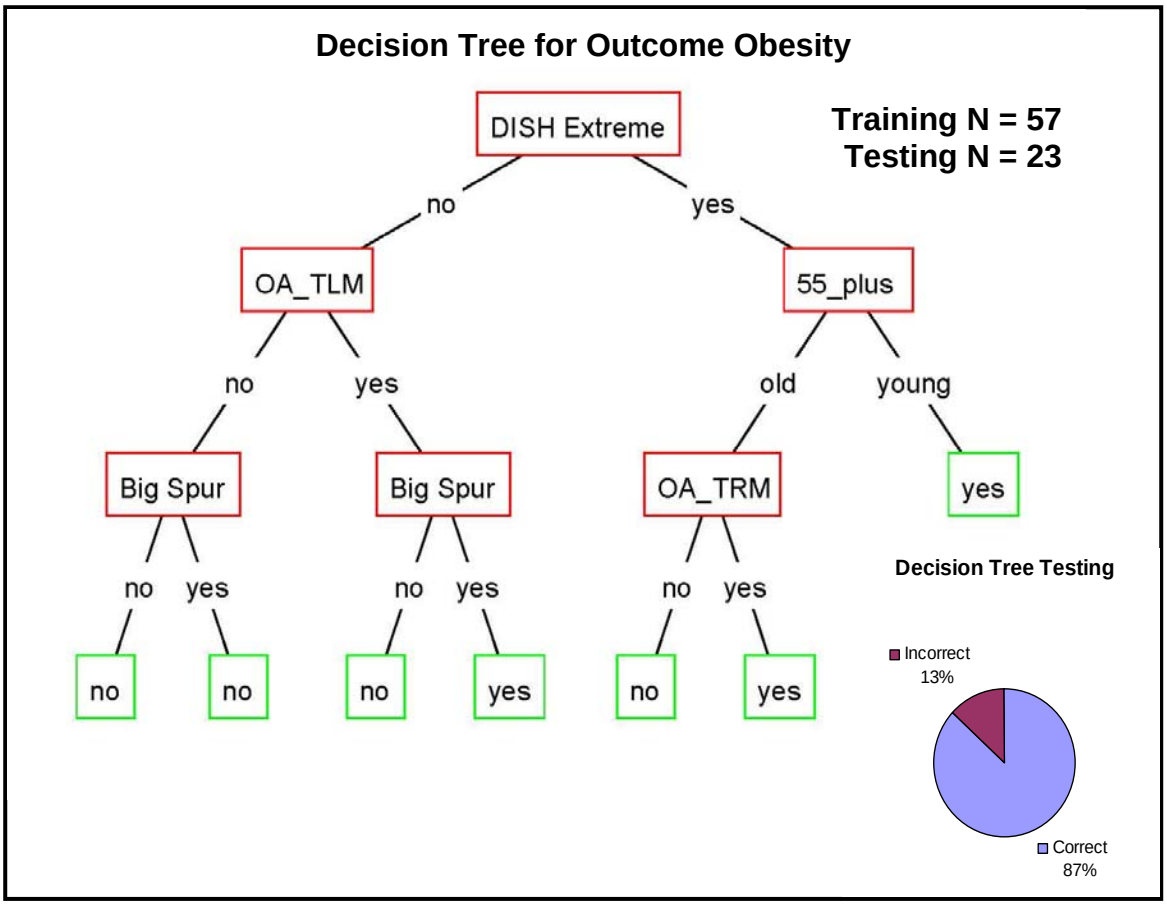

Figure 6.2. Classification Tree for Obesity with 87% accuracy

Discussion

From this data, a trend emerges for increasing pathologies in the obese and morbidly obese body mass categories. None of the emaciated individuals had moderate to severe heel spurs or osteoarthritis at any location. This finding supports early findings that osteoporosis and osteoarthritis rarely coincide, as osteoporosis is common in the emaciated. This helps to refute the suggestion that osteoporosis may help to prevent against OA, when in fact the risk factor is excessive body mass. If I were to have a sample of non-ambulatory obese, it is likely there would be both osteoporosis and osteoarthritis in the same individuals. One interesting finding is that overweight

individuals do not show signs of OA at all sites. This may be the result of sample size, but according to Messier et al. (1996), heavy normal weight adults may actually have a musculoskeletal system designed to handle larger loads.

There are significant relationships between obesity and all four pathologies considered in white females. The same relative trend is apparent in males but with less significance. Obese individuals in the sample overall are nearly eight times more likely to have DISH and OA on the left medial tibia. The medial tibia does seem to endure most of the force in both males and females. Males and females seem to favor different legs, however. Females injure the medial side more frequently and males tend to injure the right medial side.

Multiple regression equations have little predictability power for estimating weight. The best multivariate model includes heel spurs, DISH, OA of the proximal right tibia m-l breadth and right medial lipping. Previous methods to estimate body mass from the skeleton use bi-iliac breadth and diameter of the femoral head. Both of these measurements have little utility in the modern American white sample, in which obesity and emaciation are more common. The correlation between femoral head diameter ($r = 0.099$) and bi-iliac breadth ($r = 0.36$) are too low for any predictive power with this sample. That is not to say that these methods could not work for past populations. Bi-iliac breadth was not selected within the top 10 variables for a multivariate equation. The four pathological variables combined in multiple regression equations are less effective than univariate correlations of BMI with cross-sectional area of the femoral midshaft (R-squared = 0.67) and bone mineral density at the proximal femur (R-squared = 0.53) from previous chapters. The classification tree improves the predictive model by combining

the four variables and age into a simple and testable algorithm with excellent results. The decision tree is just classifying into one of two groups versus predicting weight, which is a much more difficult problem.

Chapter 7. DISCUSSION AND CONCLUSION

Introduction

From this research, we can conclude that it is possible to estimate modern human body mass from the skeleton, including the extremes of both emaciation and obesity. On one end of the spectrum with emaciation, there is an absence of hypertrophic pathologies in conjunction with low bone mineral density. On the other end of the spectrum, obese individuals are nearly eight times more likely to have diffuse idiopathic skeletal hyperostosis (DISH) in the spine. Obese individuals are seven and eight times more likely to have osteoarthritis (OA) of the right and left medial tibiae, respectively. Obesity plays a greater role in the etiology of these degenerative diseases than does aging. With 32.2% of the adult American population considered obese, biological anthropologists need to be aware of the skeletal manifestations of this recent secular trend. Some traits show a greater relationship with body weight and body mass, but by identifying the distribution pattern of these traits on the skeleton, we can distinguish random trauma from the combined effects of excessive body mass.

Though the correlations are not high in the pathological variables, classification trees combine the multiple categorical variables together into a simple and testable algorithm. Skeletal manifestations of body mass are conclusive. Male and female skeletons respond similarly, but not exactly the same, and therefore require separate consideration. All of the traits included in this analysis fit into the biomechanical method for body mass estimation. The morphometric method of bi-iliac breadth was tested here and does not appear to work for body mass estimation outside of the normal range (r =

0.3. The previous biomechanical method using the femoral head diameter does not account for the broad range of body mass in the modern human population. This is not to say that these previous biomechanical and morphometric methods do not have their utility. It is clear that obesity is only a very recent trend, so these methods could be useful for historical and prehistoric body mass estimates.

The trauma to the medial side of the knee may reflect a change in locomotion patterns and knee malalignment. Obesity is more likely to cause bilateral OA compared to normal weight counterparts. Osteoarthritis is due to either singular or multiple traumatic events. When considering the healing in normal weight individuals, by favoring one leg, there is not a high likelihood of injuring the contra-lateral leg. In obesity, however, Sharma et al. (2006) found that 46% of the most obese individuals developed osteoarthritis in the contra-lateral knee.

The findings in this dissertation support my original hypothesis that cross-sectional area and bone mineral density will have the highest correlation with body mass and body weight. It was predicted that the cross-sectional area of the midshaft would be most significant, when in fact the most proximal slice of the femur had the highest correlations. For males, the correlation between cross-sectional area at 80% and weight is $r = 0.57$ and for females, $r = 0.62$. This latter correlation in females is as high as the relationship between height and femoral length in my sample. I did not find a clear relationship between cross-sectional shape and obesity. This could either be due to the fact that activity patterns were not consistent for each of the BMI categories, or that the shape index does not truly express activity. Some length measures appear to be more reflective of body mass. Torsional strength (J) and the individual moments of inertia at

various locations along the shaft appear to reflect changes in body weight and body mass. This could be reflecting what Ford et al. (2005) wrote about strain and torque increasing in obese leading to a higher risk of injury. I did not see a decrease in the canal size in obese individuals, which does not signify endosteal apposition in adulthood is actually occurring. In a preliminary study, this was found to be the case in a sample of 24 females, looking at cross-sectional area of the femoral waist (least circumference). Perhaps this location is more important biomechanically than the midshaft, or maybe the results of my previous study were reflecting sampling error.

The lowest bone density is found in emaciated individuals and the highest bone density in the obese individuals. There were significant differences between the emaciated and the average weight and between the emaciated and obese for bone mineral density in both males and females. This relationship may reflect the change in the gait of severely obese individuals from an anterior to posterior swing of the legs to a more medio-lateral saunter. This change in gait pattern widens the proximal shaft in this medio-lateral direction, changing the shape of the shaft near the hip.

One benefit of this study is the combination of multiple indicators to provide evidence of a suite of traits. I hope that this study encourages other researchers to look at body mass estimation from a more holistic perspective. The William M. Bass Donated Skeletal Collection provides an unparalleled opportunity to explore this secular change in body mass. This large sample of modern individuals of known height and weight reflects the broad spectrum of human body mass from a BMI of 11 to 88. By using a skeletal sample, we can clearly see changes on the skeleton that would not necessarily be apparent on radiographs nor would they be symptomatic. By using a skeletal sample, we

can conduct high resolution CT scans that would expose living subjects to excessive amounts of radiation. My research shows one application of the 3-D computer models, but there are an infinite number of ways to take advantage of this technology. The models, when added to a bone atlas, can be used to automatically quantify shape. This method is similar to geometric morphometric methods on the skull using discrete landmarks. Instead of a few dozen discrete landmarks, the 3-D femoral models used here have 7,500 evenly distributed points. Another benefit of using skeletal material is the ability to standardize tissue depths with the DEXA scans. One problem with DEXA is the error involved when scanning through large amounts of soft-tissue in obese individuals. My method uses bones from a wide range of body mass index, but with the same depth of soft-tissue equivalent. Thus, any differences between bone density will reflect the actual density and not error in accounting for soft-tissues.

There are several drawbacks of my methodologies. The sample size for cross-sectional data is sufficiently large for this study, but the data on bone density is less substantial. In the near future, I will collect more DEXA scans to conduct a validation study of this method. Even with this small sample, DEXA scans prove reliable for the purpose of body mass estimation. The correlations between bone density and body mass and weight in my study are consistent with those published in the current literature (Looker et al., 2006; Wheatley, 2005), lending substantiation to my study. One problem with DEXA is that it inaccurately assumes a cylinder and it only gives area bone mineral density. DEXA has become the gold standard with bone density researcher and this allows comparisons with the clinical literature. One final flaw in my design might be the way in which I chose to collapse the BMI categories. With my BMI categories, I chose

the conservative route to collapse the overweight category with the normal weight. The justification of this is that the mean age of my sample is elderly. Recent research suggests that older individuals may be healthier up to a BMI of 28, lending credence to these findings. This would place my overweight category between 28 and 30. Other researchers have suggested that overweight individuals may actually have skeletons that are better adapted to greater loads compared to the obese (Messier et al., 1996).

Future Research

As there are so many confounding factors in the literature concerning the effects of juvenile obesity, this is a very important area of future research. At present, we have no clear idea of how obesity affects the juvenile skeleton. Recent research shows that obese juvenile females have greater bone density than their normal weight peers. When accounting for increased body mass, however, bone density was not sufficient for the increased loads, especially in the lumbar spine (Goulding et al., 2002). We need to understand the biomechanics of obesity in juveniles to ensure that overweight children are not permanently damaging joint surface or mechanical properties of their bones. Without this knowledge, any exercise regiment could potentially deform the load bearing bones for life, rendering them biomechanically disadvantaged. I intend to develop a research project that will attempt to ask two important questions. Does childhood obesity make the skeleton better adapted for adult obesity? Is there deformation of the load bearing limbs to make obese juveniles biomechanically disadvantaged and prone to injury? I believe this can be addressed using a longitudinal study of growth in obese

juveniles using DEXA and radiographs of the hip and knee. A pilot study could retrospectively survey adults who had been obese in childhood.

One relevant question not addressed in this project is the rate of bone turnover. If an obese individual lost weight, at what rate would the bone turnover become evident in a DEXA scan? One current unpublished observation from bariatric surgeons at Wright State University describes individuals after gastric bypass surgery. Surgeons have mentioned that within three years of the surgery, the formerly obese individuals became osteopenic (D. Duren, 2008, personal communication). This finding is quite remarkable and unexpected. One would expect a steep decline in bone density, but within a normal bone density range. This density decline was in spite of increased activity after the surgery. Perhaps the skeleton is accustomed to certain loads and attempts to overcompensates. Perhaps the mechanism is more chemico-physiologic and reflects overcompensation to the decrease in adipose hormones. Another recent study by Rico et al. (1994) looked at bone density changes due to seasonal weight loss in pre-menopausal Spanish females. The women lost weight over the summer, but gained in bone density. Is this a reflection of greater activity in the summer or simply due to a six month lag in bone turnover. One way to look at the effects of a change in body mass on bone density would be to conduct a longitudinal study of weight loss or weight gain for several years.

Literature Cited

Auerbach BM & Ruff CB (2004) Human Body Mass estimation: A comparison of "Morphometric" and "Mechanical" Methods. *American Journal of Physical Anthropology* 125: 331-342.

Bianchi, ML (2007) Osteoporosis in children and adolescents, *Bone* 41, 486-495.

Brahmabhatt, V, J Rho, L Bernardis, R Gillespie & I Ziv (1998) The Effects of Dietary-Induced Obesity on the Biomechanical Properties of Femora in Male Rats, *International Journal of Obesity* 22:813-818.

Brant, WE (1994) Chapter 1: Diagnostic Imaging Methods, In *Fundamentals of Diagnostic Radiology*, eds. William Brant and Clyde Helms, Williams and Wilkins, Publishers, Baltimore, MD, pp. 3-18.

Bridges, PS (1985) *Changes in Long Bone Structure with the Transition to Agriculture: Implications for Prehistoric Activities*, Ann Arbor: University of Michigan (PhD thesis), 247 p.

Bridges, PS (1991) Degenerative joint disease in hunter-gatherers and agriculturalists from the Southeastern United States, *American Journal of Physical Anthropology*, Aug; 85(4):379-391.

Buchbinder, R (2004), Clinical Practice: Plantar Fasciitis, *New England Journal of Medicine* 350(21):2159-2166.

Carter, DR, M Wong and TE Orr (1991) Musculoskeletal ontogeny, phylogeny, and functional adaptation, *Journal of Biomechanics*, 24 Supplement 1:3-16.

Coggon, D, I Reading, P Croft, M McLaren, D Barrett & C Cooper (2001), Knee osteoarthritis and obesity, *International Journal of Obesity* 25:622-627.

Cowin, SC (2001), The false premise of Wolff's Law, In Cowin, SC (ed.) *Bone Mechanics Handbook*, 2nd Ed., CRC Press, Boca Raton (FL), pp. 301-315.

Dequeker, J, P Goris & R Uytterhoeven (1983), Osteoporosis and osteoarthritis (osteoarthrosis): Anthropometric distinctions, *Journal of the American Medical Association* 249:1448-1451.

Deltoff, MN & PL Kogon (1998) Endocrine and metabolic bone disease: Chapter 7, *The Portable Skeletal X-Ray Library*, Mosby-Year Book, St. Louis, pp. 294-300.

DiMonaco, M, F Vallero, R DiMonaco, R Tappero & A Cavanna (2007), Skeletal muscle mass, fat mass, and hip bone mineral density in elderly women with hip fracture, *Journal of Bone Mineral Metabolism* 25:237-242.

Ding, C, F Cicuttini, F Scott, H Cooley & G Jones (2005) Knee Structural Alteration and BMI: A Cross-sectional Study, *Obesity Research* 13(2): 350-361.

Eckstein, F, S Faber, R Mühlbauer, J Hohe, K-H Englmeier, M Reiser & R Putz (2002) Functional Adaptation of Human Joints to Mechanical Stimuli, *Osteoarthritis and Cartilage* 10(1):44-50.

Ericksen, MF (1976), Cortical bone loss with age in three Native American populations. *American Journal of Physical Anthropology* 45: 443-452.

Felson, DT (1988), Epidemiology of Hip and Knee Osteoarthritis, *Epidemiologic Reviews* 10: 1-28.

Felson, DT, MT Hannan, A Naimark, J Berkeley, G Gordon, PWF Wilson & J Anderson (1991) Occupational Physical Demands, Knee Bending, and Knee Osteoarthritis: Results from the Framingham Study, *Journal of Rheumatology*, 18:1587-1592.

Flegal, KM, MD Carroll, RJ Kuczmarski & CL Johnson (1998), Overweight and obesity in the United States: Prevalence and trends, 1960-1994, *International Journal of Obesity* 22(1):39-47.

Ford, FM, KT Hegmann, GL White & EB Holmes (2005), Associations of Body Mass Index with Meniscal Tears, *American Journal of Preventive Medicine* 28(4): 364-268.

Francis, RM (2003), Metabolic Bone Disease: Chapter 70, *Brocklehurst's Textbook of Geriatric Medicine and Gerontology*, 6th ed., RC Tallis & HM Fillit, Eds., NY Churchill Livingstone, pp. 871-885.

Frankel, VH & M Nordin, Eds. (1980) *Basic Biomechanics of the Skeletal System*, Philadelphia, Lea and Febiger, 303 p.

Frost, HM (1993) Suggested Fundamental Concepts in Skeletal Physiology. *Calcified Tissue International* Jan 52(1):1-4.

Frost, HM (1997a) Defining Osteopenias and Osteoporoses: Another View (with insights from a new paradigm), *Bone*, May; 20(5): 385-391.

Frost, HM (1997b) Obesity, and Bone Strength and "Mass": A tutorial based on insights from a new paradigm, *Bone* (3):211-4. Review.

Frost HM (1999) An Approach to Estimating Bone and Joint Loads and Muscle Strength in Living Subjects and Skeletal Remains, *American Journal of Human Biology* 11(4):437-455.

Galli, M, M Crivellini, F Sibella, A Montesano, P Bertocco & C Parisio (2000), Sit-to-stand movement analysis in obese subjects, *International Journal of Obesity* 24: 1488-1492.

Galloway, A, P Willey, L Snyder (1997), Human Bone Mineral Densities and Survival of Bone Elements: A Contemporary Sample, In *Forensic Taphonomy: The Postmortem Fate of Human Remains*, Eds. WD Haglund and MH Sorg, CRC Press, Boca Raton, pp. 295-315.

Gennari, C, G Martini, R Nuti (1998) Secondary osteoporosis, *Aging (Milano)*, Jun; 10(3): 214-24

Gibson, JH, A Mitchell, NG Harries & J Reeve (2004), Nutritional and exercise-related determinants of bone density in elite female runners, *Osteoporosis International* 15: 611- 618.

Goulding, A, RW Taylor, IE Jones, PJ Manning & SM Williams (2002), Spinal Overload: A concern for Obese Children and Adolescents? *Osteoporosis International* 13: 835-840.

Griffin, TM & F Guilak (2005), The Role of Mechanical Loading in the Onset and Progression of Osteoarthritis, *Exercise and Sport Sciences Reviews*, 33(4):195-200.

Heaney, RP, MJ Berger-Lux, KM Davies, RA Ryan, ML Johnson & G Gong (1997) Bone Dimensional change with Age: Interactions of Genetic, Hormonal, and Body Size Variables, *Osteoporosis International* 7:426-431.

Herrington, L & C Nester (2004), Q-angle undervalued? The relationship between Q-angle and medio-lateral position of the patella, *Clinical Biomechanics* 19: 1070-1073.

Hills, AP, EM Hennig, NM Byrne and JR Steele (2002) The Biomechanics of Adiposity-Structural and Functional Limitations of Obesity and Implications for Movement, *Obesity Reviews* 3:35-43.

Hills, AP, EM Hennig, M McDonald & O Bar-Or (2001) Plantar Pressure Differences between Obese and Non-Obese Adults: A Biomechanical Analysis, *International Journal of Obesity* 25:1674-1679.

Holmberg, S, A Thelin & N Thelin (2005), Knee osteoarthritis and body mass index: a population-based case-control study, *Scandinavian Journal of Rheumatology* 34:59-64.

Horner, K, H Devlin, L Harvey (2002), Detecting patients with low skeletal bone mass, *Journal of Dentistry*, 30: 171-175.

Hough, Jr , AJ (1993) Pathology of Osteoarthritis, In *Arthritis & Allied Conditions: A Textbook of Rheumatology*, 12th Ed., Eds. DJ McCarty & WJ Koopman, Philadelphia, Lea & Febiger, pp. 1699-1721.

Hummert, JR (1983) Cortical Bone Growth and Dietary Stress among Subadults from Nubia's Batn El Hajar, *American Journal of Physical Anthropology* 62:167-176.

Jankauskas, R (2003), The Incidence of Diffuse Idiopathic Skeletal Hyperostosis and Social Status Correlations in Lithuanian Skeletal Materials, *International Journal of Osteoarchaeology* 13:289-293.

Jantz, RL & DW Owsley (1984), Temporal changes in limb proportionality among skeletal samples of Arikara Indians, *Annals of Human Biology,* Mar-Apr, 11(2):157-163.

Jones, S, D Restrepo, A Kasowitz, D Korenstein, S Wallenstein, A Schneider & MJ Keller (2007) Risk factors for decreased bone density and effects of HIV on bone in the elderly, *Osteoporosis International*, DOI.1007/s00198-007-0524-8.

Kelsey, JL (1989), Risk factors for osteoporosis and associated fractures, *Public Health Report*, Sep-Oct; 104(5): 14(7).

Kennedy, KAR (1989) Skeletal Markers of Occupational Stress, In Iscan, M.Y. and Kennedy, K.A.R. (eds.), *Reconstruction of Life from the Skeleton*, Alan R. Liss, Inc., New York, pp. 129-160.

King, CA, MY Iscan, & SR Loth (1998) Metric and Comparative Analysis of Sexual Dimorphism in the Thai Femur, *Journal of Forensic Sciences* 43(5):954-958.

Komistek, RD, TR Kane, MR Mahfouz, JA Ochoa & DA Dennis (2005), Knee mechanics: a review of past and present techniques to determine in vivo loads: *Journal of Biomechanics* 38:215-228.

Krogman, WM & MY Iscan (1986) *The Human Skeleton in Forensic Medicine*. Illinois: Charles C. Thomas.

Larsen, CS & CB Ruff (1994) The Stresses of Conquest in Spanish Florida: Structural adaptation and change before and after conquest. In: Larsen C.S., Milner G.R. eds., *Biological Landscapes of Change*. New York: Wiley-Liss, pp. 21-34.

Larsen, CS (1997), *Bioarchaeology: Interpreting Behavior from the Human Skeleton*, Cambridge, MA, Cambridge University Press, 461 p.

Legroux-Gerot, I, F Blanckaert, E Solau-Gervais, M Negahban, B Duqesnoy, ABA Delcambre & B Cortet (1999) Causes of osteoporosis in males. A review of 160 cases, *Review of Rhumatology English Edition* 66(7-9): 404-409.

Lieberman, DE, MJ Devlin & OM Pearson (2001) Articular Area Responses to Mechanical Loading: Effects of exercise, age, and skeletal location, *American Journal of Physical Anthropology* 116(4): 266-277.

Lovejoy, CO, AH Burstein & KG Heiple (1976) The Biomechanical Analysis of Bone Strength: A method and its application to platycnemia, *American Journal of Physical Anthropology* 44: 489-506.

Maffeis-Claudio & Tato-Luciano (2001), Long-term effects of childhood obesity on morbidity and mortality, *Hormone Research Basel* 55(1):42-45.

Mahfouz, MR, EE Abdel Fatah, HE Dakhakhni, RT Mesiha, KR Kesler& LN Smith (2006a) Proximal Femur 3D Morphological Analysis Utilizing Statistical Bone Atlas, 3rd Cairo International Biomedical Engineering Conference, Cairo, Egypt.

Mahfouz, MR, RE Booth, Jr, JN Argenson, BC Merkl, EE Abdel Fatah & MJ Kuhn (2006b), Analysis of Variation of Adult Femora Using Sex-Specific Statistical Atlases, 7th International Symposium on Computer Methods in Biomechanics and Biomedical Engineering, Antibes, Cote d'Azur, France.

Mahfouz, MR, A Badawi, B Merkl, EE Abdel Fatah, E Pritchard, K Kesler, M Moore, R Jantz & L Jantz (2007a), Patella sex determination by 3D statistical shape models and nonlinear classifiers, *Forensic Science International* vol. 173, pp 161-170.

Mahfouz, MR, B Merkl, EE Abdel Fatah, R Booth, Jr. & JN Argenson (2007b), Automatic methods for characterization of sexual dimorphism of adult femora: distal femur, *Computer Methods in Biomechanics and Biomedical Engineering*, vol. 10, pp 447– 456.

Mannienen, P, H Riihimäki, M Heliövaara & P Mäkelä (1996) Short Communication: Overweight, Gender, and Knee Osteoarthritis, *International Journal of Obesity* 20: 595-597.

Martin, DL, AL Magennis & JC Rose (1987) Cortical Bone Maintenance in an Historic Afro-American Cemetery Sample from Cedar Grove, Arkansas. *American Journal of Physical Anthropology* 74: 255-264.

McHenry C (1978), Multivariate subset selection. *Journal of the Royal Statistical Society Series C* 27: 291–6.

Meadows L & Jantz RL (1995), Allometric secular change in the long bones from the 1800s to the present, *Journal Forensic Sciences* 40(5):762-7.

Messier, SP, WH Ettinger Jr, TE Doyle, T Morgan, MK James, ML O'Toole and R Burns (1996), Obesity: Effects on Gait in an Osteoarthritic Population, *Journal of Applied Biomechanics* 12(2): 161-172.

Messinger-Rapport, BJ & HL Thacker (2002), Prevention for the older woman. A practical guide to prevention and treatment of osteoporosis, *Geriatrics*, Apr., 57(4):16-8, 21-4, 27.

Misra, M, R Prabhakaran, KK Miller, MA Goldstein, D Mickley, L Clauss, P Lockhart, J Cord, DB Herzog, DK Katzman & A Klibanski (2007), Prognostic Inidcators of Changes in Bone Density Measures in Adolescent Girls with Anorexia Nervosa-II, *Journal of Clinical Endocrine Metabolism*, DOI:10.1210/jc.2007-2419.

Miyabara, Y, Y Onoe, A Harada, T Kuroda, S Sasaki & H Ohta (2007), Effect of physical activity and nutritio on bone mineral density in young Japanese women, *Journal of Bone Mineral Metabolism* 25: 414-418.

Molina-Perez M, E Gonzalez-Reimers, F Santolaria-Fernandez, A Martinez-Riera, F Rodriguez-Moreno, E Rodriguez-Rodriguez, A Milena-Abril & J Velasco-Vazquez (2000), Relative and combined effects of ethanol and protein deficiency on bone histology and mineral metabolism, *Alcoholism* Jan, 20(1):1-8.

Moore, M, EA Fatah & M Mahfouz (2007) Body mass estimation from human femoral midshaft cross-sectional area, first author of poster presented at the annual meeting of the American Association of Physical Anthropologists, Philadelphia, PA.

Moro, M, MCH Van der Meulin, BJ Kiratli, R Marcus, LK Bachrach and DR Carter (1996) Body Mass is the Primary Determinant of Midfemoral Bone Acquisition during Adolescent Growth, *Bone* 19(5): 519-526.

Moskowitz, RW (1993) Clinical and Laboratory Findings in Osteoarthritis, In *Arthritis & Allied Conditions: A Textbook of Rheumatology*, 12th Ed., Eds. DJ McCarty & WJ Koopman, Philadelphia, Lea & Febiger, pp. 1735-1760.

Nagurka, ML & WC Hayes (1980), An Interactive Graphics Package for Calculating Cross-Sectional Properties of Complex Shapes, *Journal of Biomechanics* 13:59-64.

Nelson, DA, DA Barondess, SL Hendrix and TJ Beck (2000) Cross-sectional Geometry, Bone Strength, and Bone Mass in the Proximal Femur in Black and White Postmenopausal Women, *Journal of Bone Mineral Research* 15(10): 1992-1997.

Ogden, CL, MD Carroll, LR Curtin, MA McDowell, CJ Tabak & K Flegal (2006), Prevalence of Overweight and Obesity in the United States, 1999-2004, Journal of the American Medical Association, Volume 295(13): 1549-1555.

Oliveria, SA, DT Felson, PA Cirillo, JI Reed & AM Walker (1998), Body Weight, Body Mass Index and Incident Symptomatic Osteoarthritis of the Hand, Hip and Knee, *Epidemiology* 10(2):161-166.

O'Neill, K, S Sueda, W Coelho, O Chakoula, N Arksey, K Porter, B Knoll, D Poole, A Mackworth, H Hoos, P Gorniak, G Carenini & C Conati. (1999-2007), *Computational Intelligence from the University of British Columbia Decision trees 4.3.1* http://www.cs.ubc.ca/labs/lci/CIspace/index.html

Ortner, DJ (2003) *Identification of Pathological Conditions in Human Skeletal Remains,*2nd ed., Academic Press, Amsterdam, The Netherlands, 608 pp.

Paniagua, MA, JE Malphurs & LF Samos (2006), BMI and low bone mass in an elderly male nursing home population, *Clinical Interventions in Aging* 1(3): 283-287.

Patrick, PJ (2005) *Greed, Gluttony and Intemperance? Testing the Stereotype of the 'Obese Medieval Monk,'* PhD Thesis, University of London.

Pollock, NK, EM Laing, CA Baile, MW Hamrick, DB hall & RD Lewis (2007), Is adiposity advantageous for bone strength? A peripheral quantitative computed tomography study in late adolescent females, *American Journal of Clinical Nutrition* 86:1530-1538.

Porter, AMW (1996) *Physique and the skeleton*, PhD Thesis, University of London.

Porter, AMW (1999) The Prediction of Physique from the Skeleton, *International Journal of Osteoarchaeology* 9: 102-115.

Reid, IR (2002), Relationships among Body Mass, Its Components and Bone, *Bone* 31(5):547-555.

Reid, IR (2007), Relationships between fat and bone, *Osteoporosis International,* Oct. (online - ahead of print)

Riddle, DL, M Pulisic, P Pidcoe & RE Johnson (2003), Risk Factors for Plantar fasciitis: A Matched Case-Control Study, *Journal of Bone & Joint Surgery Am* 85:872-877.

Ridout, CF (1999) Old Bones in Young Bodies, *American Fitness* 14(5): 28

Robling, AG (1998), *Histomorphometric Assessment of Mechanical Loading History from Human Skeletal Remains: The Relation Between Micromorphology and Macromorphology at the Femoral Midshaft*. Columbia: University of Missouri (PhD thesis), 174 pp.

Rogers, J & T Waldron (2001) DISH and the Monastic Way of Life, *International Journal of Osteoarchaeology* 11:357-265.

Rubin CT, KJ McLeod & SD Bain (1990), Functional strains and cortical bone adaptation: epigenetic assurance of skeletal integrity, *Journal of Biomechanics* 23, Suppl 1:43-54. Review.

Ruff, CB (1981) *Structural Changes in the Lower Limb Bones with Aging at Pecos Pueblo*, PhD Thesis, University of Pennsylvania.

Ruff, CB (1987), Sexual dimorphism in human lower limb bone structure: relationship to subsistence strategy and sexual division of labor, *Journal of Human Evolution* 16:391-416.

Ruff, CB (1991), Climate, body size and body shape in hominid evolution, *Journal of Human Evolution*, 21: 81-105.

Ruff, CB (2000) Body Mass Prediction from Skeletal Frame Size in Elite Athletes, *American Journal of Physical Anthropology*, 113: 507-517.

Ruff, CB & WC Hayes (1982) Subperiosteal Expansion and Cortical Remodeling of the Human Femur and Tibia with Aging, *Science* 217(4563):945-8.

Ruff, CB & WC Hayes (1984) Bone Mineral Content in the Lower Limb: Relationship to cross-sectional geometry, *Journal of Bone and Joint Surgery* 66A:1024-1031.

Ruff, CB & FP Leo (1986) Use of Computed Tomography in Skeletal Structure Research, *Yearbook of Physical Anthropology* 29:181-195.

Ruff, CB, WW Scott & AY Liu (1991) Articular and Diaphyseal Remodeling of the Proximal Femur with Changes in Body Mass in Adults, *American Journal of Physical Anthropology* 86: 397-413.

Ruff, CB & A Walker (1993) Body Size and Body Shape, In: Walker A , Leakey R , eds. *The Nariokotome Homo erectus Skeleton*, Cambridge, MA, Harvard University Press, p 234-265.

Saitoglu, M, O Ardicoglu, S Ozgocmen, A Kamanli & A Kaya (2007), Osteoporosis Risk Factors and Association with Somatotypes in Males, *Archives of Medical Research* 38:746-751.

Schmidt-Nielson, K, (1984), *Scaling: why is animal size so important?* Cambridge: Cambridge University Press.

Sharma, L, C Lou, S Cahue & DD Dunlop (2000) The Mechanism of the Effect of Obesity in Knee Osteoarthritis: the mediating role of malalignment, *Arthritis and Rheumatism* 43(3): 568-575.

Sharma, L, D Kapoor & S Issa (2006) Epidemiology of osteoarthritis: an update, *Current Opinion in Rheumatology* 18:147-156.

Steadman, DW, BJ Adams & LW Konigsberg (2006), Statistical Basis for Positive Identification in Forensic Anthropology, *American Journal of Physical Anthropology* 131:15-26.

Stürmer, T, K-P Günther & H Brenner (2000), Obesity, overweight and patterns of osteoarthritis: the Ulm Osteoarthritis Study, *Journal of Clinical Epidemiology* 53:307-313.

Syed, IY & BL Davis (2000), Obesity and osteoarthritis of the knee: hypotheses concerning the relationship between ground reaction forces and quadriceps fatigue in long-duration walking, *Medical Hypotheses* 54(2):182-185.

Traon, AP, M Heer,, MV Narici, J Rittweger & J Vernikos (2007), From space to Earth: advances in human physiology from 20 years of bed rest studies (1986–2006), *European Journal of Applied Physiology* 101:143–194.

Trotter, M & GC Gleser, (1952) Estimation of stature from long bones of American whites and negroes, *American Journal of Physical Anthropology* 10: 463-514.

Wheatley, BP (2005), An evaluation of sex and body weight determination from the proximal femur using DXA technology and its potential for forensic anthropology, *Forensic Sci Int* 147:141-145.

Woo, SLY, SC Kuei, D Amiel, MA Gomez, WC Hayes, FC White & WH Akeson (1981) The Effect of Prolonged Physical Training on the Properties of Long Bone: A study of Wolff's Law, *Journal of Bone and Joint Surgery* 63A:780-787.

Appendix

Table A.1. Definition of Axes and Angles

Name of axis	Description
Axis x or medio-lateral axis	positive more laterally
Axis y or antero-posterior axis	positive more anteriorly
Axis z or longitudinal axis	'ideal' axis – more positive proximally = with both distal condyles on table, dorsal side down, from the midpoint in shaft from lateral view just distal to lesser trochanter to the midpoint and deepest point in the patellar groove just proximal to condyles and anterior to intercondylar notch.
Cervical axis	longitudinal axis of neck through the center of the neck to the center of the head
Mechanical axis	through distal end of femur to the midpoint to femoral head center (same axis as tibia)
Biomechanical length	average distal most projection of condyles along z axis to most superior point of neck – usually at the junction of the femoral neck to the greater trochanger just medial to the insertion for the obturator internus
Cross section locations	80%, 65%, 50%, 35%, 20% of biomechanical length
Cervico-diaphyseal angle	angle of the ideal longitudinal axis with cervical axis in frontal plane
Antetorsion angle – in transverse plane	angle between cervical axis and frontal plane of diaphysis – ideal axis
Distal condylar angle	angle between line across distal point of both condyles and the average distal point of both condyels from the frontal plane
	angle between mechanical and ideal axis
Maximum length	in frontal plane, from the greatest distance from the femoral head to the distal condyles – axis may vary depending on bone

Table A.2. Definitions of Statistical Codes

femoralNeckAnteversionPC	Antetorsion angle
proximalAngle	Cervico-diaphyseal angle
femur_length	Maximum length
F_A_per20	maximum distance along major axis from area of centroid to outer perimeter of cortical bone at 20 % Slice
F_B_per20	maximum distance along minor axis from area of centroid to outer perimeter of cortical bone at 20 % Slice
F_A_per35	maximum distance along major axis from area of centroid to outer perimeter of cortical bone at 35 % Slice
F_B_per35	maximum distance along minor axis from area of centroid to outer perimeter of cortical bone at 35 % Slice
F_A_per50	maximum distance along major axis from area of centroid to outer perimeter of cortical bone at 50 % Slice
F_B_per50	maximum distance along minor axis from area of centroid to outer perimeter of cortical bone at 50 % Slice
F_A_per65	maximum distance along major axis from area of centroid to outer perimeter of cortical bone at 65 % Slice
F_B_per65	maximum distance along minor axis from area of centroid to outer perimeter of cortical bone at 65 % Slice
F_A_per80	maximum distance along major axis from area of centroid to outer perimeter of cortical bone at 80 % Slice
F_B_per80	maximum distance along minor axis from area of centroid to outer perimeter of cortical bone at 80 % Slice
IM_A_per20	maximum distance along major axis from area of centroid to outer perimeter of IM Canal at 20 % Slice
IM_B_per20	maximum distance along minor axis from area of centroid to outer perimeter of IM Canal at 20 % Slice
IM_A_per35	maximum distance along major axis from area of centroid to outer perimeter of IM Canal at 35 % Slice
IM_B_per35	maximum distance along minor axis from area of centroid to outer perimeter of IM Canal at 35 % Slice
IM_A_per50	maximum distance along major axis from area of centroid to outer perimeter of IM Canal at 50 % Slice
IM_B_per50	maximum distance along minor axis from area of centroid to outer perimeter of IM Canal at 50 % Slice
IM_A_per65	maximum distance along major axis from area of centroid to outer perimeter of IM Canal at 65 % Slice
IM_B_per65	maximum distance along minor axis from area of centroid to outer perimeter of IM Canal at 65 % Slice
IM_A_per80	maximum distance along major axis from area of centroid to outer perimeter of IM Canal at 80 % Slice
IM_B_per80	maximum distance along minor axis from area of centroid

	to outer perimeter of IM Canal at 80 % Slice
angle3	angle between mechanical and ideal axis
angle4	Distal condylar angle
angle5	angle between mechanical and anatomical axis
femoralBMA_len	Biomechanical Length of femur
Total_AREA_20per	Total cross-sectional area
centroid_x_20per	centroid x-coordinate
centroid_y_20per	centroid y-coordinate
AREA_femur_20per	Cross-sectional area of cortical bone
AREA_IM_20per	Cross-sectional area of medullary canal
IXX_20per	second moment of inertia around x axis at 20% Slice
IYY_Comb_20per	second moment of inertia around y axis at 20% Slice
IXY_20per	cross moment at 20 % slice
Iuu_20per	centroid IXX at 20% slice
Ivv_20per	centroid IYY at 20% slice
Iuv_20per	centroid IXY at 20% slice
I1_20per	max principle moment at 20% slice
ang_20per	angle between principle and X
I2_20per	min principle moment at 20% slice
ang2_20per	angle between principle and Y
J_20per	polar moment of inertia

Table A. 3. Correlation Report Females Cross-Sectional Geometry

Page/Date/Time	**1 3/6/2008 2:04:58 PM**			
Database	**C:\Documents and Settings\Me ... \IIIsexes pooled all data.S0**			
Filter	**Sex_Code=0**			
	N = 53			
Pearson Correlations Section (Row-Wise Deletion)				
	Age	**Height_m**	**Weight_kg**	**BMI**
Age	1	0.165387	-0.044183	-0.093267
Height_m	0.165387	1	0.270945	0.01356
Weight_kg	-0.044183	0.270945	1	0.961344
BMI	-0.093267	0.01356	0.961344	1
NeckAnteversion	-0.130961	-0.023803	-0.038323	-0.053985
proximalAngle	-0.085904	0.155119	-0.08406	-0.107252
femur_length	0.102906	0.614087	0.168361	0.003045
F_A_per20	-0.1237	0.228895	0.452926	0.413838
F_B_per20	0.015812	0.392748	0.271876	0.183431
F_A_per35	-0.012044	0.38431	0.49695	0.408202
F_B_per35	-0.066936	0.377395	0.341802	0.248109
F_A_per50	-0.070782	0.331358	0.461239	0.38824
F_B_per50	0.033837	0.345864	0.405815	0.321573
F_A_per65	-0.010694	0.37333	0.500423	0.412659
F_B_per65	0.077885	0.341318	0.368279	0.293828
F_A_per80	0.11756	0.311975	0.502173	0.437593
F_B_per80	0.188343	0.332417	0.131195	0.033397
IM_A_per20	-0.126276	0.180178	0.311013	0.274209
IM_B_per20	0.047936	0.248357	0.21038	0.158727
IM_A_per35	0.060517	0.275287	0.170667	0.089398
IM_B_per35	0.132973	0.164568	0.008695	-0.050886
IM_A_per50	0.175125	0.148928	-0.058087	-0.119851
IM_B_per50	0.298583	0.05237	-0.099635	-0.126604
IM_A_per65	0.188163	-0.030333	-0.137631	-0.152331
IM_B_per65	0.386148	0.020336	-0.227069	-0.255703
IM_A_per80	0.269069	0.252054	-0.051107	-0.141569
IM_B_per80	0.357579	0.079663	-0.146115	-0.199667
angle3	0.385039	-0.106543	0.03456	0.06068
angle4	0.09994	-0.249854	-0.047228	0.00108
angle5	0.341762	-0.130936	-0.047684	-0.017893
femoralBMA_len	0.123489	0.606088	0.160379	-0.010543
IM_TotalArea_20	-0.014036	0.010962	-0.023558	-0.024764
Total_AREA_20per	-0.058811	0.339118	0.388747	0.316705
centroid_x_20per	0.156709	0.099658	0.067577	0.041435
centroid_y_20per	-0.020735	-0.084248	-0.083246	-0.048491
AREA_femur_20per	-0.052506	0.341955	0.381757	0.311015
AREA_IM_20per	-0.034923	0.245903	0.270254	0.220176
IM_Percentage_20	-0.014036	0.010962	-0.023558	-0.024764

IXX_20per	-0.037998	0.377819	0.337333	0.245689
IYY_20per	-0.01336	0.365289	0.436928	0.36012
IY_IX_20	0.073197	0.028594	0.301067	0.323275
IXY_20per	-0.072779	-0.237252	-0.120732	-0.055066
Iuu_20per	-0.070834	0.430476	0.352604	0.255234
Ivv_20per	-0.063235	0.369763	0.492747	0.420241
Iuv_20per	-0.11247	0.072096	0.367251	0.367178
Kmax_20	-0.046592	0.381275	0.21348	0.124801
I1_20per	-0.054767	0.455273	0.333416	0.228341
Imax_Imin_20	0.078349	0.222365	-0.313057	-0.387593
ang_20per	-0.053036	-0.023608	-0.103913	-0.106159
I2_20per	-0.073755	0.352026	0.492433	0.424624
Kmin_20	-0.083276	0.21812	0.441068	0.40817
Kmax_Kmin_20	0.068864	0.225551	-0.315444	-0.391764
ang2_20per	-0.052958	-0.02362	-0.103951	-0.106188
J_20per	-0.067801	0.403754	0.439313	0.354353
Ko_20	-0.072025	0.301322	0.375525	0.317138
IM_TotalArea_35	0.182124	0.00717	-0.204046	-0.232091
Total_AREA_35per	-0.211848	0.367905	0.574981	0.508002
centroid_x_35per	0.083647	0.059047	0.013234	0.000485
centroid_y_35per	0.053569	0.027262	-0.112023	-0.121039
AREA_femur_35per	-0.047047	0.425516	0.461321	0.358275
AREA_IM_35per	0.113266	0.229485	0.106148	0.032663
IM_Percentage_35	0.182124	0.00717	-0.204046	-0.232091
IXX_35per	-0.16567	0.252936	0.387024	0.334248
IYY_Comb_35per	-0.054221	0.282265	0.394178	0.335555
IY_IX_35	0.174815	0.078259	-0.007882	-0.025134
IXY_35per	0.096647	-0.179084	-0.27147	-0.236548
Iuu_35per	-0.123475	0.448071	0.444613	0.339924
Ivv_35per	-0.092846	0.426366	0.597628	0.501652
Iuv_35per	-0.04986	0.049515	0.193675	0.183511
Kmax_35	-0.054749	0.327994	0.228786	0.139297
I1_35per	-0.166561	0.453748	0.48227	0.375735
Imax_Imin_35	-0.242547	0.037462	-0.186752	-0.207514
ang_35per	0.028601	0.015863	-0.098342	-0.11739
I2_35per	-0.065005	0.441723	0.56076	0.461124
Kmin_35	0.108482	0.345517	0.388765	0.301288
Kmax_Kmin_35	-0.241231	0.034359	-0.186241	-0.206327
ang2_35per	0.035532	0.067652	0.102613	0.081688
J_35per	-0.114388	0.457418	0.53648	0.431329
Ko_35	0.031792	0.358102	0.330909	0.236985
IM_TotalArea_50	0.251625	-0.037506	-0.125716	-0.126779
Total_AREA_50per	-0.258302	0.274934	0.429931	0.375606
Area_Kshape_50per	-0.233611	0.259937	0.416903	0.366549
Area_shape_50_per	-0.192132	0.221483	0.364806	0.322779
IM_Percentage_50	0.126259	0.171747	0.037372	-0.004396
centroid_x_50per	0.213585	-0.007884	-0.165952	-0.171616

centroid_y_50per	-0.020304	0.424909	0.528273	0.428981
AREA_Femur_50per	0.238972	0.067552	-0.003066	-0.028653
AREA_IM_50per	0.251625	-0.037506	-0.125716	-0.126779
IXX_50per	-0.29015	0.215837	0.362276	0.316812
IYY_Comb_50per	-0.053733	0.274664	0.329995	0.269674
IY_IX_50	0.314697	0.142014	-0.102889	-0.141114
IXY_50per	0.191241	-0.207191	-0.305379	-0.261191
Iuu_50per	-0.175456	0.415683	0.457726	0.359897
Ivv_50per	-0.057765	0.34827	0.621503	0.545664
Iuv_50per	0.050624	-0.088529	-0.065669	-0.046812
Kmax_50	0.129779	0.225089	0.226667	0.167194
I1_50per	-0.126941	0.403192	0.538127	0.443817
Imax_Imin_50	0.022329	-0.061349	-0.113022	-0.103111
ang_50per	0.130256	-0.103557	0.02759	0.051634
I2_50per	-0.126382	0.400553	0.570565	0.480992
Kmin_50	0.102898	0.250916	0.303149	0.242214
Kmax_Kmin_50	0.022886	-0.058441	-0.111985	-0.102654
ang2_50per	0.112292	-0.121913	0.147275	0.179993
J_50per	-0.132701	0.420971	0.583543	0.487558
Ko_50	0.12396	0.260747	0.295254	0.229735
IM_TotalArea_65	0.251431	-0.063521	-0.232455	-0.243186
Total_AREA_65per	-0.209144	0.298366	0.482081	0.434863
centroid_x_65per	0.261537	0.263742	0.04562	-0.021724
centroid_y_65per	0.257543	0.00203	-0.126097	-0.145918
AREA_Femur_65per	0.034679	0.419641	0.499581	0.401308
AREA_IM_65per	0.252246	0.025585	-0.105281	-0.13551
IM_Percentage_65	0.251431	-0.063521	-0.232455	-0.243186
IXX_65per	-0.30076	0.244122	0.337527	0.295871
IYY_Comb_65per	0.047323	0.396849	0.383765	0.297904
IY_IX_65	0.348898	0.155614	-0.067172	-0.119126
IXY_65per	0.239192	-0.183074	-0.287087	-0.263125
Iuu_65per	-0.127809	0.447149	0.453257	0.348272
Ivv_65per	0.012279	0.345811	0.5753	0.500734
Iuv_65per	0.099408	0.138913	0.166702	0.123788
Kmax_65	0.199538	0.187139	0.119917	0.061426
I1_65per	-0.056002	0.399932	0.491476	0.400664
Imax_Imin_65	0.054436	-0.080612	-0.193709	-0.178438
ang_65per	-0.236767	-0.040503	0.000219	0.024511
I2_65per	-0.066843	0.430658	0.574593	0.47713
Kmin_65	0.154636	0.270436	0.268632	0.192126
Kmax_Kmin_65	0.05994	-0.083039	-0.191436	-0.175461
ang2_65per	-0.042366	-0.064648	0.093826	0.118893
J_65per	-0.064254	0.431445	0.556807	0.459031
Ko_65	0.186114	0.249722	0.215657	0.142341
IM_TotalArea_80	0.277149	-0.028806	-0.354539	-0.386616
Total_AREA_80per	-0.056295	0.377395	0.618084	0.55367
centroid_x_80per	0.447513	0.130428	0.035614	0.00219

centroid_y_80per	0.293351	0.015294	-0.085742	-0.11485
AREA_Femur_80per	0.199461	0.434334	0.401145	0.288697
AREA_IM_80per	0.301457	0.187564	-0.079525	-0.159305
IM_Percentage_80	0.277149	-0.028806	-0.354539	-0.386616
IXX_80per	0.141756	0.375715	0.45821	0.359606
IYY_Comb_80per	0.302344	0.364136	0.401331	0.322604
IY_IX_80	0.17481	-0.056379	-0.033479	-0.001511
IXY_80per	0.28577	0.127923	0.112215	0.061461
Iuu_80per	0.069929	0.383289	0.484621	0.393424
Ivv_80per	0.156004	0.436324	0.514496	0.411512
Iuv_80per	0.070492	0.110405	0.418379	0.395805
Kmax_80	0.239465	0.297019	0.016412	-0.082752
I1_80per	0.122024	0.446325	0.367193	0.252932
Imax_Imin_80	-0.029965	-0.084438	0.286863	0.330158
ang_80per	-0.021019	-0.086336	0.082536	0.113954
I2_80per	0.104424	0.37839	0.587697	0.504118
Kmin_80	0.225957	0.233201	0.354146	0.292744
Kmax_Kmin_80	0.031346	0.08397	-0.279639	-0.322116
ang2_80per	-0.018902	0.057046	-0.020961	-0.044304
J_80per_	0.121063	0.44053	0.537196	0.432823
Ko	0.276281	0.309667	0.249959	0.157954
Cronbachs Alpha = 0.715038 Standardized Cronbachs Alpha = 0.969027				

Table A.4. Correlation Report for Females – Bone Mineral Density

Bone Density	**Correlation Report Females**			
Page/Date/Time	**1 3/6/2008 2:44:26 PM**			
Database	**C:\Documents and Settings\Me ... \IIIsexes pooled all data.S0**			
Filter	**Sex_Code=0**			
	N = 28			
Pearson Correlations Section (Row-Wise Deletion)				
	Age	**Height_m**	**Weight_kg**	**BMI**
Age	1	0.436129	0.033345	-0.066303
Height_m	0.436129	1	0.419629	0.226084
Weight_kg	0.033345	0.419629	1	0.974488
BMI	-0.066303	0.226084	0.974488	1
BMD	-0.438063	0.153307	0.62265	0.637972
Neck_BMD	-0.479095	0.191945	0.563515	0.561453
Wards_BMD	-0.470267	0.185659	0.428404	0.427264
Troch_BMD	-0.34944	0.194871	0.610225	0.616094
Shaft_BMD	-0.433445	0.124429	0.638115	0.659355
Cronbachs Alpha = 0.398797 Standardized Cronbachs Alpha = 0.875525				

Table A.5. Correlation Report Males – Cross-sectional Geometry

Page/Date/Time	**1 3/6/2008 1:30:47 PM**			
Database	**C:\Documents and Settings\Me ... \IIIsexes pooled all data.S0**			
Filter	**Sex_Code=1**			
	N = 75			
Pearson Correlations Section (Row-Wise Deletion)				
	Age	**Height_m**	**Weight_kg**	**BMI**
Age	1	-0.436679	-0.263096	-0.179118
Height_m	-0.436679	1	0.411749	0.176165
Weight_kg	-0.263096	0.411749	1	0.966592
BMI	-0.179118	0.176165	0.966592	1
NeckAnteversion	0.097171	-0.170702	-0.113568	-0.083818
proximalAngle	0.000923	0.009751	-0.086422	-0.107629
femur_length	-0.230254	0.597205	0.068091	-0.086967
F_A_per20	-0.092443	0.401855	0.471186	0.405917
F_B_per20	0.017956	0.402165	0.242316	0.155444
F_A_per35	0.01289	0.423603	0.398333	0.323933
F_B_per35	-0.06256	0.440298	0.422509	0.340385
F_A_per50	-0.080741	0.379941	0.378975	0.30857
F_B_per50	0.091004	0.376796	0.494617	0.429635
F_A_per65	-0.025206	0.296728	0.387449	0.346479
F_B_per65	0.143618	0.333478	0.401158	0.333537
F_A_per80	0.125687	0.286137	0.468513	0.423576
F_B_per80	0.078989	0.35192	0.221622	0.149634
IM_A_per20	0.006272	0.373788	0.323242	0.25088
IM_B_per20	0.194197	0.253534	0.112556	0.053825
IM_A_per35	0.247522	0.052376	-0.11684	-0.141748
IM_B_per35	0.171504	0.338647	0.181008	0.110681
IM_A_per50	0.261587	-0.070898	-0.230871	-0.236032
IM_B_per50	0.313137	0.193113	0.029674	-0.015902
IM_A_per65	0.280684	-0.033048	-0.247008	-0.262617
IM_B_per65	0.385311	0.013508	-0.067846	-0.080663
IM_A_per80	0.268745	0.122986	-0.003646	-0.042889
IM_B_per80	0.338301	0.137147	-0.062428	-0.107748
angle3	0.388388	-0.141634	0.103438	0.150723
angle4	-0.006747	-0.10733	-0.050324	-0.020669
angle5	0.395528	-0.250947	0.015509	0.079761
femoralBMA_len	-0.172197	0.593286	0.060914	-0.094426
IM_TotalArea_20	0.293149	0.113032	-0.06585	-0.103479
Total_AREA_20per	-0.386237	0.291999	0.462515	0.426848
centroid_x_20per	0.0721	0.022964	0.031396	0.033703
centroid_y_20per	-0.093629	-0.023071	-0.055425	-0.060422
AREA_femur_20per	-0.041585	0.427509	0.3926	0.31194
AREA_IM_20per	0.120036	0.332849	0.222885	0.151811
IM_Percentage_20	0.293149	0.113032	-0.06585	-0.103479

IXX_20per	-0.172732	0.278988	0.338576	0.29671
IYY_20per	-0.189478	0.378392	0.499304	0.441493
IY_IX_20	-0.09155	0.195163	0.329844	0.304889
IXY_20per	0.011317	-0.069936	-0.088411	-0.080282
Iuu_20per	-0.200356	0.397742	0.402991	0.331474
Ivv_20per	-0.248399	0.442514	0.591995	0.52378
Iuv_20per	-0.20478	0.227729	0.371401	0.349702
Kmax_20	-0.021648	0.390327	0.277694	0.204921
I1_20per	-0.233107	0.437748	0.45735	0.3823
Imax_Imin_20	0.043735	-0.035745	-0.213146	-0.214251
ang_20per	0.099401	-0.119765	-0.224207	-0.219774
I2_20per	-0.230841	0.425107	0.562236	0.494513
Kmin_20	-0.022784	0.390636	0.428054	0.358673
Kmax_Kmin_20	0.019788	-0.009155	-0.173601	-0.177039
ang2_20per	-0.046477	0.097468	0.121032	0.115435
J_20per	-0.238968	0.443526	0.537016	0.464193
Ko_20	-0.019567	0.426439	0.397744	0.319889
IM_TotalArea_35	0.135509	0.168222	0.045909	0.020091
Total_AREA_35per	-0.17744	0.188311	0.305405	0.267471
centroid_x_35per	-0.004974	0.173541	0.091543	0.053532
centroid_y_35per	-0.014188	-0.033519	0.114252	0.126478
AREA_femur_35per	-0.020279	0.456287	0.433487	0.349966
AREA_IM_35per	0.124418	0.308468	0.189704	0.136072
IM_Percentage_35	0.135509	0.168222	0.045909	0.020091
IXX_35per	-0.071191	0.201909	0.15137	0.109158
IYY_Comb_35per	-0.10062	0.354669	0.3783	0.311131
IY_IX_35	-0.016132	0.157797	0.284373	0.258377
IXY_35per	0.069832	-0.203012	-0.139361	-0.094597
Iuu_35per	-0.084037	0.405951	0.406786	0.331003
Ivv_35per	-0.131767	0.453791	0.559666	0.480654
Iuv_35per	-0.061939	-0.027498	0.058483	0.081223
Kmax_35	-0.021577	0.440361	0.356655	0.279026
I1_35per	-0.155879	0.454827	0.503262	0.421792
Imax_Imin_35	-0.220123	0.072405	0.020191	0.009107
ang_35per	0.009533	0.050879	0.189023	0.183263
I2_35per	-0.070505	0.425131	0.483769	0.406807
Kmin_35	0.08973	0.393873	0.334111	0.264426
Kmax_Kmin_35	-0.218975	0.079551	0.03118	0.018967
ang2_35per	-0.084039	0.159488	0.113638	0.083446
J_35per	-0.111728	0.4459	0.500692	0.420379
Ko_35	0.04044	0.428944	0.355297	0.279525
IM_TotalArea_50	0.363991	0.009346	-0.091054	-0.100999
Total_AREA_50per	-0.319592	0.325214	0.491362	0.44153
Area_Kshape_50per	-0.343065	0.319551	0.432855	0.378232
Area_shape_50_per	-0.316805	0.271889	0.332373	0.281428
IM_Percentage_50	-0.005922	0.232568	0.16747	0.121393
centroid_x_50per	0.087066	-0.153216	0.057568	0.095239

centroid_y_50per	0.020447	0.411584	0.489323	0.415986
AREA_Femur_50per	0.343859	0.115878	0.03231	0.00349
AREA_IM_50per	0.363991	0.009346	-0.091054	-0.100999
IXX_50per	-0.16055	0.297722	0.225025	0.167235
IYY_Comb_50per	-0.120366	0.353871	0.403566	0.34056
IY_IX_50	0.067111	0.052693	0.229124	0.223843
IXY_50per	0.171934	-0.30875	-0.242849	-0.183239
Iuu_50per	-0.073003	0.407817	0.491227	0.418378
Ivv_50per	-0.072598	0.4362	0.576914	0.50159
Iuv_50per	0.158874	-0.278088	-0.189055	-0.120371
Kmax_50	0.216918	0.328173	0.362775	0.306499
I1_50per	-0.037515	0.435577	0.581819	0.50926
Imax_Imin_50	0.160971	-0.064258	0.056567	0.08194
ang_50per	0.107975	-0.07403	0.10865	0.12348
I2_50per	-0.099228	0.421573	0.511605	0.434824
Kmin_50	0.089519	0.327196	0.281617	0.215497
Kmax_Kmin_50	0.155592	-0.058679	0.058867	0.083255
ang2_50per	0.138555	-0.101704	0.154352	0.200566
J_50per	-0.076509	0.443369	0.560862	0.483014
Ko_50	0.15228	0.351005	0.337279	0.270659
IM_TotalArea_65	0.219522	0.078906	-0.002064	-0.004121
Total_AREA_65per	-0.182651	0.189705	0.37748	0.334881
centroid_x_65per	0.037897	0.293748	0.217731	0.166791
centroid_y_65per	0.139431	-0.220671	-0.004268	0.049613
AREA_Femur_65per	0.068961	0.340233	0.432077	0.372951
AREA_IM_65per	0.22358	0.135917	0.051528	0.036447
IM_Percentage_65	0.219522	0.078906	-0.002064	-0.004121
IXX_65per	-0.146979	0.308531	0.258293	0.191919
IYY_Comb_65per	-0.05329	0.331239	0.406332	0.344859
IY_IX_65	0.126104	-0.028423	0.118711	0.133008
IXY_65per	0.178011	-0.327557	-0.205841	-0.132001
Iuu_65per	0.031782	0.280645	0.436929	0.394072
Ivv_65per	0.049528	0.274784	0.439731	0.388858
Iuv_65per	0.294643	-0.245596	0.082761	0.160181
Kmax_65	0.268348	0.181862	0.215896	0.185662
I1_65per	0.121818	0.251524	0.41629	0.369335
Imax_Imin_65	0.249389	-0.0913	-0.107715	-0.110042
ang_65per	-0.118721	0.214802	0.14058	0.08727
I2_65per	-0.023583	0.30779	0.47016	0.421905
Kmin_65	0.092296	0.245204	0.280182	0.249715
Kmax_Kmin_65	0.253483	-0.09311	-0.10383	-0.105763
ang2_65per	0.035241	-0.031102	0.167254	0.198561
J_65per	0.042646	0.291726	0.4604	0.411199
Ko_65	0.17746	0.229185	0.264751	0.232756
IM_TotalArea_80	0.371251	-0.054448	-0.263105	-0.272072
Total_AREA_80per	-0.185768	0.342087	0.568142	0.521649
centroid_x_80per	0.128179	0.250426	0.126271	0.077778

centroid_y_80per	0.179915	-0.168182	-0.085979	-0.05423
AREA_Femur_80per	0.115104	0.361587	0.375796	0.307963
AREA_IM_80per	0.313409	0.151045	-0.034463	-0.07872
IM_Percentage_80	0.371251	-0.054448	-0.263105	-0.272072
IXX_80per	0.025762	0.254711	0.415885	0.372141
IYY_Comb_80per	0.017662	0.362775	0.41573	0.353875
IY_IX_80	-0.068027	0.113334	-0.05952	-0.079088
IXY_80per	0.183022	-0.071156	0.073234	0.091029
Iuu_80per	0.022429	0.329155	0.489992	0.435638
Ivv_80per	0.04417	0.339075	0.426016	0.365701
Iuv_80per	0.16465	0.05395	0.387867	0.385535
Kmax_80	0.185401	0.260617	0.165714	0.11052
I1_80per	0.017004	0.333823	0.411451	0.354338
Imax_Imin_80	-0.07325	0.011551	-0.143292	-0.147896
ang_80per	-0.213047	0.024023	-0.165354	-0.177692
I2_80per	0.046684	0.343573	0.501841	0.442621
Kmin_80	0.22889	0.248229	0.280335	0.229337
Kmax_Kmin_80	-0.06816	0.00924	-0.147393	-0.151659
ang2_80per	0.099983	-0.129834	0.097371	0.137407
J_80per_	0.03548	0.35195	0.480931	0.420452
Ko	0.227504	0.27552	0.253117	0.195787
Cronbachs Alpha = 0.796684	Standardized Cronbachs Alpha = 0.976767			

Table A.6. Correlation Report for Males – Bone Mineral Density

Bone Density **Correlation Report – Males**
Page/Date/Time **1 3/6/2008 2:48:49 PM**
Database **C:\Documents and Settings\Me ... \IIIsexes pooled all data.S0**
Filter **Sex_Code=1**
N = 24

Pearson Correlations Section (Row-Wise Deletion)

	Age	**Height_m**	**Weight_kg**	**BMI**
Age	1	-0.525944	-0.491166	-0.437415
Height_m	-0.525944	1	0.559098	0.368096
Weight_kg	-0.491166	0.559098	1	0.973628
BMI	-0.437415	0.368096	0.973628	1
BMD	-0.715575	0.204104	0.498015	0.518446
Neck_BMD	-0.774431	0.28383	0.579998	0.580954
Wards_BMD	-0.786075	0.236032	0.461979	0.468485
Troch_BMD	-0.652497	0.249266	0.468968	0.47583
Shaft_BMD	-0.68207	0.149703	0.477373	0.512023

Cronbachs Alpha =- 0.087184 Standardized Cronbachs Alpha = 0.822576

Table A.7.

Female Counts					
	TLM_lip				
BMI_Code	0	1	2	3	Total
Emaciated	2	3	0	0	5
Normal	8	8	0	1	17
Overweight	0	3	0	0	3
Obese	1	5	3	0	9
Morbid Obese	0	1	2	2	5
Total	11	20	5	3	39

Table A.8.

Female Percentages					
	TLM_lip				
BMI_Code	0	1	2	3	Total
Emaciated	40	60	0	0	100
Normal	47.1	47.1	0	5.9	100
Overweight	0	100	0	0	100
Obese	11.1	55.6	33.3	0	100
Morbid Obese	0	20	40	40	100
Total	28.2	51.3	12.8	7.7	100

Table A.9.

Female Counts					
	TLL_lip				
BMI_Code	0	1	2	3	Total
Emaciated	2	3	0	0	5
Normal	7	7	2	1	17
Overweight	1	2	0	0	3
Obese	1	5	2	1	9
Morbid Obese	0	1	0	4	5
Total	11	18	4	6	39

Table A.10.

Female Percentages					
	TLL_lip				
BMI_Code	0	1	2	3	Total
Emaciated	40	60	0	0	100
Normal	41.2	41.2	11.8	5.9	100
Overweight	33.3	66.7	0	0	100
Obese	11.1	55.6	22.2	11.1	100
Morbid Obese	0	20	0	80	100
Total	28.2	46.2	10.3	15.4	100

Table A.11. Males

CountsMales					
	Spur_L				
BMI_Code	0	1	2	3	Total
Emaciated	4	2	0	0	6
Normal	16	1	5	0	22
Overweight	2	4	0	1	7
Obese	3	3	3	0	9
Morbid Obese	3	1	1	3	8
Total	28	11	9	4	52

Table A.12.

Counts Males					
	TRM_lip				
BMI_Code	0	1	2	3	Total
Emaciated	3	2	0	0	5
Normal	11	12	0	0	23
Overweight	5	1	0	1	7
Obese	2	5	1	1	9
Morbid Obese	3	2	4	0	9
Total	24	22	5	2	53

Table A.13.

Row Percentages Males					
	TRM_lip				
BMI_Code	0	1	2	3	Total
Emaciated	60	40	0	0	100
Morbid Obese	33.3	22.2	44.4	0	100
Normal	47.8	52.2	0	0	100
Obese	22.2	55.6	11.1	11.1	100
Overweight	71.4	14.3	0	14.3	100
Total	45.3	41.5	9.4	3.8	100

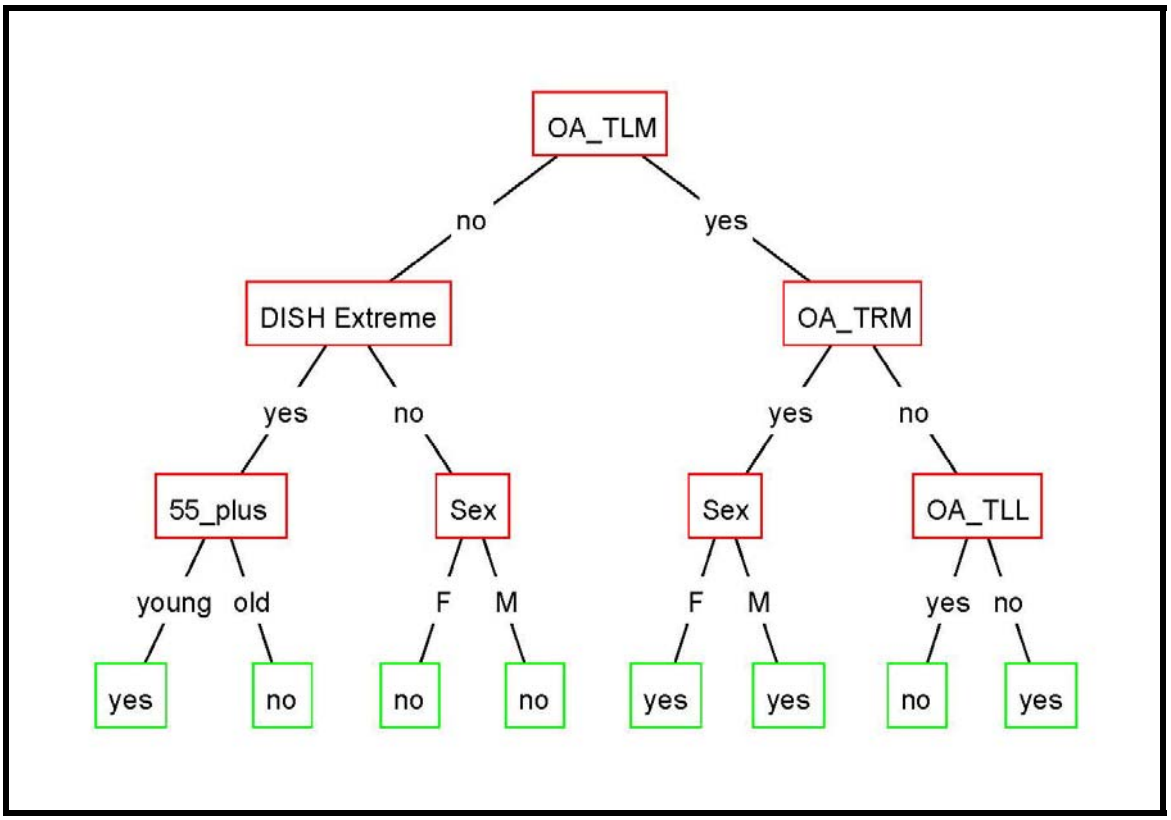

Figure A.1. Classification Tree Solving for Obesity with 83% Correct Classification

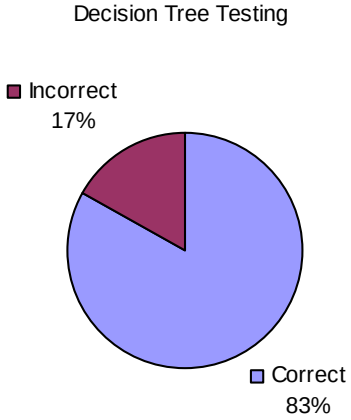

Figure A.2. Results Solving for Obesity with 83% Correct Classification

Vita

Megan Katrina Moore was born in Columbus, Ohio, on December 22, 1975. She went to went to grade school at Montrose Elementary in Bexley, Ohio, and McCord Middle School in Worthington, Ohio. For high school, she spent her Freshman and Sophomore years at Grandview Heights High School and graduated a year early from Worthington Kilbourne High School in 1993. She spent a year studying fine arts at Columbus College of Art and Design on a scholarship. She received her B.A. with honors distinction in Anthropology with a minor in French from The Ohio State University in 1998. Megan completed her M.S. in Anthropology at the University of Oregon. Megan completed her doctoral degree in Anthropology from the University of Tennessee in May 2008. She is to be married at the end of the summer of 2008 to John Thomas Nipper of Cookeville, Tennessee.